THE UNIVERSITY OF ALBERTA

AN INTERFEROMETRIC STUDY OF THE $Zn - ZnSO_4$ SYSTEM

A THESIS

SUBMITTED TO THE FACULTY OF GRADUATE STUDIES

IN PARTIAL FULFILMENT OF THE REQUIREMENTS FOR

THE DEGREE OF MASTER OF SCIENCE

DEPARTMENT OF MINING AND METALLURGY

BY

FREDERICK WILLIAM YAKYMYSHYN

EDMONTON, ALBERTA

APRIL, 1962.

UNIVERSITY OF ALBERTA

FACULTY OF GRADUATE STUDIES

The undersigned certify that they have read and recommend to the Faculty of Graduate Studies for acceptance, a Thesis, entitled "An Interferometric Study of the Zn - $ZnSO_4$ System", submitted by Frederick William Yakymyshyn, B.Sc. (Metallurgical Engineering, U. of A. 1959) in partial fullfilment of the requirements for the degree of Master of Science.

ACKNOWLEDGEMENT

The experimental work described in this thesis was sponsored by a grant from the National Research Council. The author would like to express his gratitude to Dr. J. Leja and Dr. R. N. O'Brien for their assistance while the experiments were being carried out and for their helpful discussion of the data obtained. The author would also like to express his gratitude to Mr. R. Scott of the Department of Mining and Metallurgy for his assistance in photographical work.

A paper, based on a portion of the results presented here, will be given by Dr. R. N. O'Brien at the Los Angeles Meeting of the Electrochemical Society on May 7th, 1962.

ABSTRACT

An interferometric study of the refractive index gradients existing in an electrolyte while current is being passed through it has been carried out using Fizeau type fringes. It was found that the type of fringe patterns obtained depended greatly on the position of the electrodes. The positions of the narrow-faced electrodes (2 mm x 25 mm) were as follows: (1) shallow vertical, (2) deep vertical, (3) horizontal anode over cathode and (4) horizontal cathode over anode.

Two systems were studied: aqueous $CuSO_4$ electrolyte between polycrystalline copper electrodes and aqueous $ZnSO_4$ between polycrystalline zinc electrodes. Photographs of the fringe patterns in each of the positions are shown and the corresponding voltage-current density data are given. Most of the work was carried out using 0.10 M solutions; however, some results were also obtained for 0.001 M, and 0.010 M and 0.25 M $ZnSO_4$. Fringe patterns formed by temperature gradients and by alternating current are also included.

Refractive index data were obtained for aqueous H_2SO_4, aqueous $ZnSO_4$ and for mixtures of aqueous H_2SO_4 and $ZnSO_4$. A Pulfrich Refractometer was used to obtain these data.

TABLE OF CONTENTS

TABLE OF CONTENTS (Cont.)

LIST OF TABLES

LIST OF FIGURES

LIST OF FIGURES (Cont.)

LIST OF FIGURES (Cont.)

LIST OF INTERFEROGRAMS

LIST OF INTERFEROGRAMS

INTRODUCTION

A knowledge of the exact concentration of electrolyte at all points between the electrodes in an electrodeposition cell has been sought by electro-chemists for a long time. In the present work, an electrodeposition cell has been so constructed that it is also an interferometer. The interference fringes produced in the apparatus enable measurement of concentration differences, with reference to the bulk of the electrolyte, which are smaller than 0.10 grams/litre for aqueous solutions of $ZnSO_4$ or $CuSO_4$. A further advantage of this method is that the concentration of the electrolyte can be determined, at any given point between the electrodes, relative to the bulk of the electrolyte.

Prior to electrolysis in systems such as $ZnSO_4$ electrolyte between zinc electrodes or $CuSO_4$ electrolyte between copper electrodes the concentration of the electrolyte between the electrodes is essentially constant. However, as soon as electrolysis is started the electrolyte at the anode interface is enriched due to the ionization of atoms on the anode and the electrolyte at the cathode interface is depleted due to the deposition of ions. Since the transfer of ions from the enriched zone or to the depleted zone is determined by the coefficient of diffusion of the ion being deposited on the cathode and to a smaller extent the voltage across the cell, a concentration gradient determined by these factors is set up very quickly at the electrode faces.

If conditions are such that natural convection currents are not set up in the electrolyte (e.g. using very thin electrodes or in the cathode over anode position) the concentration gradients will progress from the electrodes towards each other until the appropriate concentration difference between the anode and cathode is established for the given current density. The concentration gradient between the electrodes will therefore have the shape of an S-curve at low current densities and a straight line at high current densities.

However, if conditions are such that natural convection currents are set up, the shape of the concentration gradient will be changed. Since the convection currents operate mainly in the bulk of the electrolyte, the concentration gradient at the electrode interface will be the same as that obtained for no convection. However, the electrolyte in the bulk will be transferred at a faster rate than that due to diffusion alone and a smaller overall concentration difference between the anode and cathode is produced.

When a fluid is set in motion due to localized differences in density which accompany differences in concentration, the movement is said to be taking place due to "natural convection" (laminar flow). Natural convection is thus deferentiated from "forced convection" which is produced by mechanical agitation such as stirring or pumping.

In 1888 Nernst defined concentration polarization by the

Equation

$$E_p = \frac{RT}{nF} \ln \frac{C}{C_o}$$

where E_p is the concentration polarization in volts, R the universal gas constant, T the absolute temperature, n the number of electrons transferred in the electrode process per reacting molecule or ion, F the Faraday, C the concentration of the electrolyte at the electrode face and C_o the concentration of the bulk of the electrolyte. Although the equation is written using concentration the activity of the electrolyte at the two points should be used.

Haring[1] was the first to attempt to measure the concentration of the electrolyte at the electrode face, in his case the cathode. His method involved removing the cathode quickly from the electrolyte while electrolysis was being carried out, collecting the solution adhering to the face and then analysing the solution thus obtained. This same method was also used by Brenner who later developed an improved method for determining the variation in the concentration of the electrolyte at an electrode face. A freezing solution was injected into a hollow electrode immediately after the current was switched off, thus freezing the electrolyte onto the electrode. Layers of electrolyte were then machined off the face and analysed. Brenner found that at a distance of 0.2 m.m. or less from the cathode face the concentration was reduced to approximately one half the concentration of the bulk. The pin-hole method which was developed by Read and Graham has also been used. In this method a small hole is drilled through the electrode and capped

of the electrolyte near the electrode face are removed by a capillary tube during electrolysis.

The main fault with these methods is that only average values of the concentration of the electrolyte are obtained; Haring's method gives only one value, Brenner's method gives two to four values and, it was found, that Read and Graham's method gives values which are dependent on the size of hole and the sampling rate.

The first person to apply an interferometric method to study the concentration variation of the electrolyte between two working electrodes was Samartsev [2] in 1934. Working with $ZnSO_4$ between amalgamated zinc electrodes, he was able to measure the concentration gradients at the cathode and thus calculate the coefficient of diffusion of zinc ions at various concentrations of $ZnSO_4$ electrolyte. His apparatus consisted of the interferometer of Lebedev combined with a polarizing microscope. The electrodes were placed one above the other, with the cathode on top, to prevent the establishment of convection currents.

The interferometric method proved to be a much better method for studying concentration polarization because values of the actual concentration of the electrolyte could be obtained at any distance from the electrode. However, since the maximum separation between the two coherent rays in Lebedev's interferometer was only 0.063 m.m., both rays passed through the diffusion layer and a true picture of the concentration distribution across the whole distance between the electrodes was not obtained.

Samartsev's work went unnoticed for many years, for in 1947, Berg[3] suggested that an interferometer similar to that used by Scott[4] could be used to study concentration polarization. Scott had been studying the concentration gradients at the advancing face of a growing salt crystal.

The work of Ibl[5] in 1955, on $CuSO_4$ using a Jamin type of interferometer showed that at relatively high current densities an "anomalous maximum" at the cathode and an "anomalous minimum" at the anode was obtained in addition to the concentration gradient in the diffusion layer. He postulated at this time that these maxima and minima are due to natural convection in the cell. The electrodes in the cell used by Ibl were positioned in such a way that the faces were vertical. In a second paper[6] Ibl developed an equation relating the amount of convection to the height of the electrode and the current density. He was also able to check the results obtained by the formula by adding collophonium to the electrolyte and photographing the rate of movement of the particles in the convection currents. His observed and calculated values of the convection currents agreed to two significant figures.

Like the interferometer of Lebedev the Jamin interferometer also relies on splitting a beam of light into two coherent rays before the light enters the electrolyte. However, since the separation between the two coherent rays can be made as great as 8 mm., the Jamin interferometer gives a much better picture of the concentration distribution of an electrolyte between two working electrodes.

Working independently O'Brien[7] developed an optical system in which the light beam was not split until after it had entered the electrolyte

between the electrodes. Although O'Brien's interferometer is very simple to construct and set up for a run it has one great disadvantage relative to the Jamin interferometer in that the size of the electrolysis cell must be kept quite small. Unless extreme precautions are taken the separation between the glass flats can't be greater than about 4 mm.

O'Brien also studied $CuSO_4$ system between copper electrodes. Most of his work was carried out at high current densities (10-40 ma./cm^2) where the "anomalous maxima and minima", which O'Brien called the "second wave", existed.

Rosenfield[8] also studied the copper-$CuSO_4$ system using O'Brien's interferometer. She postulated that the second wave may not be a concentration gradient, but rather, is due to a purely optical effect to be expected when ion-pairs dissociate, the free ions having a higher intrinsic refractive index than the ion-pairs. This conclusion was arrived at mainly on the strength of two observations. The fact that the second wave, while following the decay of the patterns after the current was switched off, disappeared about 60 times faster than the first wave and also that this second wave was not observed in $NiSO_4$ or Ag ClO_4 electrolytes at comparable current densities. Rosenfield felt that ion-pairs should not be detected in $NiSO_4$ or Ag ClO_4 by optical means. She also felt that her cell (2 mm x 3 mm x 20 mm) was too small to support convection currents.

The results incorporated in this thesis were obtained using the system of aqueous $ZnSO_4$ electrolyte between polycrystalline zinc electrodes and aqueous $CuSO_4$ electrolyte between polycrystalline copper electrodes.

The interferometer used was similar to that used by O'Brien and Rosenfield. The nomenclature given to the fringe patterns by O'Brien is illustrated in Fig. 1 and it will be used throughout this thesis.

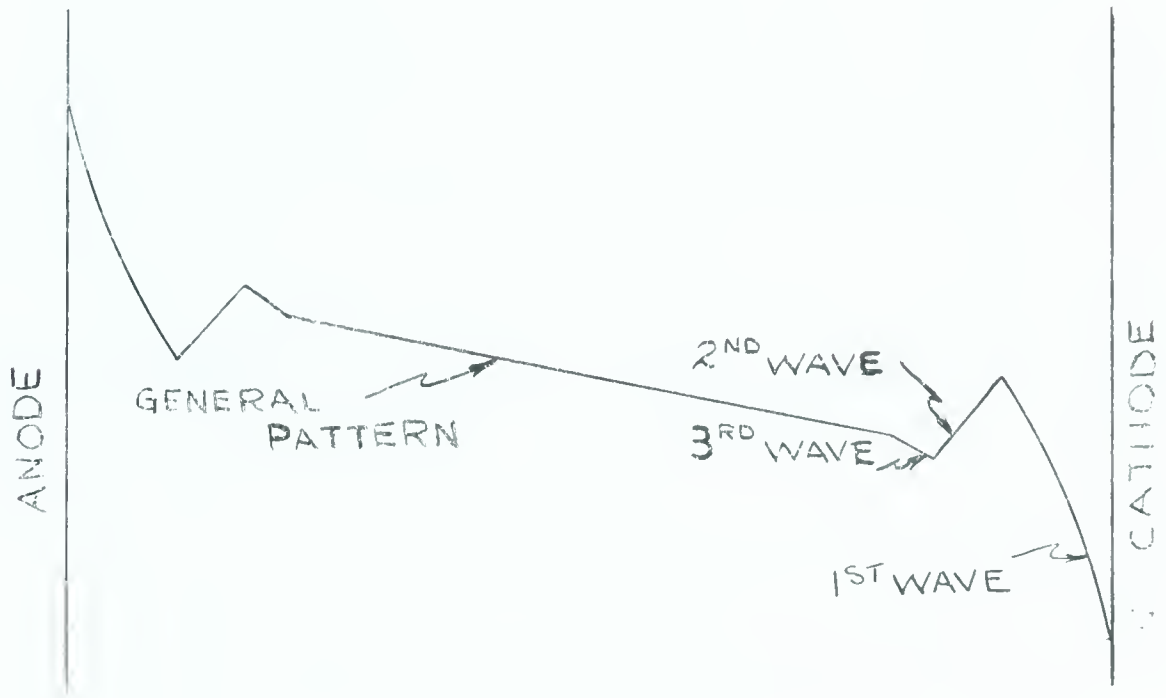

FIG. 1 O'Brien's Nomenclature for Fully Developed Fringe Pattern.

The amount of fringe shift that is observed in first, second or third wave is proportional to the corresponding refractive index change, therefore, in order to correlate the fringe shift to a concentration change, the relationship between refractive index and concentration must be known. This relationship was obtained using a Pulfrich refractometer.

Voltage-current density relationships were obtained for various concentrations of $ZnSO_4$ and the fringe patterns obtained at each current density were photographed. In order to determine whether convection of any type did play a part in the transfer of ions from the anode to the cathode, fringe patterns together with the voltage-current density data

were obtained with the cell in various positions, i.e., when the electrode faces were horizontal, vertical or one above the other. The results obtained in Zn-$ZnSO_4$ system were then compared to the results obtained from similar experiments in the system of aqueous $CuSO_4$ electrolyte between copper electrodes. Results were also obtained in the Cu-$CuSO_4$ system while bringing the electrode faces closer together in steps from a separation of 3.25 mm. to a separation of 0.52 mm.

It is hoped that the data and observations will be of use to other investigators studying concentration polarization interferometrically.

THEORY

A - INTERFEROMETRY[9]

LIGHT SOURCES

For chromatic fringes, which are formed by white light, any convenient white source may be used. According to the light intensity required, one may use an incandescent lamp or a high current carbon arc. For monochromatic fringes, the light source depends on the type of investigation to be carried out. Therefore, the source can vary from the broad wavelength band transmitted by a colored glass filter to the sharp bright monochromatic line sources. Generally, for monochromatic fringes, when the order of interference is high the monochromatism must also be high.

INTERFERENCE BY DIVISION OF AMPLITUDE

Division of [redacted] amplitude is brought about by simple reflection. Thus when light falls on a thin film, say, of glass or mica, part of the amplitude of the incident wave is reflected at the first face of the film met and the remainder continues until it meets the second face where a similar fraction is reflected. Since these two fractions are coherent and have travelled different path lengths, they are in a condition to interfere.

The effects produced depend on whether the faces of the film are parallel or are inclined to each other. The "Cosine Law" which governs the fringe separation is more simply deduced from the interference effect in the parallel-sided film.

If parallel rays A and A^1 meet the surface B^1B of a plane parallel sheet of material of thickness t and refractive index μ, the ray A^1B^1 refracts to C^1 where it reflects to B and is refracted and combined with the reflected ray AB at B. From B both rays travel towards C and are in a position to interfere. The path difference of the two rays A^1B^1 and AB in the air is DB. In the medium the path length is $B^1C^1 + C^1B$. Since the time taken for B^1 to reach D^1 in the medium is the same as that for D to reach B in the air, the path difference between the two rays equals $B^1C^1 + C^1B - B^1D^1$ in the medium. If B^1C^1 is produced its own length to E and BE joined, it is easily seen that the path difference in the medium equals D^1E and since BE = 2t,

$2t \cos \theta = \delta =$ path difference in the medium, where θ is the angle of refraction in the medium.

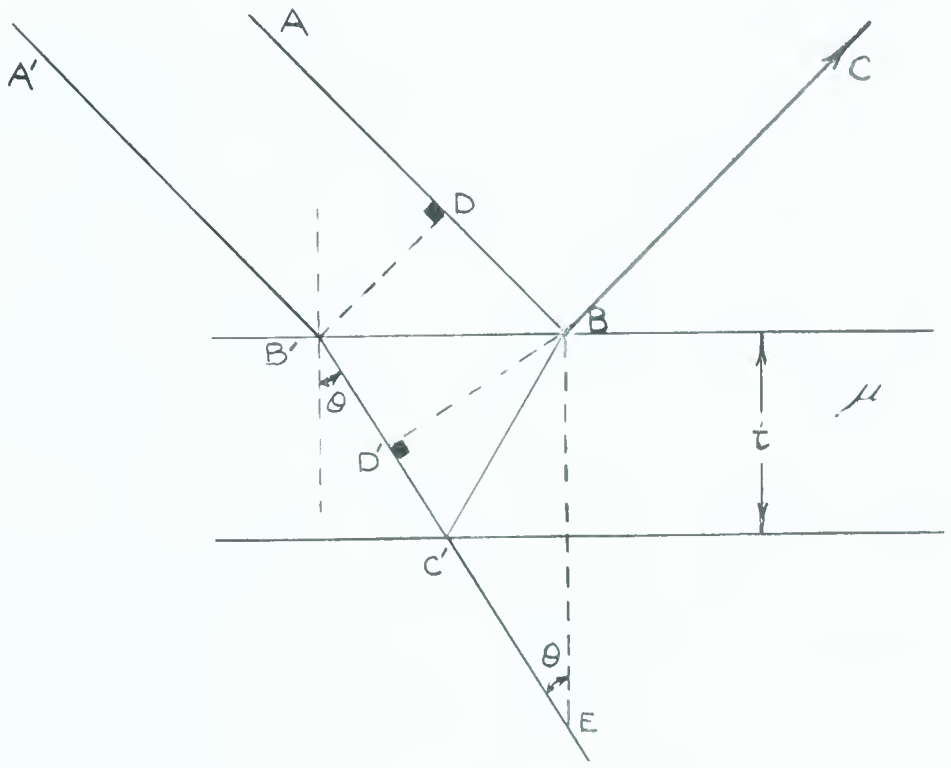

FIG. 2 Cosine Law

In the air the equivalent path difference is $2\mu t \cos\theta$. Reflection of the ray AB at B introduces a phase change of π i.e. the path length is altered by $\lambda/2$. Therefore, whenever the path difference δ equals $n\lambda$, where n is an integer and λ is the wave length of the light, dark fringes will be obtained and when

$(n + 1/2)\lambda = 2\mu t \cos\theta$ bright fringes will be obtained.

In the formula $n\lambda = 2\mu t \cos\theta$ the variables are λ, μ , t and θ . Since λ is usually kept constant and μ cannot easily be varied, the only true variables are t and θ and the following clasification of fringes can be made:

NATURE OF LIGHT	CONSTANT	VARIABLE	NATURE OF FRINGE
λ constant	θ	t	equal thickness
λ constant	t	θ	equal inclination

FRINGES OF EQUAL INCLINATION

This type of fringe is produced when the thickness is kept constant and the angle of incident light is varied. For this purpose an extended source, which is in the focal plane of a lens, must be used. From the formula $n\lambda = 2\mu t \cos\theta$ it is seen that successive fringes will appear for those values of θ for which n is a constant; the particular values being determined by the values of μt and λ .

All the light incident at an angle θ_1 , falls along the surface of a cone of semi-angle θ_1 and therefore the fringe produced is a circular ring. Further, since the reflecting surfaces are parallel

the rays which combine to interfere will also emerge parallel. For this reason these fringes are described as being localized at infinity because the beams can only be brought to interfere by a lens or seen by an eye relaxed at infinity.

Fringes of equal inclination are not equally spaced but become closer spaced as the distance from the center increases. The order of interference n is a maximum at the center and diminishes progressively towards the outer rings.

FRINGES OF EQUAL THICKNESS

Fringes of equal thickness are produced when θ is held constant and the thickness between the reflecting surfaces is varied. If the reflecting surfaces are flat then t is varied by placing the surfaces in such a position that a wedge angle exists between them. If this wedge angle is small the basic formula $n\lambda = 2\mu t \cos\theta$ holds closely enough. Fringes of equal thickness will be equally spaced and straight if the reflecting surfaces are flat and if μ is kept constant. For the case of normal light, i.e., $\cos\theta = 1$, the fringes are localized on one of the reflecting surfaces (the exact surface depends on whether the fringes are produced by reflection or transmission) and will occur at positions where the product μt is equal to $\lambda/2$, λ, $3\lambda/2$, 2λ, - - - - - - - -, $\frac{n}{2}\lambda$. Each fringe is the locus of points for which n, the order of interference, is constant.

Since fringes of this type are localized it is a very simple matter to photograph them.

FIZEAU FRINGES

In order to obtain precise sharp localization of fringes on a wedge it is necessary to use strictly parallel light. Since parallel light can only be produced from a point source at the focus of a perfectly corrected lens, it is very difficult to produce parallel light. If an extended source is used packets of parallel light, each having a different angle of incidence to the wedge will be produced. This range of incident angles causes all the bright fringes to broaden out on the side corresponding to greater wedge thickness. The amount of broadening depends on the wedge thickness, therefore, if strictly collimated light is used one is not restricted to using only thin films but separations of many centimeters may be used. Experimentally a compromise must be made between the degree of collimation and the retention of sufficient light so that photographs may be taken.

B - REFRACTIVE INDEX

In order to interpret fringe shifts, the variation of refractive index with concentration must be known. Refractive index of a medium is defined as the ratio of the velocity of light in a vacuum to the velocity in the medium. Mathematically this is stated as

$\frac{U_1}{U_2} = \frac{\sin \theta_1}{\sin \theta_2} = \mu$ where U_1 and U_2 are the phase velocities of light in the two media, θ_1 is the angle between the incident beam of light and the normal to the surface separating the two media, θ_2 denotes the corresponding angle for the refracted ray and μ is the refractive index of the medium other than vacuum.

The index of refraction can be measured by various types of refractometers. Examples are the Abbe refractometer where a drop of solution is placed between two prisms and the angle of total reflection measured; the differential refractometer where the refractive index of one solution may be compared to another and the Pulfrich which will be desribed later.

White light may be used for both the Abbe and differential refractometers but for the Pulfrich, monochromatic light must be used.

Refractive index differences or gradients can be measured very accurately using various types of interferometers. A Fizeau type interferometer which was used to obtain refractive index gradients due to concentration polarization in an electrolytic cell will be described later.

DISPERSION

The index of refraction is not a constant but increases as the frequency of light is increased, i.e., μ is greater for violet light than for red light of the visible spectrum. Therefore, in order to obtain comparable results, it is necessary to use a monochromatic source of known frequency. Usually, light corresponding to the A or D line of the sun spectrum or the α or γ lines of the hydrogen spectrum is employed.

For most solutions and liquids the refractive index varies quite uniformly with frequency in the visible range of the spectrum. However, in certain materials such as organic liquids which contain conjugated systems of double bonds and solutions of some inorganic salts, chelated and unchelated, a very rapid change in refractive index with frequency has been observed. This phenomenon is known as anomalous refractive dispersion.

INTERPRETATION OF FRINGE SHIFTS

The basic formula for the position of fringes on a wedge is

$$n\lambda = 2\mu t \cos\theta \ .$$

For the case of normal incidence $\cos\theta = 1$, therefore,

$n\lambda = 2\mu t$ where n is the order of interference, μ the refractive index, λ the wave length of light used and t the thickness between the reflecting surfaces (i.e., the thickness of the wedge at a given point).

If we assume that fringes are generated in a medium of refractive index μ, between the reflecting surfaces in such a manner that the fringes are a distance d_1 apart, then, from Fig. 3, it follows that

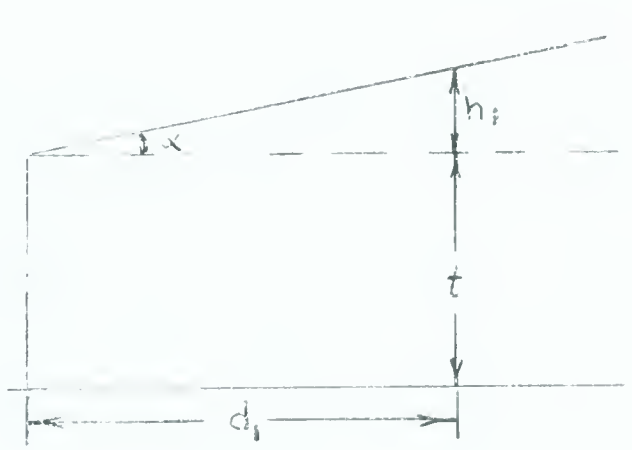

FIG. 3 Position of Fringes on a Wedge

$\tan\alpha = \dfrac{h_1}{d_1}$ and $\lambda = 2\mu h_1$, where α is the wedge angle.

Therefore

$$\tan\alpha = \frac{\lambda}{2\mu d_1} \qquad (1)$$

If medium (1) is removed and replaced with a second medium of refractive index μ_2 the corresponding relationship

$$\tan \alpha = \frac{\lambda}{2\mu_2 d_2} \quad \text{---} \quad (2)$$

will be obtained. Combining equations (1) and (2) the relationship

$$\frac{\mu_1}{\mu_2} = \frac{d_2}{d_1} \quad \text{----} \quad (3)$$

is obtained.

The accuracy of measurements of refractive index changes made in this way depends on the accuracy with which d_1 and d_2 can be measured. In work of the type carried out in this project, it was possible to measure these values to three figures. This means a percentage error of about $\pm$ 0.3% or less.

However, if a refractive index gradient is produced in a medium which causes the fringes to deviate from a straight line, very accurate measurements can be made on the gradient. In the electrolytic cell used in this work the wedge angle was arranged so that the fringes were parallel to each other and perpendicular to the electrodes. The current was then turned on establishing a refractive index gradient at the electrode faces. This condition is illustrated in Fig. 4.

From case I the following equations are obtained:

$$n_{AA}\lambda = 2\mu_1 t \quad \text{\_\_\_\_\_} \quad (4)$$

and $$\tan \alpha = \frac{\lambda}{2\mu_1 d_1} \quad \text{\_\_\_\_\_} \quad (5)$$

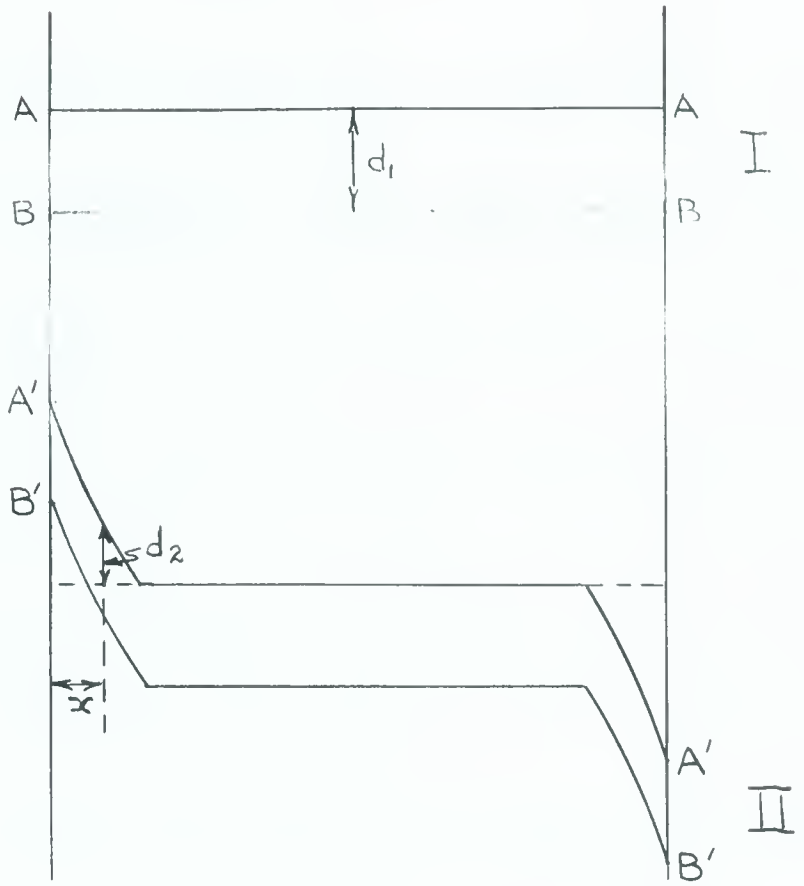

FIG. 4 Fringe Shift Calculations

The equation for fringe A^1A^1 in case II is

$$n_{A^1A^1}\,\lambda = 2\mu_2\,(t \pm h) \qquad \text{(6)}$$

where h is the change in the thickness of the wedge at the point x on the fringe A^1A^1. Since the order of interference n is constant for the fringes AA and A^1A^1 the following relationship

$$\frac{n_{AA}\,\lambda}{2} = \frac{n_{A^1A^1}\,\lambda}{2}$$ can be written.

Therefore $$\mu_1 t = \mu_2\,(t \pm h) \qquad \text{(7)}$$

From a diagram similar to Fig. 3 it can be shown that

$$\tan \propto = \frac{h}{d_2} \qquad \text{(8)}$$

By combining equations (5) and (8), the equation

$$\frac{h}{d_2} = \frac{\lambda}{2\mu_1 d_1}$$

$$\text{or} \qquad h = \frac{\lambda d_2}{2\mu_1 d_1} \qquad \text{——— (9)}$$

is obtained. By substituting this value for h into equation (7) we get:

$$\mu_1 t = \mu_2 \left[t \pm \frac{\lambda d_2}{2 d_1} \right]$$

With the use of the relationship given in equation (4) the above equation can be reduced to

$$\mu_1 = \mu_2 \pm \frac{\mu_2 d_2}{n_{AA} d_1}$$

$$\text{or} \qquad \mu_2 = \frac{\mu_1}{1 \pm \frac{F}{n}} \qquad \text{——— (10)}$$

where $F = \frac{d_2}{d_1}$ and is called the fringe shift.

The deviation of a fringe from the horizontal position can be measured to approximately 0.1 of a fringe shift. Measurements on t can be made to ± 0.001 cm. The order of interference n for a cell 0.200 cm. thick will be

$$n = \frac{2\mu t}{\lambda} = \frac{2 \times 1.33534 \times 0.200}{5893 \times 10^{-8}} = 9060$$

for the case of 0.10 M $ZnSO_4$ at 25.0°C using sodium D light.

The factor $\frac{F}{n}$, for the smallest refractive index change detectable, is equal to $\frac{1}{10 \times 9060} = 0.000011$. This means that a concentration difference of 0.0005 M $ZnSO_4$ or 0.08 grams $ZnSO_4$ per liter can be observed and measured.

If the distance between fringes is 0.0300 cm. the value of the wedge angle α is

$$\tan \alpha = \frac{\lambda}{2\mu d} = \frac{5893 \times 10^{-8}}{2 \times 1.33534 \times 0.0300}$$

$$= 0.736 \times 10^{-3}$$

or $= 2.5$ minutes.

If the length of the cell is 2.5 cm., the difference in the thickness of the wedge from one end of the cell to the other is $0.736 \times 10^{-3} \times 2.5$ $= 0.0017$ cm.

Equation (1) can be further reduced to yield the equation for

$$\Delta\mu = \mu_1 - \mu_2 = \pm \frac{\mu_2 F}{n}$$

combining this with equation (6) we get

$$\Delta\mu = \pm \frac{\mu_2 \lambda F}{2\mu_2 (t \pm h)}$$

and since h is very small

$$\Delta\mu = \pm \frac{\lambda F}{2t}$$

For the case where F is one fringe shift $\Delta\mu$ will be 0.00015 if λ equals 5893 A^o and t is 0.200 centimeters. Table I shows the change in concentration, ΔC, that is required to produce a change in the refractive index of 0.00015 at the various concentrations.

TABLE I - CHANGE IN CONCENTRATION REQUIRED TO PRODUCE ONE FRINGE SHIFT

Conc. $ZnSO_4$ MOLAR	μ_1	ΔC moles/liter	ΔC gms/liter
0.009	1.33274	0.0048	0.77
0.094	1.33518	0.0054	0.87
0.235	1.33900	0.0055	0.89
0.469	1.34528	0.0056	0.90
0.938	1.35701	0.0061	0.98

INHERENT DIFFICULTIES OF THE FIZEAU TYPE INTERFEROMETER

The first difficulty is that the fringes are indistinguishable, that is, it is impossible to tell one fringe from another. This makes it very difficult to measure the absolute movement of a fringe. While it is easy to measure a refractive index gradient it is difficult to determine whether a fringe moves up or down due to a change in the refractive index in the bulk of the solution. It is true that if there is a movement of the fringes up or down then there will also be a change in the distance between the fringes, however, this change can only be measured to about 0.3%. Therefore, the concentration of $ZnSO_4$ could change by as much as 0.14 M before it could be detected by a change in the distance between fringes.

However, if the fringe movements are photographed with a movie camera, the absolute movements of the fringe can be measured and concentration changes as low as 0.0005M $ZnSO_4$ can be determined in the bulk of the electrolyte.

The second difficulty is due to a characteristic of light and therefore cannot be avoided. When light travels through a medium it always takes the shortest path length (μt) in going from one point to another. If there is a refractive index gradient in the medium, the light ray will be bent in the direction of decreasing refractive index. The amount of bending per passage of light can be calculated using the following formula [1] for the simple case where the refractive index is proportional to the distance from the electrode face.

$$x_2 - x_1 = \frac{\mu_1}{K} \left(\cosh \frac{kt}{\mu_1} - 1\right)$$

$$= \frac{kt^2}{2\mu_1} + \frac{k^3t^4}{24\mu_1^3} + \frac{k^5t^6}{720\mu_1^5} + - - -$$

where $x_2 - x_1$ is the displacement due to the bending of the light per passage of the light from on reflecting surface to the other, x is the distance from the electrode face, t is the distance between the reflecting surfaces and k is the proportionality constant relating the refractive index, μ, to the distance x. μ_1 is the refractive index at x_1.

Taking the example where k = 0.00022 per mm. t = 2.00 mm. and μ_1 = 1.33500 the amount of displacement $x_2 - x_1$ per passage will be 0.0033 mm. The value of k was calculated for the case where a shift of three fringes occurs within a distance of 0.20 mm. Since the rays of light make, on the average, 2 to 3 passes between the reflecting surfaces, this displacement becomes an observable value and produces a blurring effect on the fringes, especially at the anode, where the bend

is in towards the bulk of the solution. This bending of the light causes the fringe shift at the anode to appear greater than at the cathode even though the same concentration gradient exists at both electrodes.

In order to determine whether a fringe shift is related to an increasing or decreasing refractive index, the direction of the wedge angle α must be known. This cannot be easily determined with complete assurance that the correct direction was obtained. One method that can be used to determine the direction of α involves the use of an electrode through which a coolant may be passed. The direction of the fringe shift when the electrolyte is cooled near the electrode can be observed. The temperature of the electrolyte is then equalized and a current passed between the electrodes so that the direction of the fringe shift at a known electrode can be observed. The two fringe shifts can then be related and the fringe shift at a known working electrode can be used as a standard.

APPARATUS

The arrangement of the apparatus used to obtain interference fringes was similar to that used by O'Brien and Rosenfield. Fringes are produced by 1/4" x 1 1/2" diameter glass flats (obtained from Liberty Mirror Division, Libbey-Owens-Ford Glass Company, Brackenridge, P.A.) which have partially reflecting coatings on one side and non-reflecting coatings on the other. Fig. 5 shows the arrangement of all the apparatus for the case of fringes produced by transmission and Fig. 6 shows the arrangement of cell, mirror and camera for the case of reflection.

The light, from a sodium vapor lamp, was partially collimated by two sets of slits placed about one foot and 1 1/2 foot from the mirror. The first slit, about one inch wide, was stationary while the second slit of 0.2" could be moved to the most suitable position. A distance of approximately five feet was maintained between the lamp and the mirror.

The 2" x 3" mirror was prepared by evaporating a coat of aluminium on glass in a vacuum. In the case of transmission a 100% reflecting coat was used and in reflection a 50% reflecting coat. The mirror was supported by a tripod so that adjustments could easily be made to aline the light with respect to the cell.

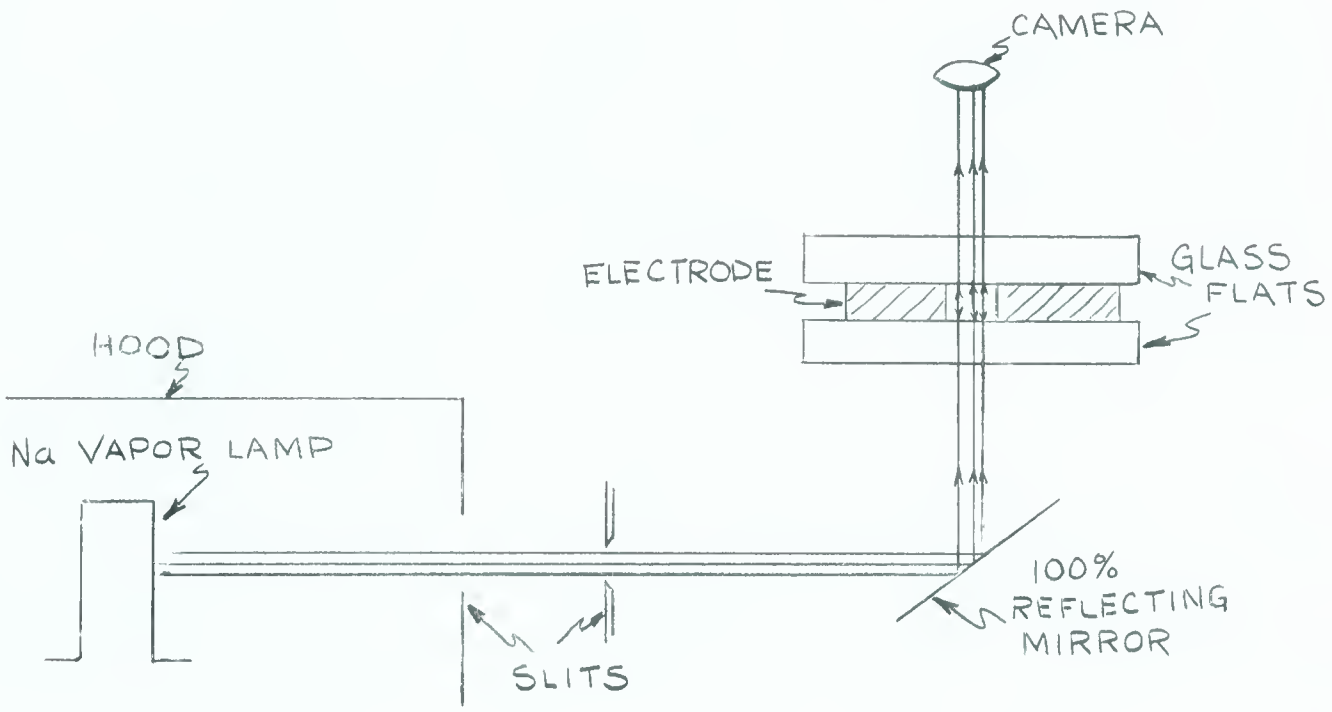

FIG. 5 Assembly of Apparatus For Fringes Produced by Transmission

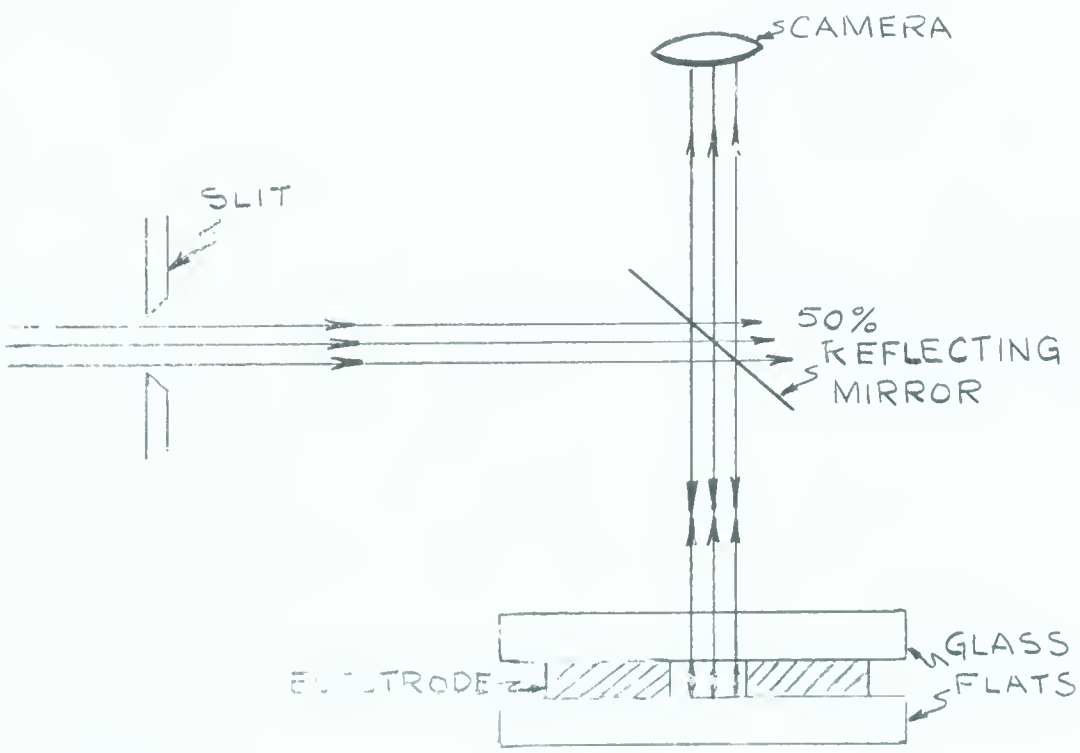

FIG. 6 Assembly for Fringes Produced by Reflection

Photographs of the fringe patterns were taken with a 35 mm. camera with bellows attached. This enabled the lens of the camera to be within three inches of the solution between the electrodes. Focusing was obtained by extending or shortening the bellows while observing the fringes by a "through the lens sight".

The photographs were taken using Ilford H.P.S. film at exposures of 1/10 second. The negatives were developed and printed using solutions to obtain maximum contrast. Photographs were printed at an enlargement of 35 times. The magnification could be further increased if desired by photographing this enlarged picture and enlarging again.

Some color photographs were also taken. Kodak high speed ektachrome film, at 1 sec. exposures, was used for this purpose.

Construction of Cell

The cell consists of four components:

(a) the walls of the cell through which constant temperature water is circulated;

(b) the top glass flat holder;

(c) the bottom glass flat holder;

(d) the electrodes and electrode holder.

The assembly of the components of the cell is shown in Fig. 7.

The cell walls were cast in two steps from an Epoxy resin supplied by C.I.B.A. (Araldite 502 resin and Araldite H N 951 hardener) and machined to correct dimensions on a lathe. The product of the first cast was a 4" clyinder of O.D. 2" and I.D.1 1/4". After machining the

O.D. of this cylinder to 1.885" a 2" coil of 1/8" O.D. copper tubing was wound tightly around the cylinder. A second casting was then made around this making the O.D. of the final cylinder 3". The inside of the cylinder was then machined to make the I.D. 1.825", leaving a shell only 0.030" thick to isolate the copper tubing from the solutions in the cell.

A Jabsco, model AL, rubber impeller pump was used to circulate water from a constant temperature bath, maintained at ± 0.1°C, through the cell. The cell was placed on the suction side of the pump to prevent heating of the water by the pump.

It was found that the 1/8" O.D. tubing offered too high a resistance to the flow of water, so most of the copper tubing was removed by circulating nitric acid through it. This procedure enabled a flow of 750 cc/min. of water to be obtained and also afforded a faster heat transfer between the circulating water and the solution in the cell.

The glass flats were held in position by mounts machined from polyethylene. The bottom glass flat holder was attached, through ball and socket type joints, to a three screw tripod which was used to adjust the wedge angle between the glass flats.

In order to prevent leakage of the solution past the bottom mount a rubber O-ring was installed which fitted snugly against both the mount and the cell wall. O-rings were also used to support the glass flats in the mounts. As well as preventing leaks these O-rings served as cushions for the glass flats. This prevented scratching of the coating

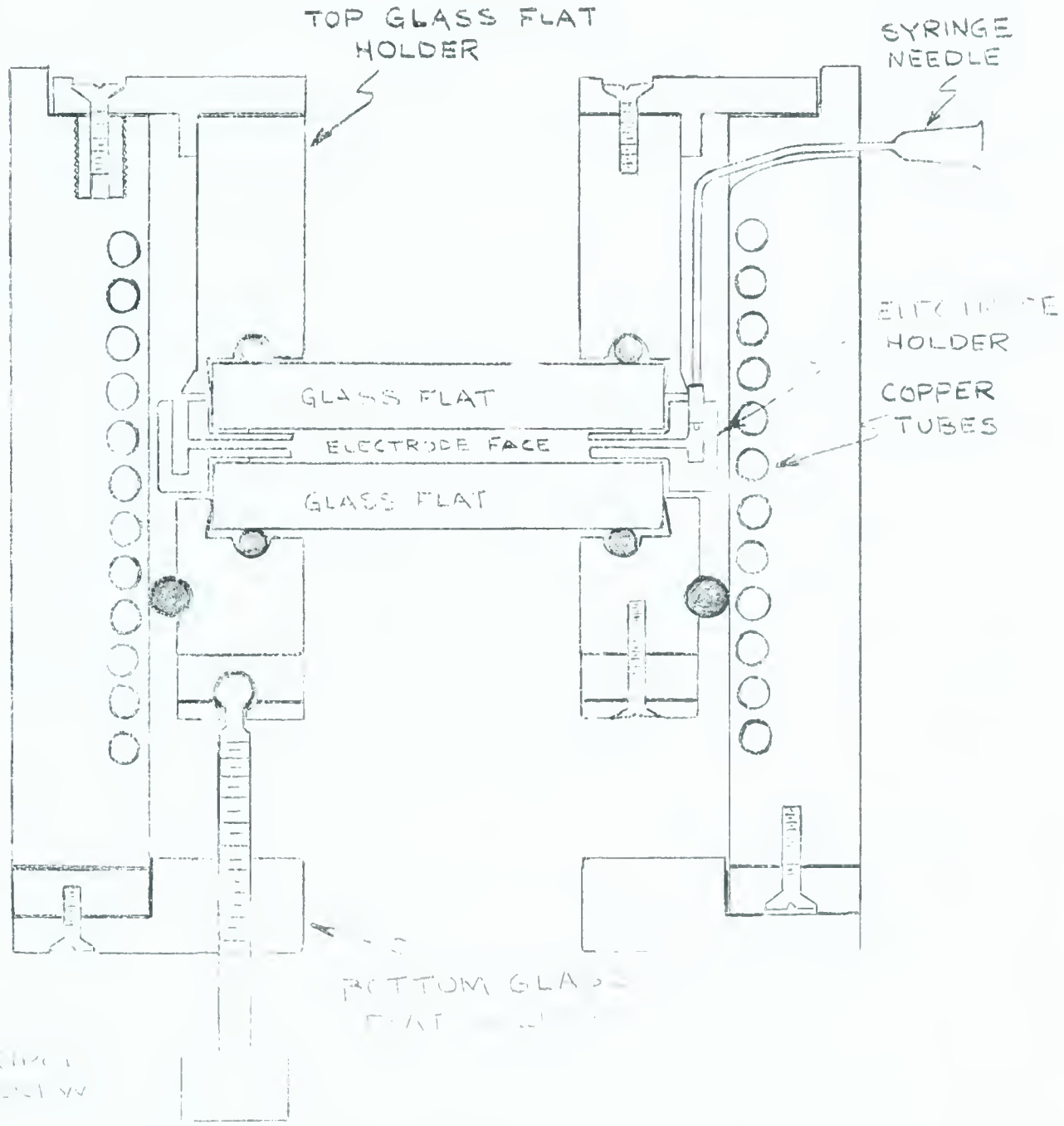

FIG. 7 Cross Section of Assembled Cell.

on the flats when the flats were brought up against the electrodes.

The separation between the electrodes was maintained constant by means of an electrode holder (Fig. 8). A separate holder was made for each set of electrodes by casting epoxy resin around the electrodes positioned in a mold with a 25mm. long by 3 mm. wide spacer set between them. Covering the electrodes with silicone vacuum grease prevented the epoxy resin from adhering to them. It was, therefore, easy to punch the electrodes out of the mold when the casting was machined down. The part of the holder between the glass flats was machined until its thickness was slightly less than that of the electrodes. Holes were drilled in the electrode holder for mounting a 20 gauge syringe needle (for the purpose of changing the solution in the cell at any desired time) and for the electrical leads to the electrodes.

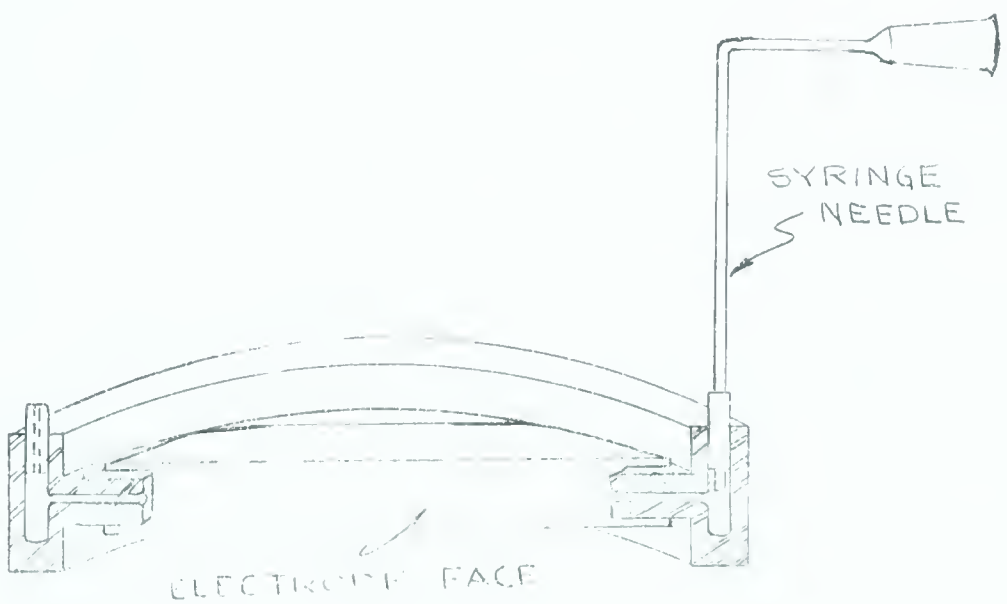

FIG. 8 Electrode Holder

PREPARATION OF ELECTRODES

Four sets of two electrodes each were prepared from 99.999% zinc obtained from Consolidated Mining and Smelting, Trail, B C. The zinc was received in the as-cast condition in bars approximately 1" x 1" x 8". Electrode sets No. 2 and No. 3 were prepared from zinc remelted in an induction heating unit under argon and cast into carbon black coated copper molds while No. 1 and No. 4 were prepared from the as-received material.

The zinc castings or slabs cut from the as-received bars were machined down to a thickness of 3 mm. Each disk thus obtained was then cut in two to form an electrode pair. This procedure was adopted to eliminate, as much as possible, any differences in chemical composition or grain size between the electrodes in each set.

When each electrode had been reduced to the dimensions of 1 cm. x 3 cm. x 0.25 cm. on belt grinders, holes 3/64" in diameter were drilled into the back of the electrodes to a depth of 3 to 4 mm. so that electrical leads could be attached to the electrodes. Further reduction of the thickness of the electrodes was accomplished on 240 to 600 grit emery paper. Measurement of the thickness of the electrodes were made with a micrometer scaled in millimeters until the thickness was constant within ± 0.01 mm. at a thickness of about 2.0 mm.

The area of each electrode face in contact with the electrolyte was approximately 0.5 cm^2 for the case of electrode sets No. 1, 2 and 3. Electrode set No. 4 was 3.56 mm. thick and had a surface area of 0.876 cm^2.

When the disk, from which the No. 3 set of electrodes was made, had been machined to a thickness of 3 mm. it was lightly cold worked and then heated for 3 hours at a temperature of 200°C. An equiaxed grain structure was thereby obtained which contained about 70 grains/cm^2 as compared to the columnar grain structure, containing about 40 grains/cm^2 in the as-cast condition.

After the electrodes were reduced to the appropriate dimensions each set was placed in an oven at 120°C for 4 1/2 hours in an attempt to eliminate strains that were produced during machining and polishing. The electrode faces were then polished on 600 grit emery paper and etched in dilute H_2SO_4 solution until the grain structure was visible. Similar polishing and etching of the electrode faces was carried out before every series of experiments.

Early experiments were carried out using copper wire leads to the electrodes. Although the copper wire and the electrodes were coated with polyurethane it was felt that some interfering voltages due to a galvanic couple may be set up. Zinc wire was, therefore, produced by taking appropriate cuts while machining high purity zinc on a lathe, and used as electrical leads. The leads were fitted snugly into the holes provided in the electrodes to ensure good electrical contact.

The copper electrodes were prepared from high purity copper, received as 2" diameter rod, by machining and polishing to the proper dimensions. A dilute nitric acid solution was used to etch the electrode faces. The grain size of the copper electrodes was very small compared to that in the zinc electrodes.

After the electrodes were placed in the cell and the glass flats adjusted, solution was introduced into the cell through the syringe needle. When the solution had come to the cell temperature a potential of approximately 0.5 volts was applied across the cell for 6 minutes in one direction and then 3 minutes in the other direction. The old solution was then removed and fresh solution injected. When the fresh solution came to the cell temperature a series of runs was started. Runs were continued until a needle-like deposit was noticed on the cathode or for not more than 3 hours.

PREPARATION OF SOLUTIONS

(a) For Refractive Index Determinations

In all cases the solutions were prepared from high purity reagents. Sulfuric acid was of 95.5% minimum strength while the zinc sulphate was obtained as crystalline $ZnSO_4 \cdot 7H_2O$. All water used in making the solutions was doubly distilled (with the addition of potassium permanganate in the second distillation). The water was then boiled before preparing the solutions in order to remove dissolved CO_2. The pH of this water was found to be 6.8 and the conductivity 1.5μmhos per cm. These data were obtained using a Beckman Zeromatic pH meter and a Betz Laboratories Conducto-Bridge Model X-50, Purity Meter.

Approximately one molar solution of H_2SO_4 and $ZnSO_4$ were prepared and titrated against Na OH and E.D.T.A. respectively. Solutions of lower concentrations were then prepared by dilution of the titrated stock solutions to make 200 cc. quantities of the required strength.

Solutions containing both H_2SO_4 and $ZnSO_4$ were prepared from approximately one molar H_2SO_4 (determined by refractive index) and weighed amounts of $ZnSO_4 \cdot 7H_2O$.

It was found that if $ZnSO_4 \cdot 7H_2O$ was weighed out to make 0.750 and 1.000 molar solutions the respective titrated values were 0.774 and 1.027 molar. This corresponds to values of 6.50 and 6.58 for the number of water molecules of hydration rather than 7. The formula $ZnSO_4 \cdot 6.54\ H_2O$ was therefore used to weigh out appropriate amounts of zinc sulfate to make 200 cc. solutions containing both H_2SO_4 and $Zn\ SO_4$.

The solutions were stored in 250 cc. polyethylene bottles. In most cases the determinations at the four temperatures were carried out within two to three days. If the solutions were stored for more than five days their refractive indicies were checked at a previously used temperature in order to ascertain that no change in concentration took place due to evaporation.

(b) Interferometric studies

All solutions were prepared by weighing out the appropriate amount of crystalline zinc sulfate or copper sulphate and dissolving it in doubly distilled and boiled water to make either 500 or 1000cc. of solution in a volumetric flask. Only the concentration of the 0.1 M solutions were checked by the refractive index of the solutions at 20.0°C.

Recording Cell Temperature

Electrodes No. 1 were prepared, especially for the purpose of observing the temperature within the cell. Holes 3/64" in diameter were drilled from the back of the electrodes to within 1 to 1.5 millimeters

of the electrode face. Chromel-alumel thermocouples made from 28 gauge wire and coated with polyurethane (obtained from Plastiglo Industries Ltd. Edmonton) were then inserted into the holes in each of the electrodes. The coating of polyurethane was used to insulate the thermocouples from the electrodes through which current was passed and from the solution which would short circuit the thermocouples.

The thermocouples were calibrated against a thermometer reading to 0.1°C. It was found that the thermocouples produced 0.040 millivolts per °C in the range 15 to 30°C. The value obtained from tables is 0.0400 to 0.0406 mv/°C between 10 and 40°C. Readings were taken with the thermocouples to determine at what temperature the bath water should be kept in order to obtain the correct temperature in the cell, how much time was required before a constant temperature was reached in the cell and whether there was any change in temperature of the electrolyte in the cell at large current densities between the electrodes.

It was found that a constant temperature was obtained rather quickly(5-10 min) for temperatures between 20 to 30°C and could be maintained within ± 0.2°C of any desired temperature in this range. If no fringe shift could be seen near the electrodes the temperature could be assumed constant since a temperature change of 0.2°C would produce a 0.14 fringe shift which is within the measurable range.

This criterion could not always be applied because at higher concentrations (around 0.25 M $ZnSO_4$) a slight bend in the fringes could be detected near the electrodes. This bend did not disappear as would

be expected if it was due to temperature and was most evident if there was a large potential (5 mv or greater) between the electrodes at no imposed current or after a loose needle-like deposit had been produced on the cathode.

RESULTS

PART A - REFRACTIVE INDEX STUDY

The refractive index data were obtained using a Pulfrich refractometer for the sodium D line with reference to air. In the Pulfrich refractometer the light is focussed on to the liquid contained in a small glass cylinder (tabulure) cemented on to a carefully ground glass prism as shown in Fig. 9.

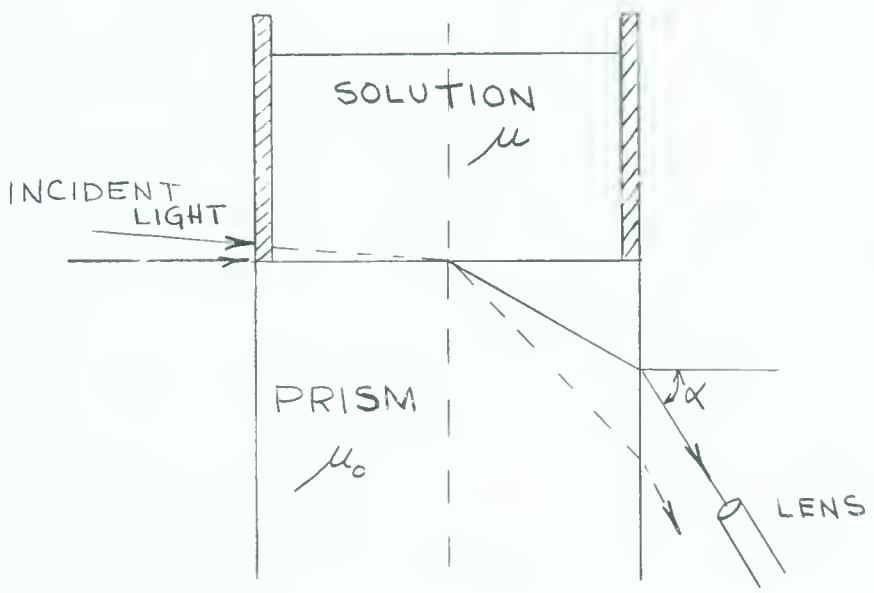

FIG. 9 Pulfrich Refractometer

The angle which the refracted beam makes with the vertical increases as the incident beam approaches the horizontal and reaches a maximum when the beam enters parallel to the interface between the solution and the prism. The refractive index of the solution μ is related to

the refractive index of the prism μ_o and the angle α by the formula

$$\mu^2 = \mu_o^2 - \sin^2\alpha$$

The angle α was measured on a graduated circle with vernier attachment to the nearest 0.5 minutes. After the values of μ were calculated they are appropriately corrected to account for the change in refractive index of the prism due to temperature.

Before the solution was placed in the tabulure, the instrument was allowed to come to the desired temperature by circulating water for 30 minutes to one hour from a constant temperature bath. The water was circulated at the rate of 400 cc/min. around the prism and through a silver vessel which dips into the tabulure. After the solution (about 1.5 cc.) had been placed in the tabulure the silver vessel was dipped into place. It was found, by observing the refractive index change with time, that 5 minutes was sufficient time for the solution to reach a constant temperature.

The refractive index of a solution of a given concentration was determined by taking the average of several readings on each of two separate samples. After removing the old solution from the tabulure with a squeeze bottle adapted for this purpose, the tabulure, prism surface and silver vessel were washed three times with water, three times with acetone and then dried. The same three components were then rinsed three times with solution of the next concentration to be observed before a sample of the solution was left in the tabulure to reach a constant temperature.

When the silver vessel was lowered into position a rubber gasket, which was also washed in the way described above, fitted snugly against the top of the tabulure. It was found that a one molar solution of $ZnSO_4$ could be left in the tabulure for 30 minutes at 35°C before there was any change in the refractive index due to evaporation.

The temperature of the solution in the tabulure was taken to be the same as that of the circulating water which was measured with a thermometer, graduated in 0.1°C divisions, placed with its mercury bulb inside the silver vessel. The accuracy of the instrument was checked by determining the refractive index of water at various temperatures and comparing these values to those obtained in the literature.

The refractive indices obtained for H_2SO_4 and $ZnSO_4$ are given in Tables III and IV for the temperatures 20.0, 25.0, 30.0 and 40.0°C. Values obtained at the various temperatures for H_2SO_4 and $ZnSO_4$ are plotted in Figures 10 and 11 respectively against the values obtained at 17.5°C from the Landolt-Bornstein tables. Figure 12 gives the variation of refractive index with temperature for various concentrations of $ZnSO_4$ and H_2SO_4.

TABLE II - REFRACTIVE INDEX OF WATER

$T^{0}C$	μ_D (Measured)	μ_D (Reference Values)	
20.0	1.33295	1.33299 (10)	1.33300 (11)
24.0		1.33262	
25.0	1.33246		1.33248
26.0		1.33241	
30.0	1.33189	1.33192	1.33194
40.0	1.33057	1.33051	

TABLE III - REFRACTIVE INDEX OF H_2SO_4 (Measured)

Molarity	μ_D^{20}	μ_D^{25}	μ_D^{30}	μ_D^{40}
0.052	1.33361	1.33316	1.33255	1.33123
0.104	1.33425	1.33376	1.33317	1.33173
0.261	1.33599	1.33546	1.33479	1.33337
0.521	1.33878	1.33819	1.33747	1.33599
0.782	1.34164	1.34096	1.34019	1.33856
1.042	1.34438	1.34365	1.34278	1.34110
1.675	1.35088	1.34995	1.34893	1.34706

TABLE IV - REFRACTIVE INDEX OF $ZnSO_4$ (Measured)

Molarity	μ_D^{20}	μ_D^{25}	μ_D^{30}	μ_D^{40}
0.009	1.33322	1.33274	1.33220	1.33088
0.047	1.33432	1.33388	1.33329	1.33196
0.094	1.33568	1.33518	1.33459	1.33325
0.235	1.33955	1.33900	1.33848	1.33711
0.469	1.34581	1.34528	1.34462	1.34324
0.704	1.35178	1.35124	1.35056	1.34914
0.938	1.35774	1.35701	1.35636	1.35485
0.774		1.32397		
1.027		1.35896		

TABLE V - REFRACTIVE INDEX OF $ZnSO_4 + H_2SO_4$ (Measured)

H_2SO_4 Molarity	$ZnSO_4$ Molarity	μ_D^{25}	μ_D^{40}
0.10	0.01	1.33392	1.33200
"	0.05	1.33498	1.33298
"	0.10	1.33626	1.33428
"	0.25	1.34021	1.33814
"	0.50	1.34662	1.34456
"	0.75	1.35277	1.35066
0.50	0.01	1.33819	1.33599
"	0.05	1.33920	1.33699
"	0.10	1.24031	1.33805
"	0.25	1.34402	1.34158
"	0.50	1.34990	1.34743
"	0.75	1.35601	1.35347

TABLE VI - REFRACTIVE INDEX OF H_2SO_4 + $ZnSO_4$ (Measured)

Molarity H_2SO_4 M	Molarity $ZnSO_4$ M	μ_D^{20}	μ_D^{25}	μ_D^{30}	μ_D^{40}
$[SO_4^=] = 0.100M$					
0.025	0.075	1.33549	1.33495	1.33436	1.33299
0.050	0.050	1.33501	1.33448	1.33390	1,33256
0.075	0.025	1.33456	1.33407	1.33348	1.33208
$[SO_4^=] = 0.250M$					
0.025	0.225	1.33954	1.33895	1.33835	1.33702
0.050	0.200	1.33909	1.33854	1.33790	1.33657
0.125	0.125	1.33783	1.33728	1.33661	1.33525
0.200	0.050	1.33661	1.33607	1.33543	1.33401
0.225	0.025	1.33623	1.33574	1.33507	1.33361
$[SO_4^=] = 0.50M$					
0.050	0.450	1.34566	1.34504	1.34440	1.34297
0.100	0.400	1.34468	1.34411	1.34337	1.34196
0.150	0.350	1.34400	1.34335	1.34262	1.34109
0.250	0.250	1.34233	1.34164	1.34104	1.33945
0.350	0.150	1.34063	1.34004	1.33927	1.33773
0.400	0.100	1.33993	1.33925	1.33861	1.33704
0.450	0.050	1.33923	1.33868	1.33796	1.33644
$[SO_4^=] = 0.75M$					
0.050	0.700	1.35196	1.35138	1.35070	1.34919
0.150	0.600	1.35049	1.34982	1.34914	1.34757
0.250	0.500	1.34863	1.34801	1.34726	1.32570
0.350	0.400	1.34700	1.34634	1.34568	1.34391
0.420	0.330	1.34589	1.34536	1.34441	1.34279
0.500	0.250	1.34470	1.34402	1.34335	1.34158
0.660	0.150	1.34340	1.34259	1.34181	1.34013
0.650	0.100	1.34260	1.34186	1.34111	1.33955
0.700	0.050	1.34189	1.34138	1.34049	1.33883

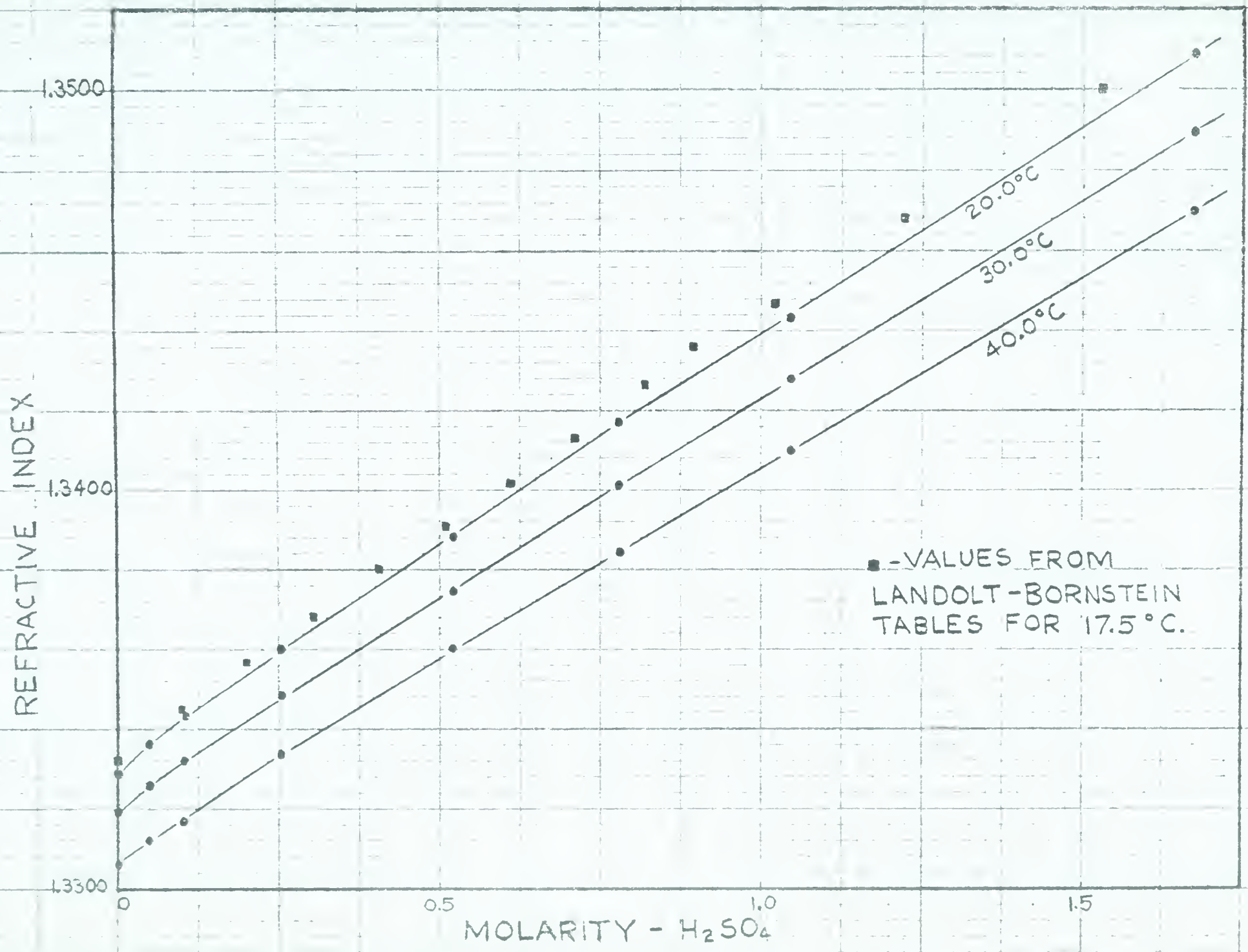

FIG.10 - REFRACTIVE INDEX OF H_2SO_4.

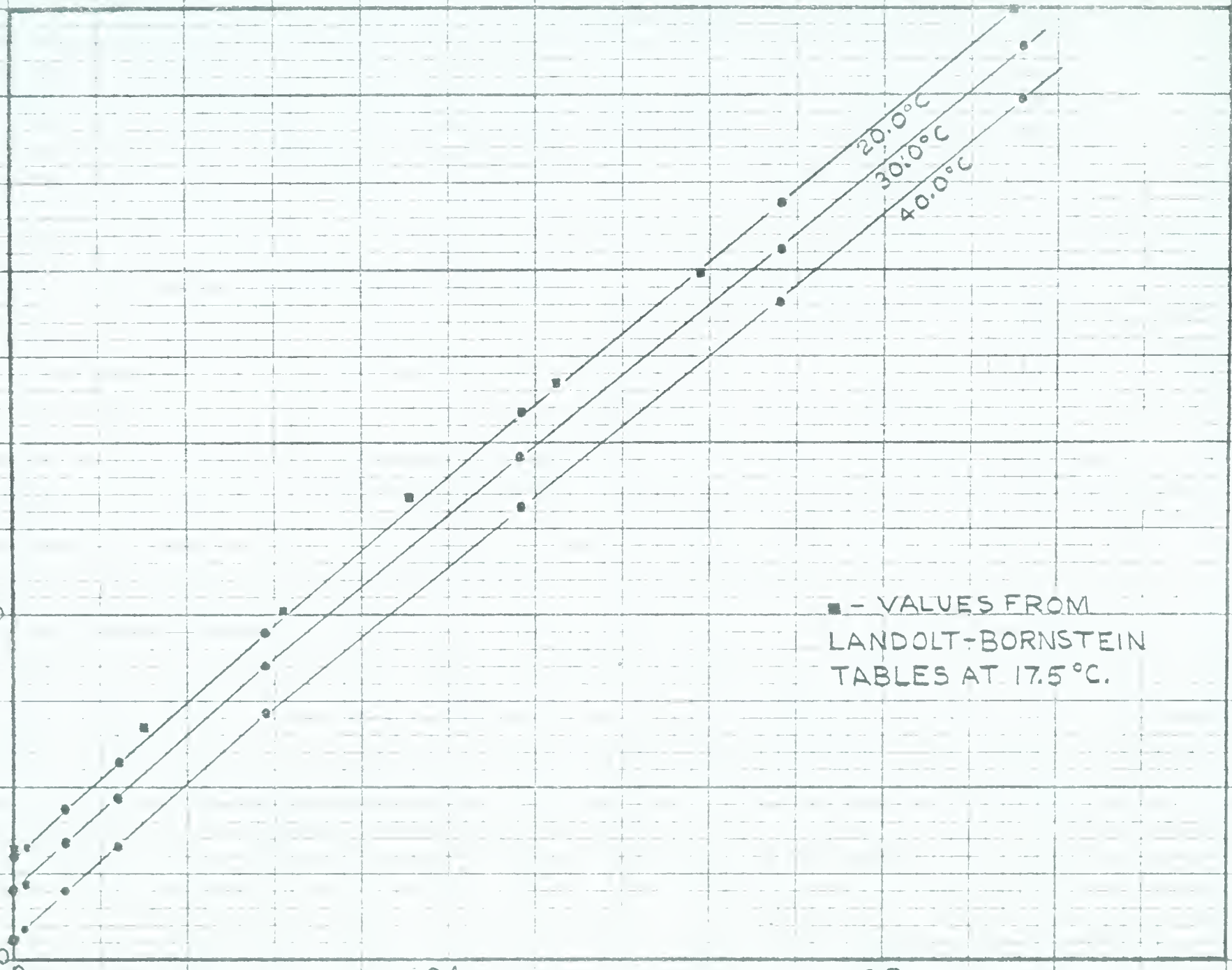

FIG. 11 — REFRACTIVE INDEX OF $ZnSO_4$.

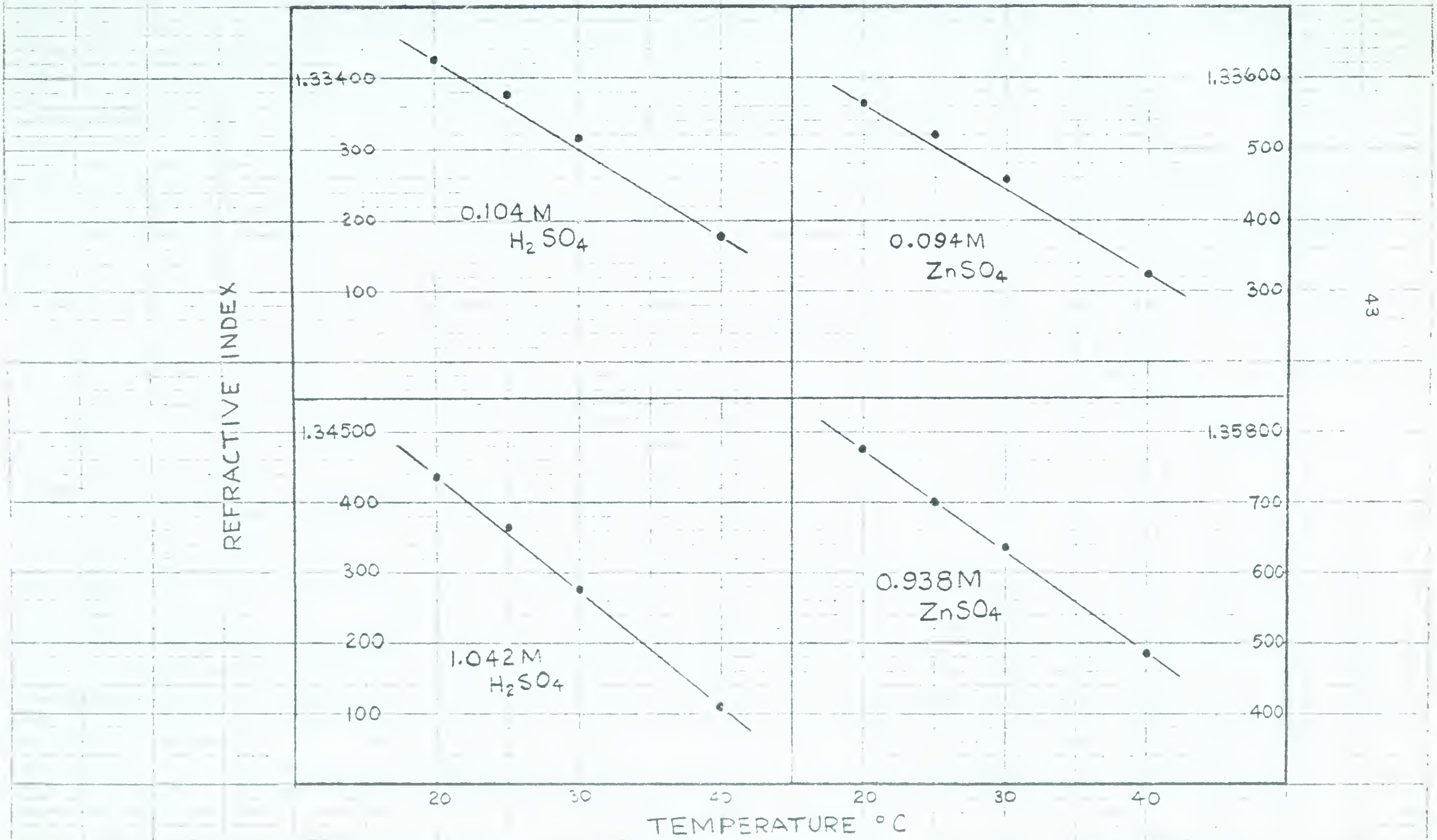

FIG. 12 - VARIATION OF REFRACTIVE INDEX WITH TEMPERATURE.

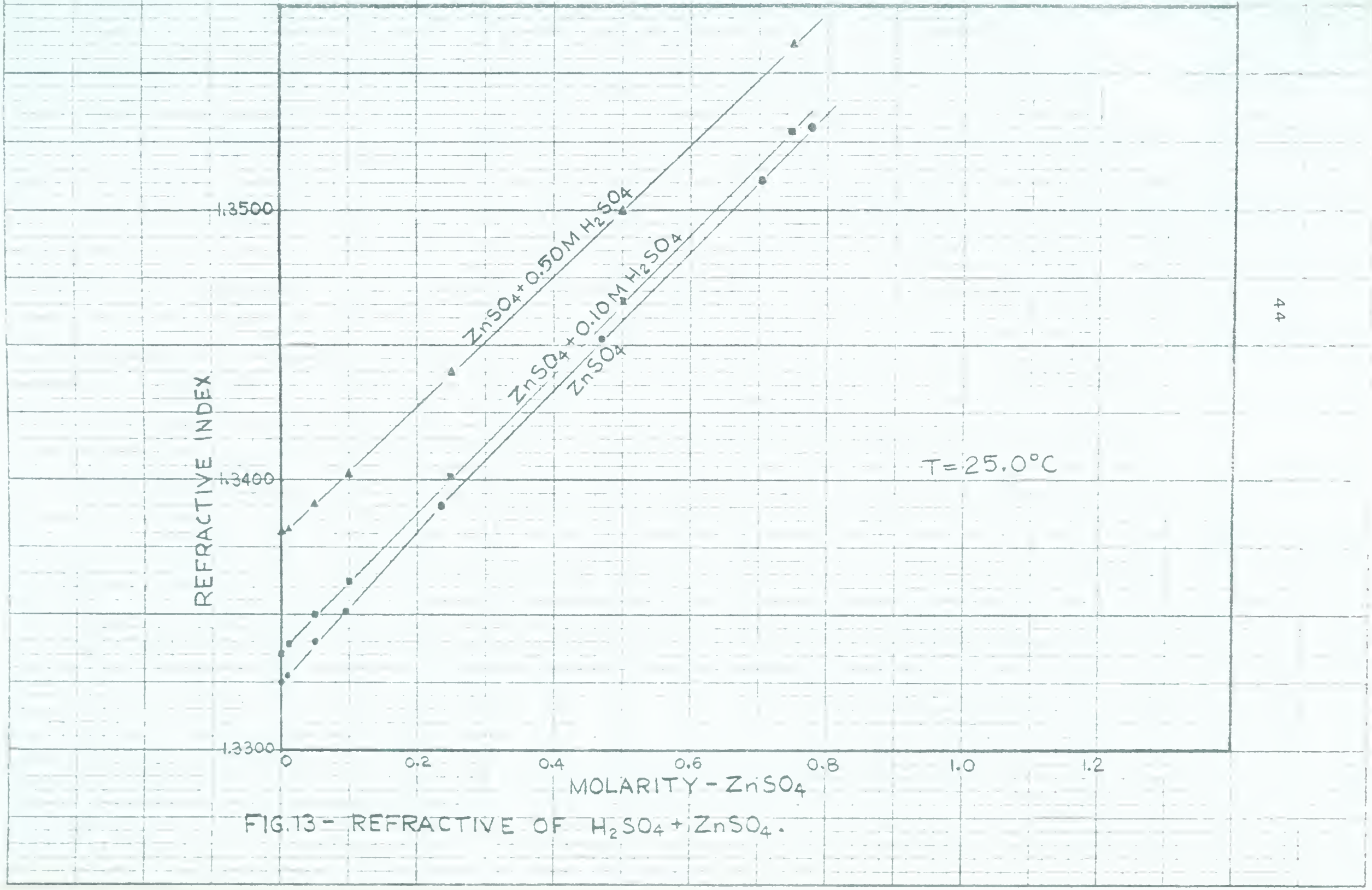

FIG.13 - REFRACTIVE OF $H_2SO_4 + ZnSO_4$.

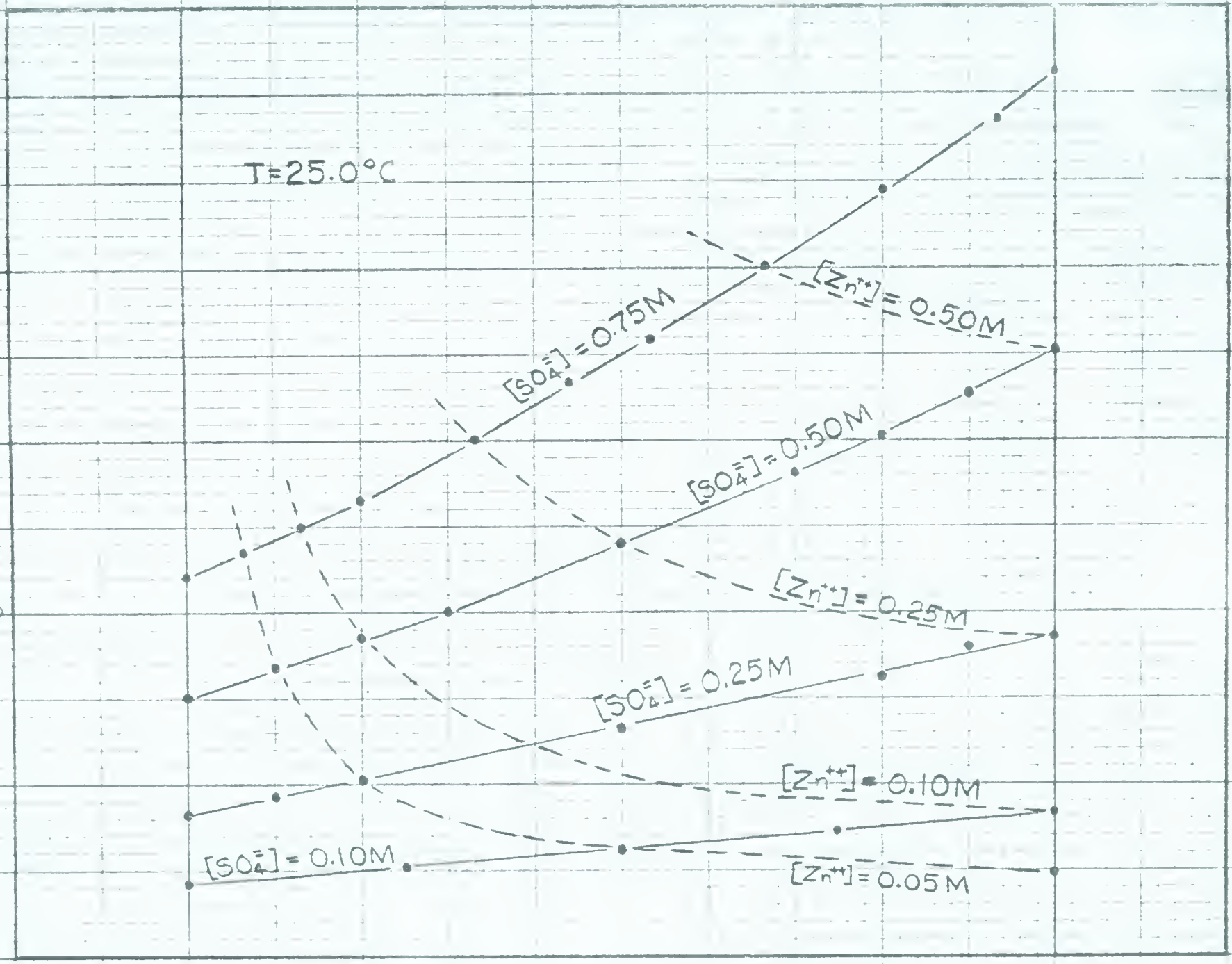

FIG. 14 - REFRACTIVE INDEX OF $H_2SO_4 + ZnSO_4$.

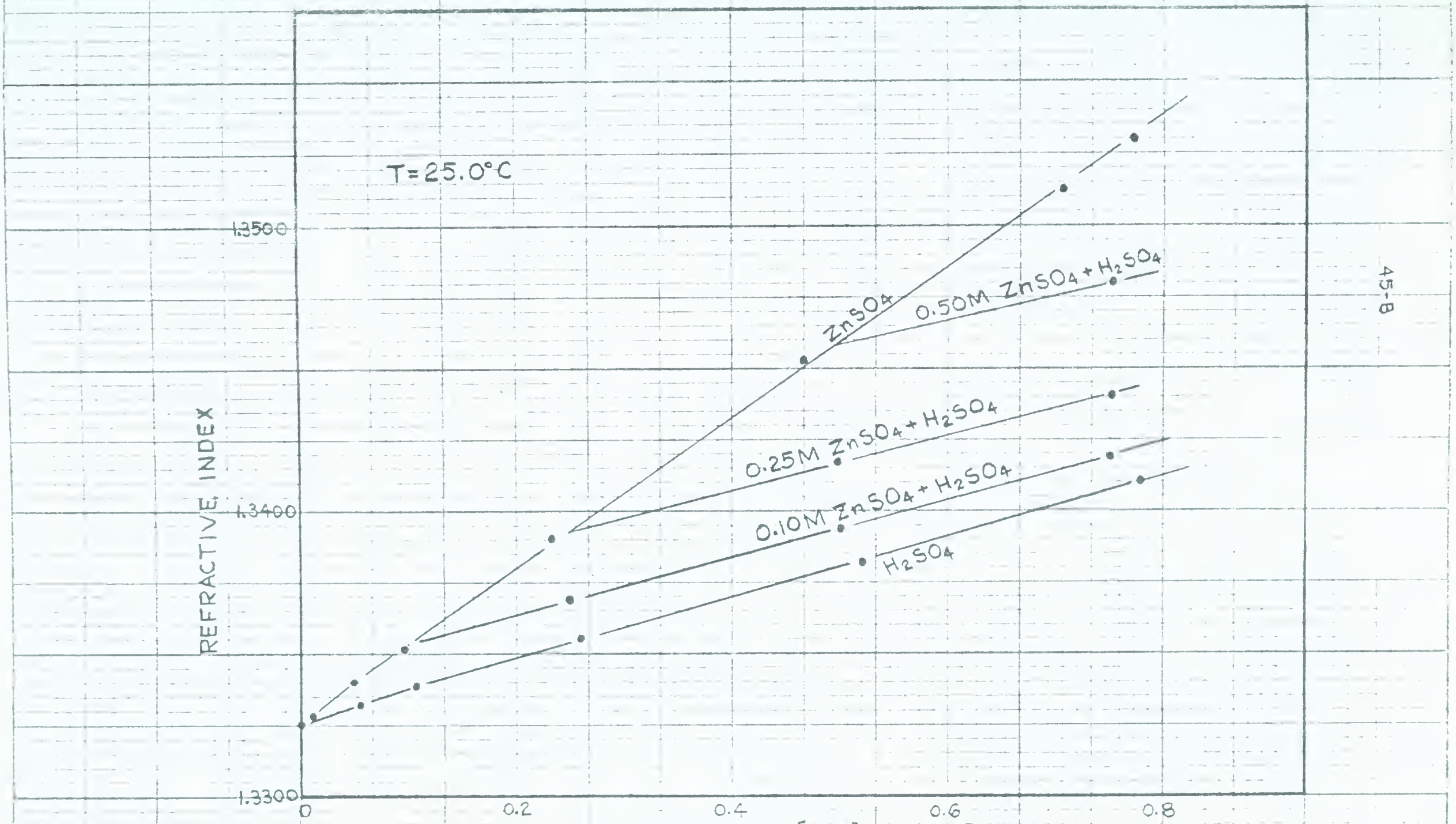

FIG. 15 - REFRACTIVE INDEX OF $ZnSO_4 + H_2SO_4$.

TablesV and VI give the variation of refractive index with concentration of mixtures of H_2SO_4 and $ZnSO_4$. In Table V the concentration of H_2SO_4 is kept constant while the concentration of $ZnSO_4$ is varied. In Table VI the concentration of both H_2SO_4 and $ZnSO_4$ is varied in such a way that the $SO_4^=$ concentration remains constant at values of 0.1, 0.25, 0.50 and 0.75 molar. Figure 13 is a plot of the data in Table V at 25.0°C. Figure 14 shows a plot of the data given in Table VI at 25.0°C. Points which have the same $ZnSO_4$ concentration are indicated by the broken lines. These broken lines are replotted against $SO_4^=$ concentration in Figure 15.

B. INTERFEROMETER STUDIES

Tha apparatus was originally designed so that both fringes of equal thickness and equal inclination could be obtained. The results obtained by the two systems of fringes could then be compared. However, after a few trials it was found that photographs of fringes of equal inclination could not be obtained easily, therefore, all work was carried out using fringes of equal thickness. It was also found that fringes produced by transmission photographed with more contrast than those produced by reflection. The most probable reason for this is that less stray light is picked up by the camera when the fringes are produced by transmission because the lens can be placed within 1/4" of the top of the cell.

The best results were obtained when a 90% reflecting coating was used on the bottom glass flat and a 70% reflecting coating on the top flat and a distance of 2.10 mm. between the glass flats.

FRINGES PRODUCED BY TEMPERATURES GRADIENTS

A special electrode, through which ethanol cooled with dry ice could be passed, was made from copper. Photographs (a) and (b) in Fig. 1 show the fringe patterns developed when ice is formed on the electrode face. Photographs (c) and (d) show the fringe patterns formed by cooling 0.10 M $ZnSO_4$ at an electrode face and by passing a direct current through 0.01 M $ZnSO_4$. It can be seen that the fringe shift at the anode is in the same direction as that at the electrode which is cooled (indicated as the anode in the photograph), thereby showing that the fringe shift at the anode is in the direction of increasing concentration. The wedge angle is in the same direction for both photographs (c) and (d).

VOLTAGE - CURRENT DENSITY CURVES

Early experiments showed that a white precipitate was formed on the glass when current was passed through the $ZnSO_4$ electrolyte at current densities greater than 5 m.a./cm^2. This caused the fringes to become blurred so that they could no longer be photographed. The precipitate adhering to the reflecting coatings on the glass flats was soluble in either dilute HNO_3 or H_2SO_4.

It was found that if the electrodes were coated on all surfaces except the working face with polyurethane the precipitate did not form in any noticeable amount. The electrodes were coated evenly (average thickness of coating was 0.03 mm.) with polyurethane and then placed under an infra-red lamp for 12-18 hours at about 75°C. This coating would usually last for one to two weeks before it would start to peel. When this happened the existing coating was removed with acetone and a fresh coating applied. If 0.1% by weight of epoxy resin hardener was

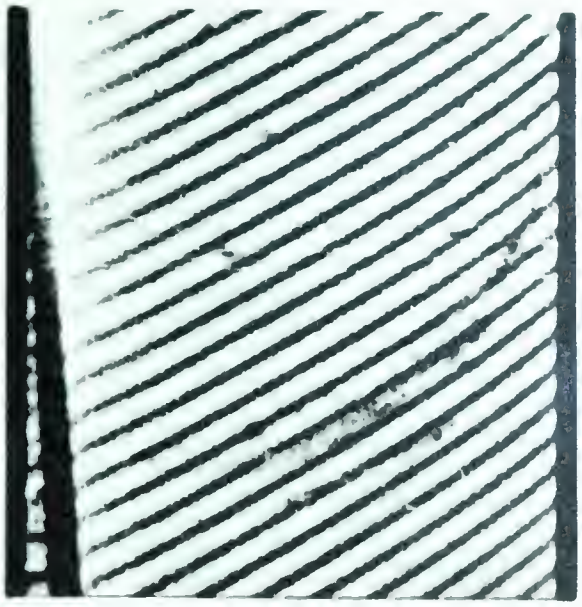

(a) Advancing Ice Interface in Water

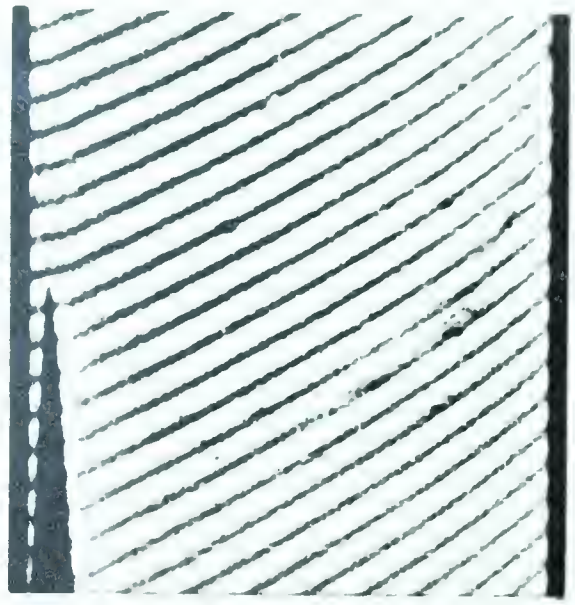

(b) Receding Ice Interface in Water

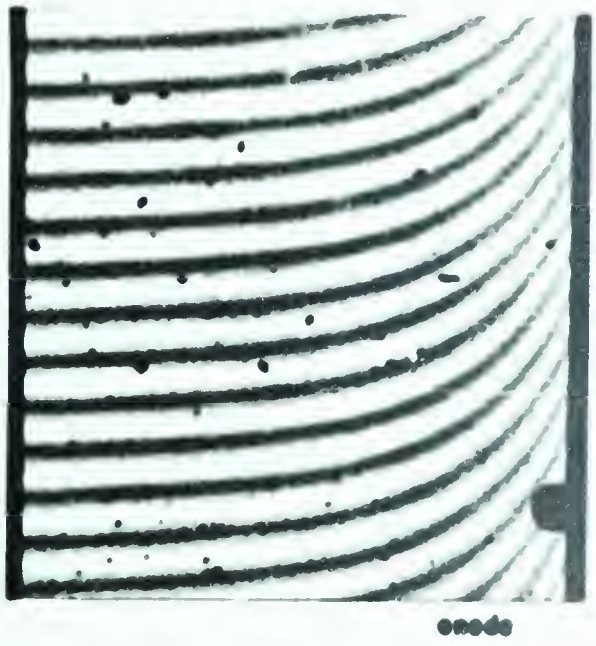

(c) Cooling 0·1M $ZnSO_4$ at anode

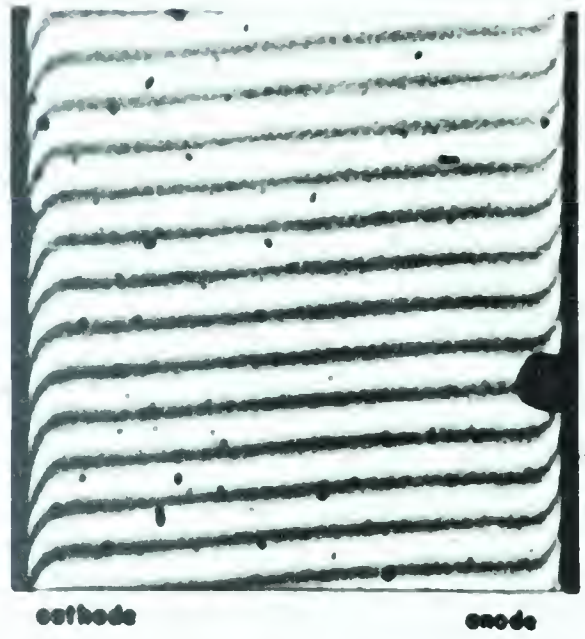

(d) Passage of Direct Current– 0·1M $ZnSO_4$

Fig I FRINGES PRODUCED BY TEMPERATURE GRADIENTS

NORMAL POSITION

added to component A before component B was added a more durable coating of polyurethane was obtained.

The earliest results were obtained, using a voltohmyst obtained from R.C.A. to measure both voltage and current, with a circuit as shown in Fig. 16.

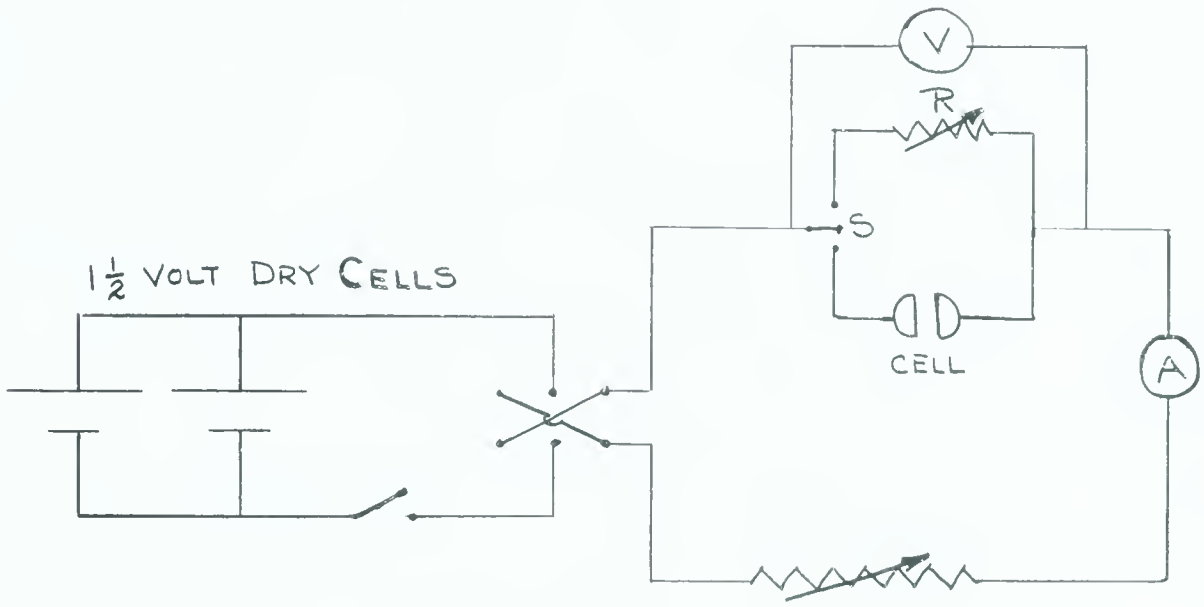

FIG. 16 Wiring Diagram Using Voltohmyst

A switch, S, was arranged such that the current could be passed either through the cell or through the resistance box. A position on the resistance box was found where the voltage drop across the resistance box was the same as that across the cell. This resistance was then taken as the resistance of the cell and the value of the current was obtained by a separate measurement. These readings were taken

three minutes after the current was turned on.

Figure 17 shows the results obtained using this circuit for 0.10 M $ZnSO_4$ at 20.0°C. The poor reproducibility obtained was thought to be due to the method used to obtain the results so the circuit was redesigned using a potentiometer to obtain readings of the potential drop across a known resistance (R) and across the cell (Fig. 18). A calibration of the potentiometer used, against a Cambridge Instruments Co.Ltd. potentiometer No. L-347849 using a Weston Normal Cell No. L-353404 "A", is given in Table VII. An 800 ohm resistance was also calibrated and any other resistance used in the circuit was checked against this resistance.

TABLE VII

CALIBRATION OF PORTABLE POTENTIOMETER

TYPE 3184D NO. 20298

MANUFACTURED BY TINSLEY INSTRUMENTS

CAMBRIDGE INST. (VOLTS)	TINSLEY INST. (VOLTS)
0.07874	0.0787
0.14924	0.1492
0.24814	0.2481
0.35750	0.3575
0.47769	0.4777
0.65300	0.6529
0.95046	0.9505
1.03353	1.0335
1.24972	1.2498
1.57282	1.5731
1.76575	1.7660

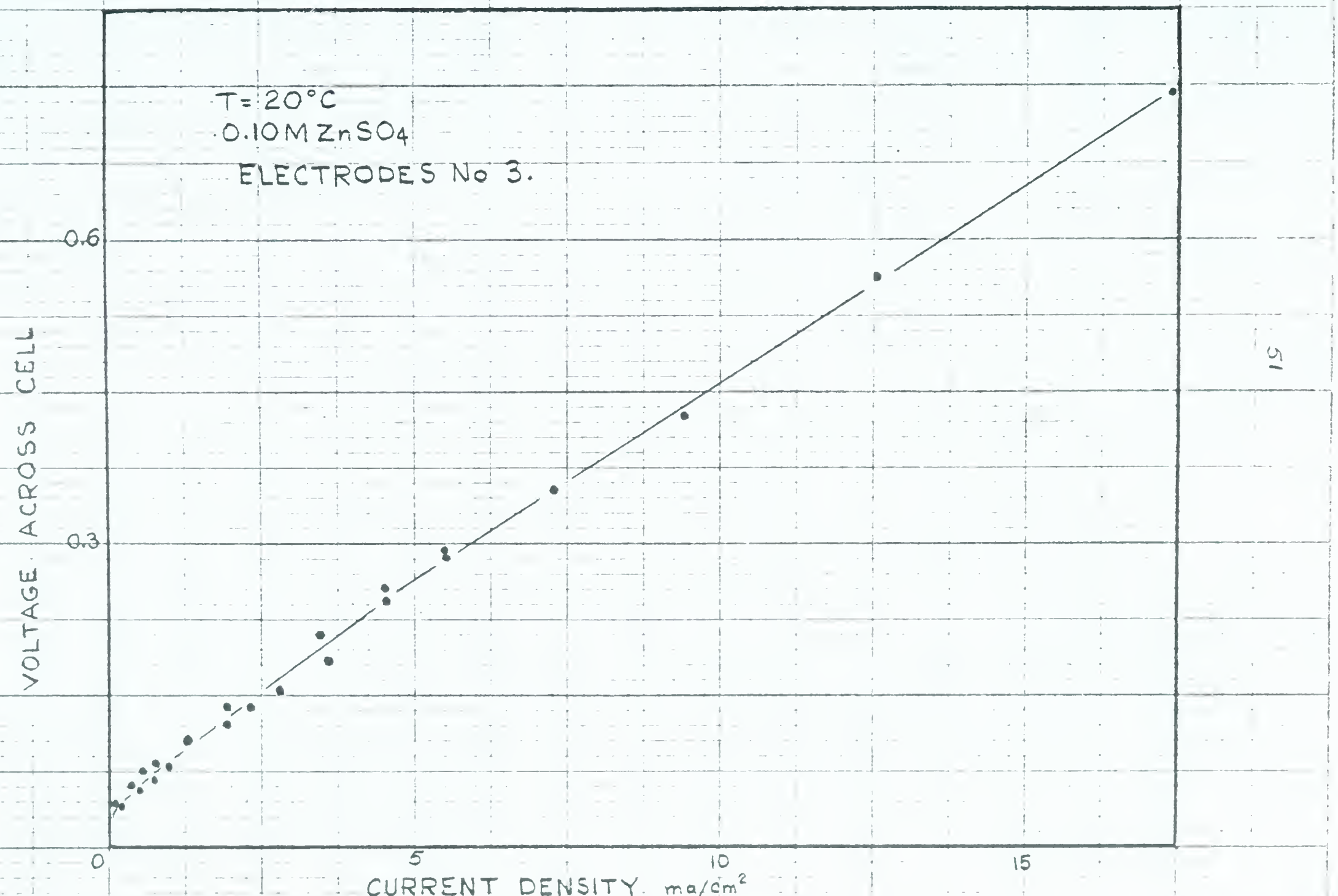

FIG. 17 - MEASUREMENTS MADE WITH VOLTOHMYST.

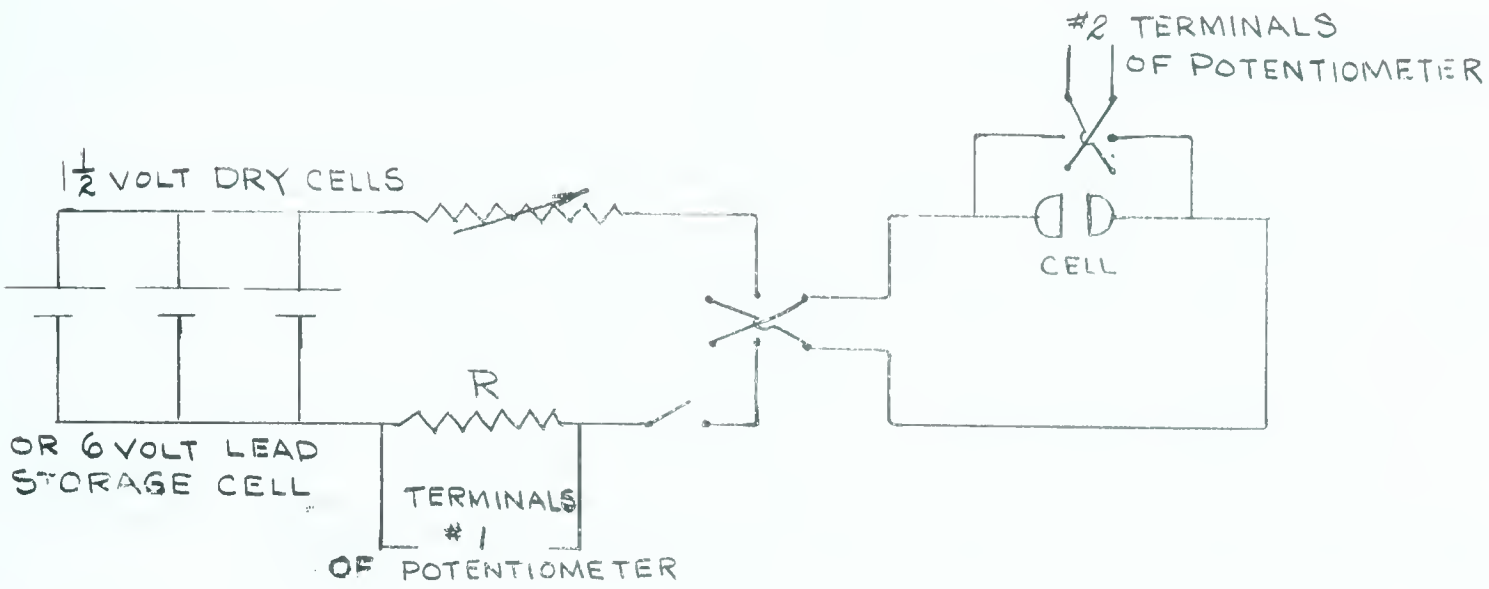

FIG. 18 Wiring Diagram Using Potentiometer

Results were obtained by measuring the potential drop across the known resistance at 2 minutes after the current had been switched on and the potential drop across the cell at 1 and 3 minutes. This was done because it was found that the voltage across the cell varied with time.

Figure 19 illustrates some of the results obtained using the new circuit. As can be seen there is a marked difference in the results obtained for No. 1 and No. 3 electrodes.

During a run fresh solution was injected into the cell at intervals of 4 to 5 points. Readings were taken by passing the current in one direction for one point and then reversing the direction of the flow of current for the next point.

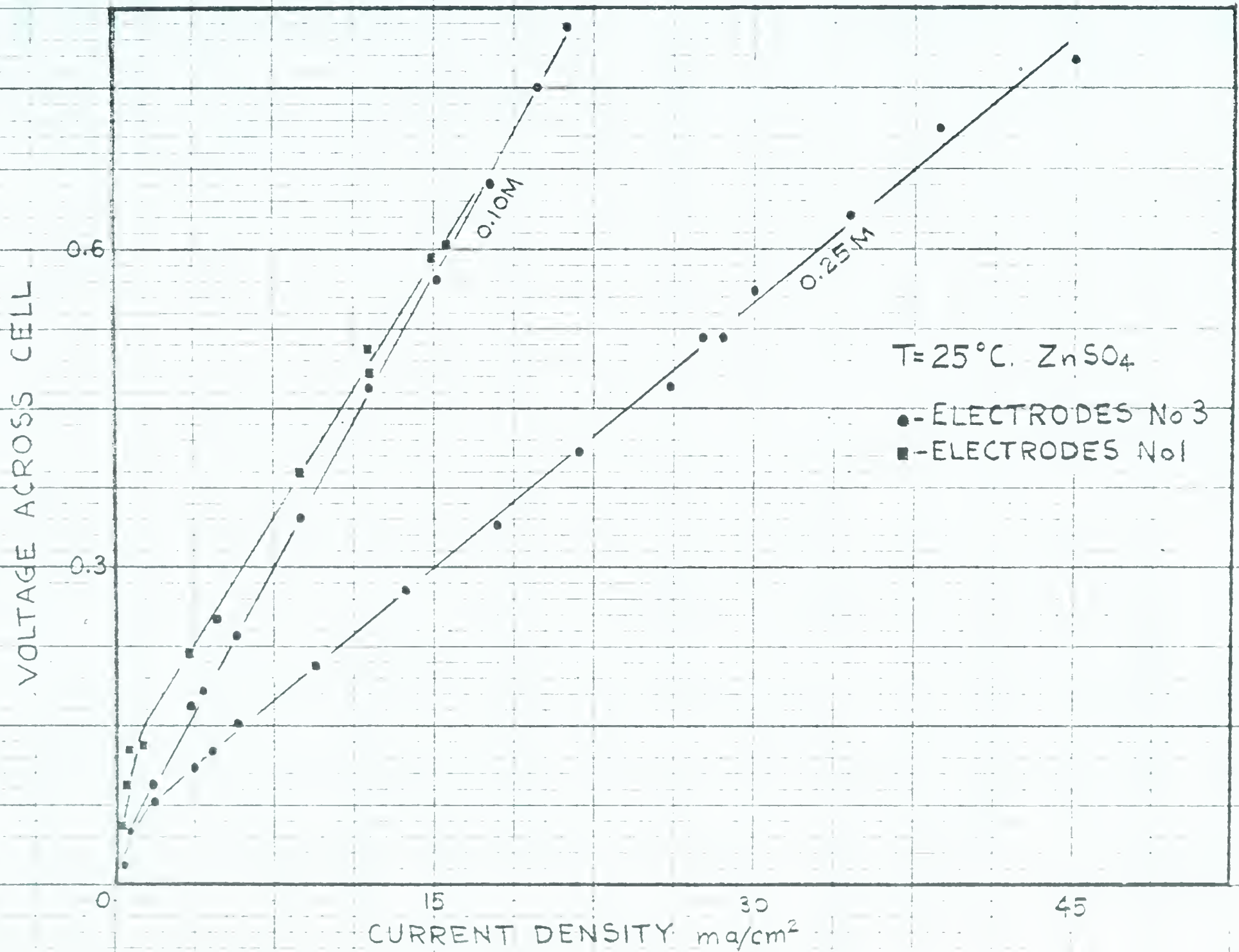

FIG. 19 - EARLY RESULTS USING POTENTIOMETER.

VOLTAGE ACROSS CELL WITH NO IMPOSED CURRENT

One of the first observations made with the new circuit was that a voltage existed between the zinc electrodes even when no current was being imposed. It was first thought that a reaction between the zinc electrodes and the coatings on the glass flats might be occuring. However, this idea was rejected when it was found that the potential existed whether the electrodes were in contact with the glass flats or in a separate beaker of $ZnSO_4$ solution. The value of this potential was usually between ± 5 mv., however values as high as 15 m.v. have been obtained.

Coating of the electrodes with polyurethane did not have any apparent effect on this potential. The value could be reduced to near zero by passing direct current between the electrodes, first in one direction and then in the other, or by passing alternating current for 5 minutes at about one volt. However, if, after obtaining a zero potential, direct current was passed in either direction, the potential across the cell would not return to zero after the current was shut off. It was observed that the time required for this potential to attain a constant value after fresh solution was injected into the cell decreased as the concentration of the $ZnSO_4$ increased.

From these observations it seemed that the potential existing at no impressed current was due to surface effects between the zinc electrodes and the $ZnSO_4$ solution. An attempt was made to measure the voltage difference between the zinc electrodes and the solution by dipping a copper wire into the solution to a distance of about 0 .5 cm. from the

electrode faces. The values obtained are shown in Fig. 20.

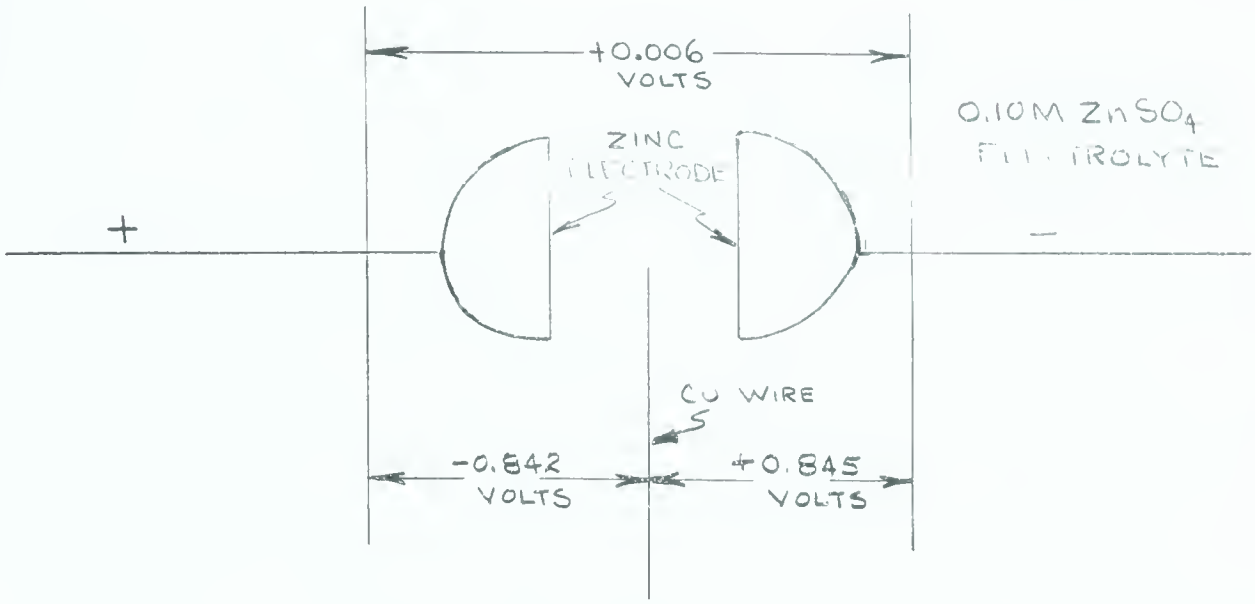

FIG. 20 Voltage Across Cell at no Imposed Current

It was also found that bubbles were formed at the zinc solution interface when no current was passed through the solution. The time required for this to occur in fresh solution was one to two hours if the electrodes were freshly etched and only about 10 minutes if high currents had been previously passed so that a needle-like deposit existed on the electrodes.

It was discovered that if a resistance was placed in parallel with the cell, the voltage across the cell remained quite constant with time while a current was being imposed and the voltage across the cell at no imposed current was practically zero. The highest value recorded was 0.1 m.v. The reproducibility of the voltage-current density curves

for five separate runs obtained in this manner is shown in Figure 21.

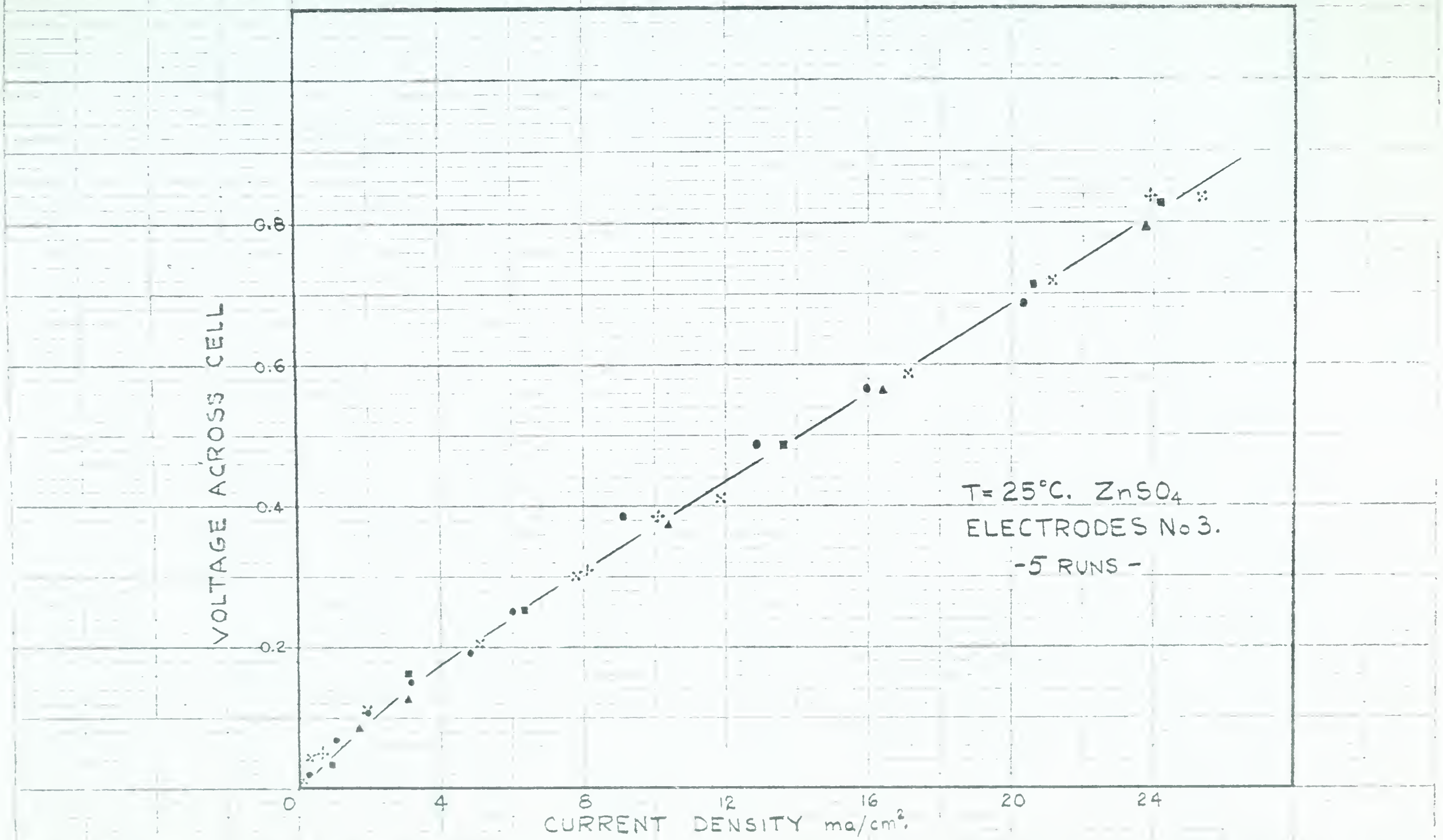

FIG. 21- REPRODUCIBILITY USING A RESISTANCE IN PARALLEL WITH THE CELL.

VOLTAGE TIME CURVES

Since a method, by which reproducible results could be obtained was not found, it was decided to obtain voltage-time curves at each current density for various concentrations of $ZnSO_4$. Four runs were carried out for each current density, using fresh solution for each run and reversing the direction of the current after each run. Fig. 22 indicates the type of reproducibility obtained for the various concentrations at relatively low current densities. The reproducibility becomes worse as the current density is increased. Fig. 23 and 24 indicate the type of voltage-time curves obtained at various current densities for each concentration of $ZnSO_4$ used.

Due to the variation in the shape of the curves it was decided to use the average of the first points (usually obtained 5-10 seconds after the current was switched on) to be used as the value of the voltage for the corresponding current density. Table VIII gives the results obtained in this way for water and various concentrations of $ZnSO_4$. The results given in Table VIII are plotted in Fig. 25 and 26. As can be seen in Fig. 25 the points obtained for 0.010 M $ZnSO_4$ are scattered. It was found that at this concentration metallic zinc was plated out on the glass flats at voltages greater than 0.5. It was also noted that the fringe patterns in 0.001 M $ZnSO_4$ became distorted at the cathode at voltages greater than 0.3 volts. It is felt that this effect in 0.001 M $ZnSO_4$ may be connected with the formation of bubbles which were observed at the cathode at these voltages.

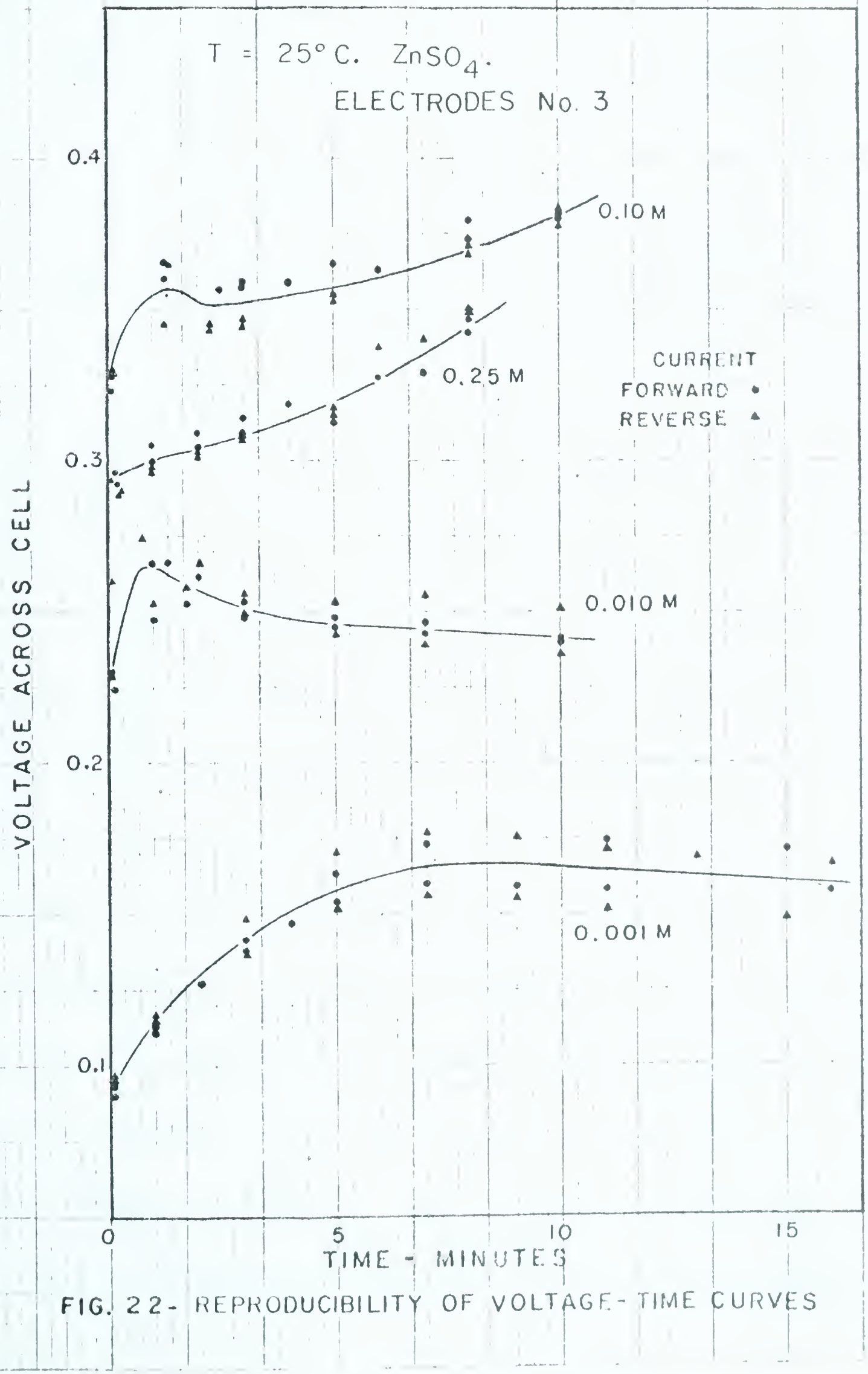

FIG. 22- REPRODUCIBILITY OF VOLTAGE-TIME CURVES

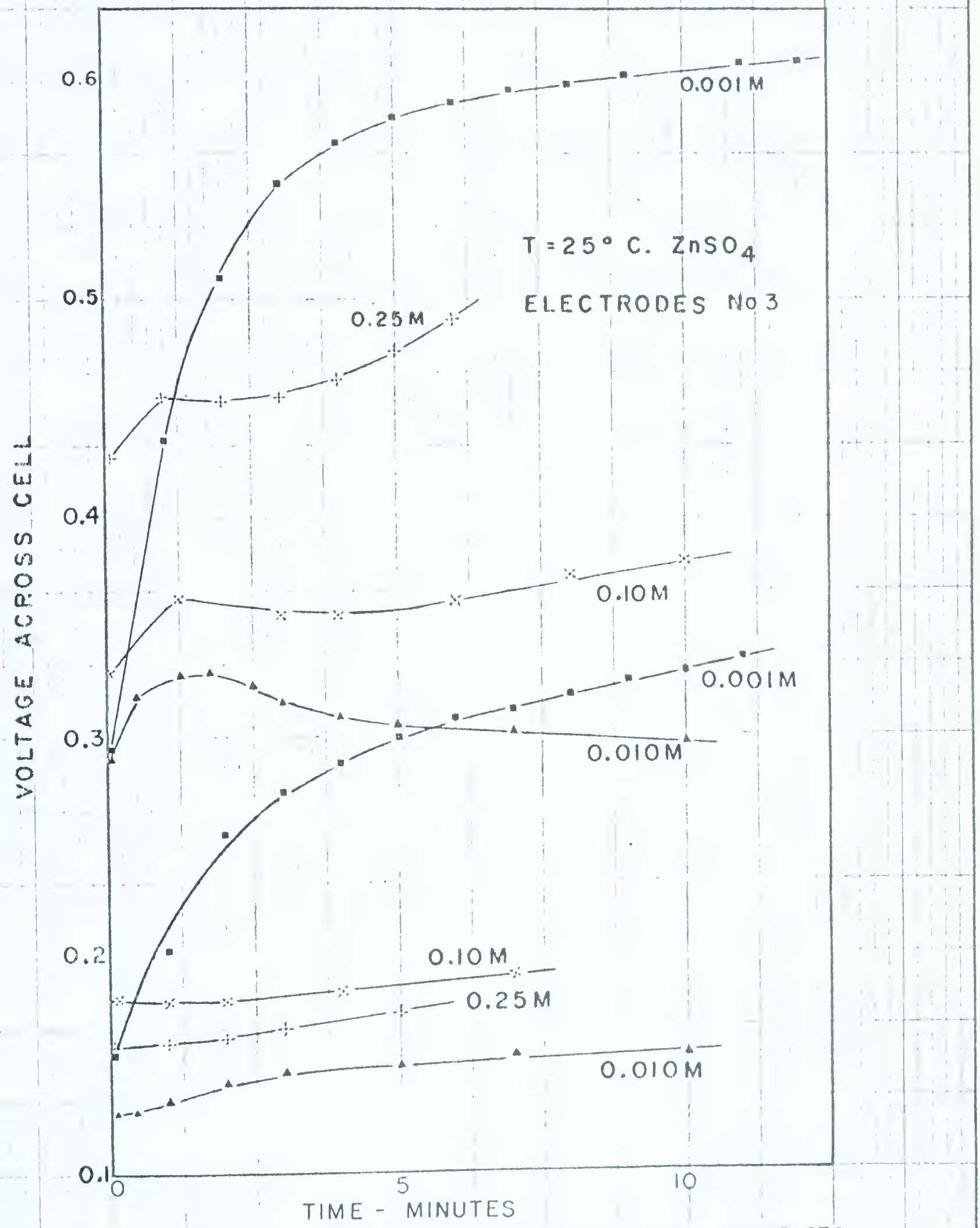

FIG. 23- VARIATION OF VOLTAGE WITH TIME - LOW VOLTAGES

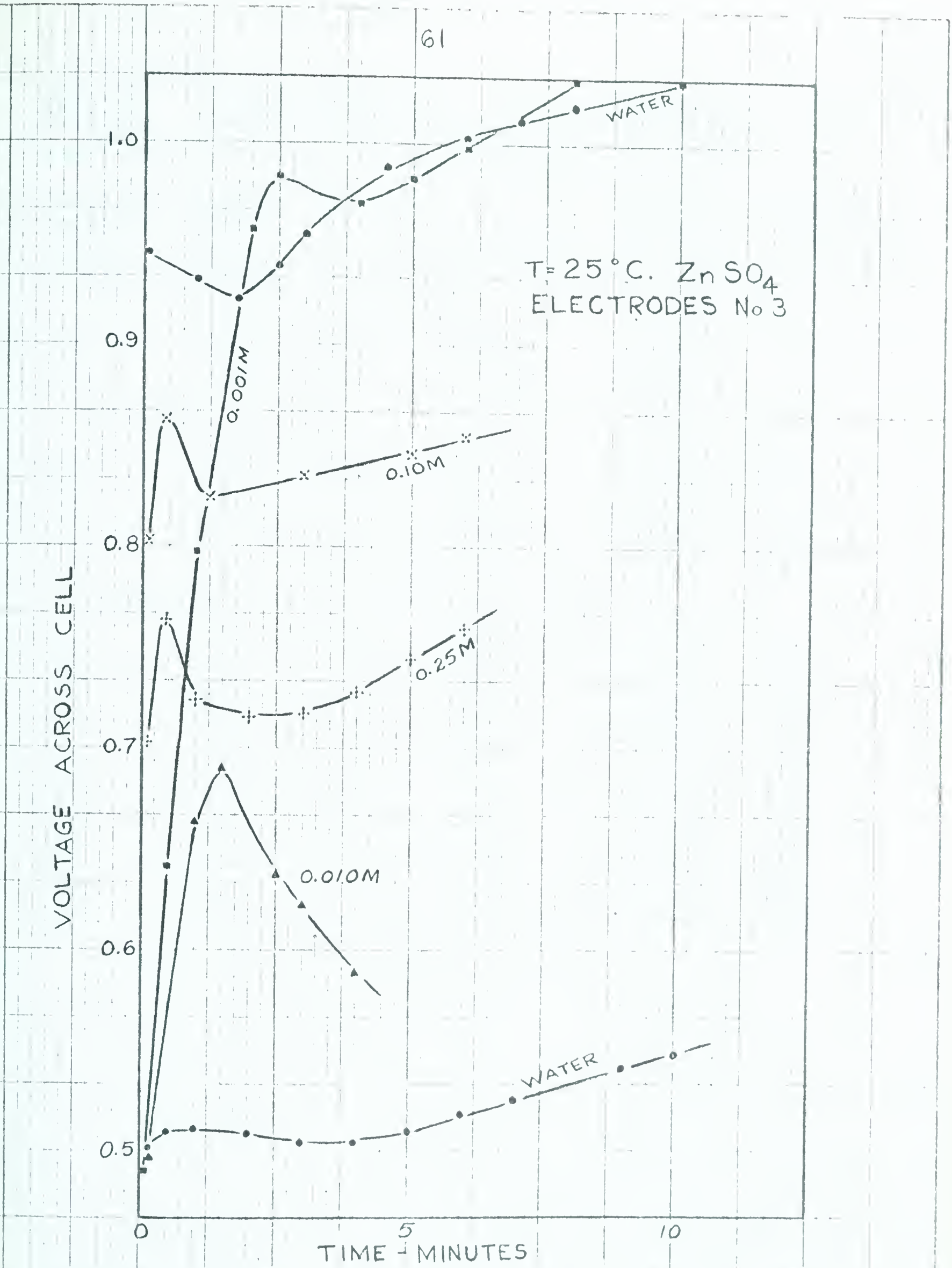

FIG. 24 - VARIATION OF VOLTAGE WITH TIME - HIGH VOLT.

TABLE VIII - VOLTAGE-CURRENT DENSITY RESULTS IN NORMAL POSITION

ELECTRODE SET NO. 3, AREA = 0.4897 cm^2, T = 25.0°C

VOLTAGE ACROSS CELL VOLTS	CURRENT DENSITY ma/cm^2	DIST. BET. ELECTRODES cm	RESISTIVITY ohm cm.	SPECIFIC CONDUCTIVITY $mho\ cm^{-1}$	EQUIVALENT CONDUCTIVITY
A - DOUBLY-DISTILLED AND BOILED WATER					
0.499	0.0137	0.322	113,000	$8.85x10^{-6}$	
0.950	0.0251	0.322	117,000	$8.55x10^{-6}$	
B - 0.001 M $ZnSO_4$					
0.093	0.080	0.307	3730	$2.68x10^{-4}$	134
0.154	0.123	0.307	4100	$2.44x10^{-4}$	122
0.296	0.235	0.307	4100	$2.44x10^{-4}$	122
0.480	0.374	0.307	4180	$2.39x10^{-4}$	120
C - 0.010 M $ZnSO_4$					
0.046	0.112	0.297	1380	$0.72x10^{-3}$	36.0
0.076	0.111	0.297	2280	$0.44x10^{-3}$	22.0
0.137	0.346	0.297	1330	$0.75x10^{-3}$	37.5
0.235	0.798	0.297	991	$1.01x10^{-3}$	50.5
0.290	1.117	0.297	874	$1.14x10^{-3}$	57.0
0.427	1.393	0.297	1030	$0.97x10^{-3}$	48.5
0.488	1.958	0.297	839	$1.17x10^{-3}$	59.5
0.537	2.211	0.297	818	$1.22x10^{-3}$	61.0
0.699	3.510	0.297	669	$1.49x10^{-3}$	74.5

TABLE VIII - Cont.

VOLTAGE ACROSS CELL VOLTS	CURRENT DENSITY ma/cm^2	DIST. BET. ELECTRODES cm	RESISTIVITY ohm cm.	SPECIFIC CONDUCTIVITY $mho\ cm^{-1}$	EQUIVALENT CONDUCTIVITY
D. 0.10 M $ZnSO_4$, pH = 6.0					
0.020	0.125	0.298	553	$1.81x10^{-3}$	9.05
0.041	0.492	"	286	$3.50x10^{-3}$	17.5
0.075	1.229	"	206	$4.85x10^{-3}$	24.3
0.116	2.555	"	153	$6.54x10^{-3}$	32.7
0.175	4.682	"	131	$7.63x10^{-3}$	38.2
0.327	9.203	"	119	$8.40x10^{-3}$	42.0
0.473	13.82	"	114	$8.77x10^{-3}$	43.9
0.636	19.15	"	110	$9.09x10^{-3}$	45.5
0.802	24.95	"	105	$9.52x10^{-3}$	47.6
E. 0.25 M $ZnSO_4$, pH = 5.6					
0.014	0.210	0.297	232	$4.31x10^{-3}$	8.62
0.023	0.506	"	156	$6.41x10^{-3}$	12.8
0.047	1.744	"	92.3	$10.8x10^{-3}$	21.6
0.082	3.974	"	70.5	$14.2x10^{-3}$	28.4
0.143	8.758	"	60.0	$16.7x10^{-3}$	33.4
0.292	17.20	"	58.0	$17.2x10^{-3}$	34.4
0.424	26.44	"	53.7	$18.6x10^{-3}$	37.2
0.579	36.67	"	52.2	$19.2x10^{-3}$	38.4
0.699	44.82	"	50.7	$19.7x10^{-3}$	39.4
0.823	61.97	"	52.0	$19.2x10^{-3}$	38.4
F. 0.25 M $ZnSO_4$ + 1.00 M Na_2SO_4					
0.022	0.355	0.307	211	$0.47x10^{-2}$	
0.037	1.233	"	98.3	$1.02x10^{-2}$	
0.045	2.022	"	71.6	$1.40x10^{-2}$	
0.060	3.984	"	49.1	$2.02x10^{-2}$	
0.118	12.36	"	31.1	$3.22x10^{-2}$	
0.132	17.74	"	24.2	$4.13x10^{-2}$	
0.188	24.77	"	24.6	$4.07x10^{-2}$	

TABLE VIII - Cont.

VOLTAGE ACROSS CELL VOLTS	CURRENT DENSITY ma/cm^2	DIST. BET. ELECTRODES cm	RESISTIVITY ohm cm	SPECIFIC CONDUCTIVITY mho cm^{-1}	EQUIVALENT CONDUCTIVITY
G - 0.10M $ZnSO_4$ + H_2SO_4 pH = 3.5					
0.080	0.352	0.323	702	1.42×10^{-3}	7.1
0.115	0.607	"	584	1.71×10^{-3}	8.6
0.144	1.199	"	371	2.70×10^{-3}	13.5
0.165	1.977	"	257	3.89×10^{-3}	19.5
0.223	2.857	"	186	5.38×10^{-3}	26.9
0.302	7.424	"	126	7.94×10^{-3}	39.7
0.412	11.72	"	109	9.17×10^{-3}	45.9
0.552	16.44	"	104	9.62×10^{-3}	48.1
0.744	22.43	"	102	9.80×10^{-3}	49.0
H - 0.10 M $ZnSO_4$, ELECTRODES No. 4, AREA = 0.8758 cm^2					
0.047	0.692	0.324	210	4.76×10^{-3}	23.8
0.061	1.130	"	166	6.02×10^{-3}	30.1
0,141	3.262	"	134	7.46×10^{-3}	37.3
0.242	6.140	"	122	8.20×10^{-3}	41.0
0.413	11.06	"	114	8.77×10^{-3}	43.9
0.594	16.25	"	111	9.01×10^{-3}	45.1

TABLE IX - VOLTAGE-CURRENT DENSITY RESULTS FOR COMPARISON PURPOSES

CONC.	VOLTAGE	CURRENT DENSITY	EQUIVALENT CONDUCTIVITY
0.001 M	0.300	0.24	124
0.010 M	"	1.17	58.0
0.10 M	"	8.52	42.4
0.25 M	"	18.1	35.8

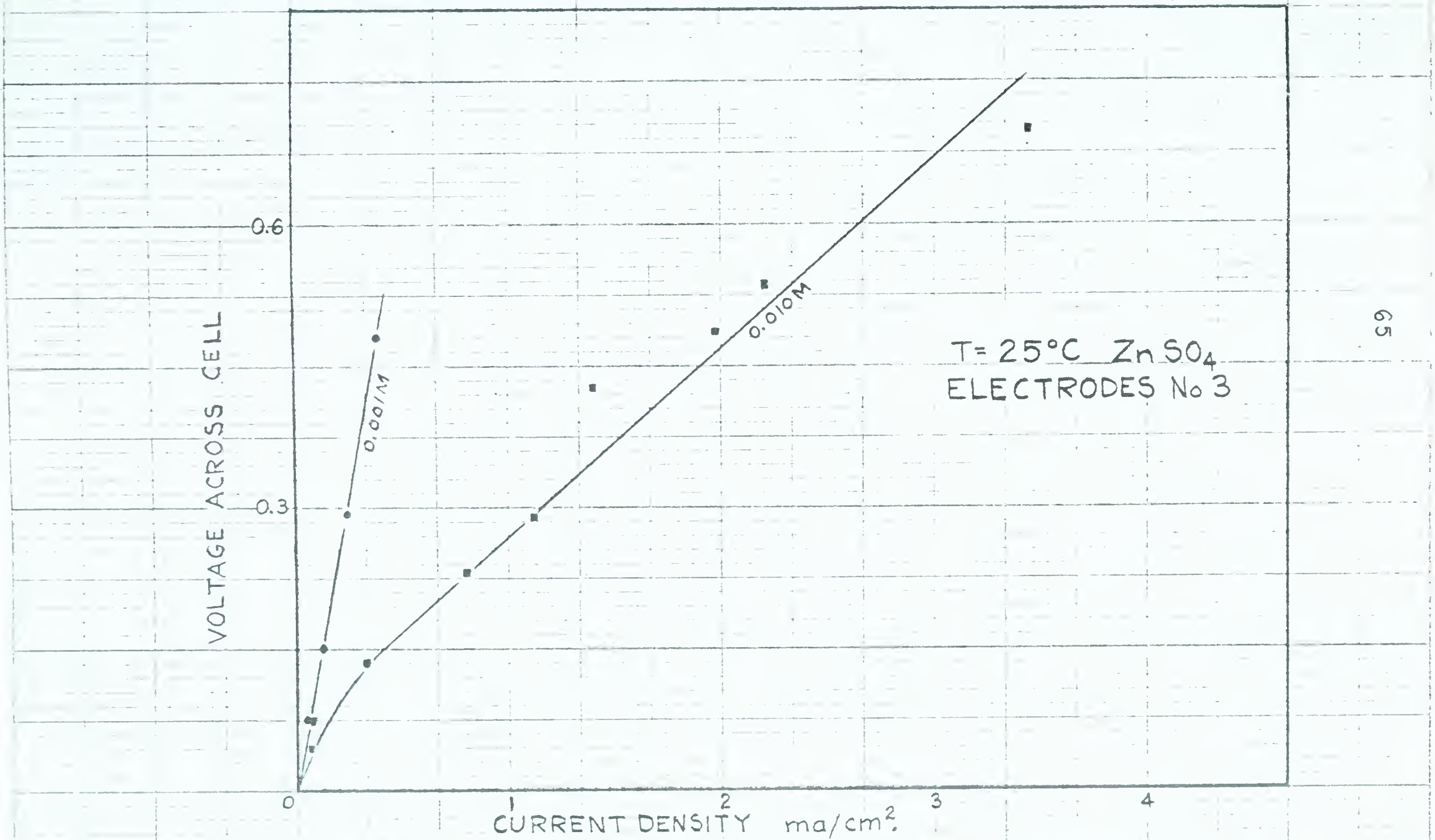

FIG. 25 - VOLTAGE - CURRENT DENSITY CURVES. LOW CONCENTRATIONS.

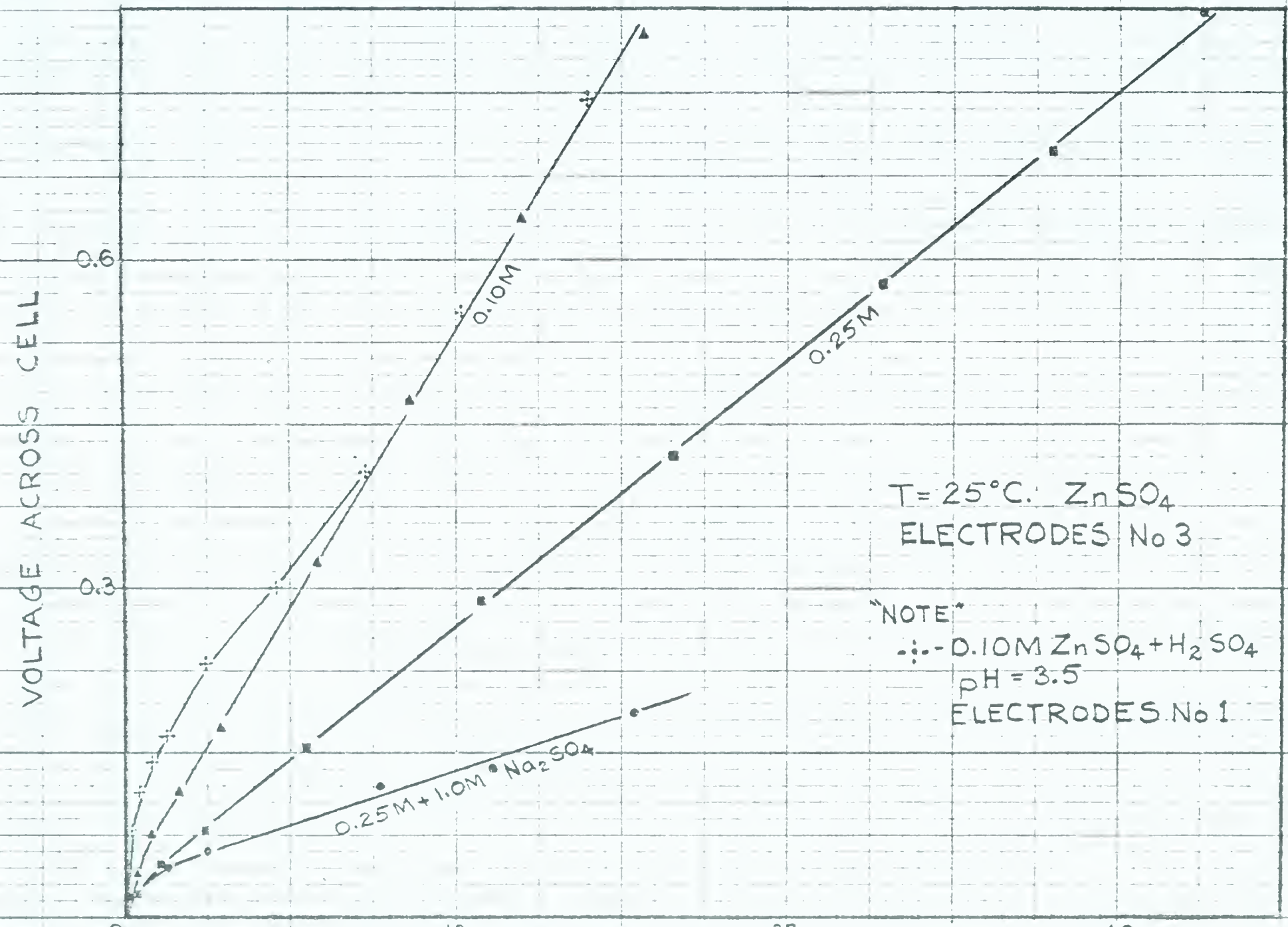

FIG. 26 - VOLTAGE - CURRENT DENSITY CURVES. HIGHER CONCENTRATIONS.

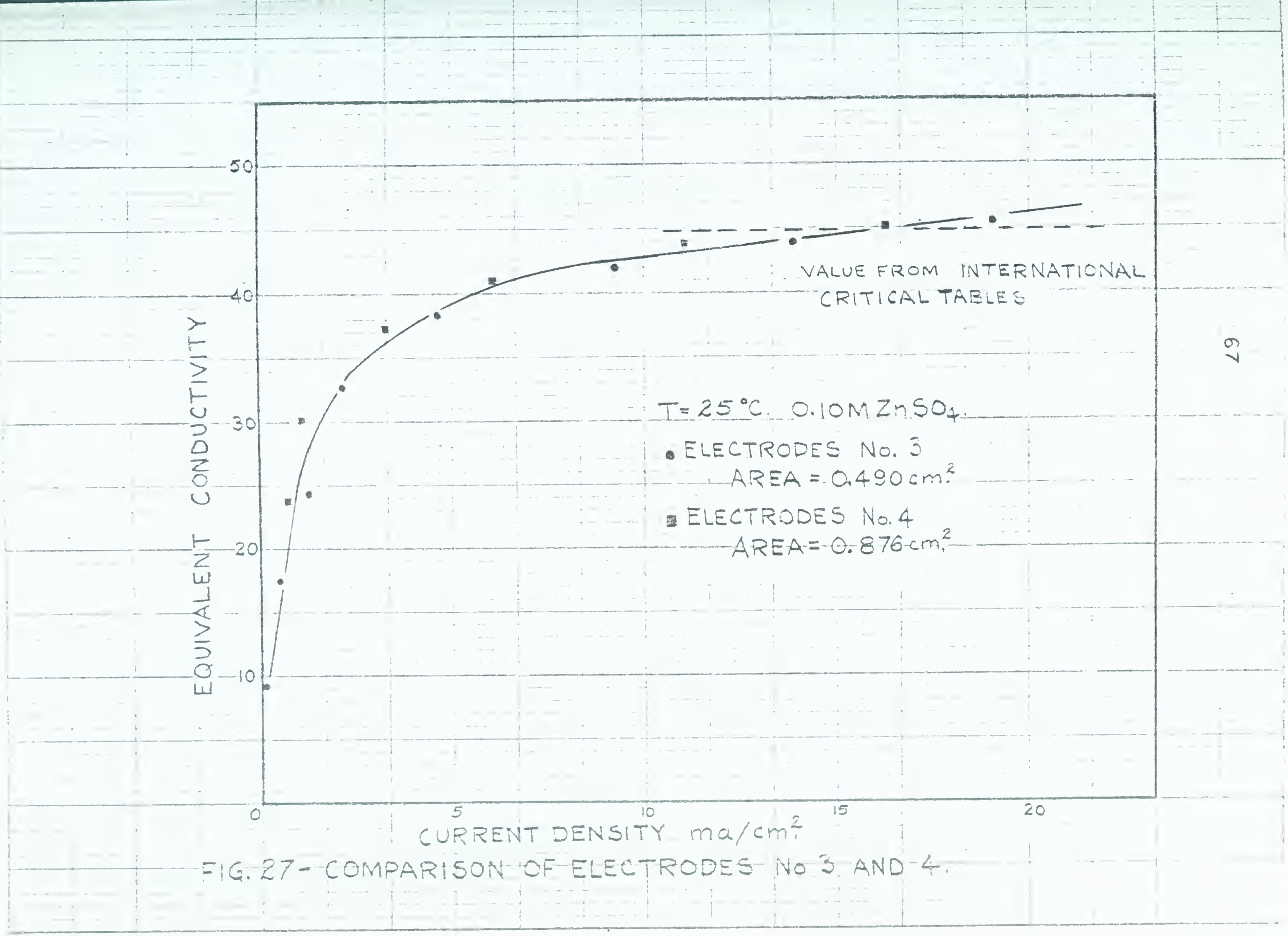

FIG. 27 - COMPARISON OF ELECTRODES No 3 AND 4.

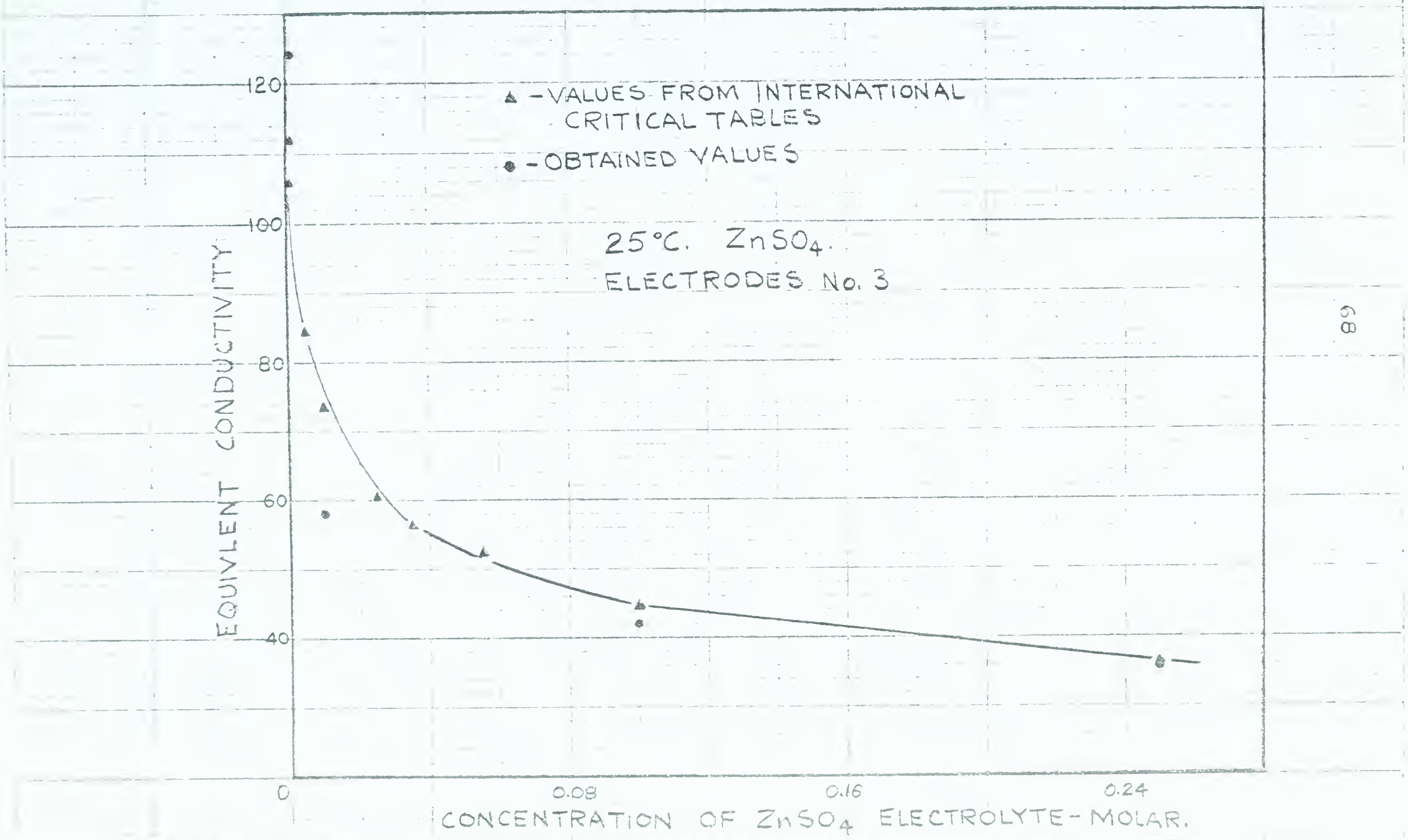

FIG. 28 - VARIATION OF CONDUCTANCE WITH CONCENTRATION.

Similarly, when an attempt was made to impose a potential drop of more than 0.23 volts across the cell with 0.25 M $ZnSO_4$ + 1.00 M Na_2SO_4 as the electrolyte, the potential drop increased rapidly with time reaching a value over 0.6 volts within two minutes. However, with 0.10 M or 0.25 M $ZnSO_4$ alone, potential drops of more than 1.2 volts across the cell were obtained and held reasonably constant. At these voltages bubbles were rapidly produced at the electrodes.

Fig. 27 indicates the shape of the equivalent conductivity versus current density curves obtained for 0.10 M $ZnSO_4$ using electrodes No. 3 and 4. Current density values at 0.300 volts for the various concentrations of $ZnSO_4$ were obtained from Fig. 25 and 26 and the respective equivalent conductivities were calculated for these values. These results are shown in Table IX and are compared to values obtained from the International Critical Tables for 25.0°C. in Fig. 28.

MEASUREMENTS ON FRINGE PATTERNS

Photographs were taken of the fringe patterns obtained at each current density for each concentration of $ZnSO_4$ used. The corresponding concentration change at the electrode faces was then obtained by measuring the fringe shift in the first wave with a 6" x 5" plastic graticule containing 25 lines to the inch.

It was found that about 90 seconds was required, after the current was turned on, for the fringe pattern to stabilize. Photographs were therefore taken 3 minutes after the current was turned on.

Table X gives the results obtained for the concentration change expressed by the first wave at the anode and at the cathode. These results are plotted in Fig. 29. Values of the concentration change

occurring at the electrodes could not be obtained for current densities greater than about 3 ma/cm^2 because the first wave becomes indistinguishable at higher current densities.

EXPERIMENTS ON CAUSE OF SECOND WAVE

A controversy existed as to the cause of the second wave. O'Brien and Rosenfield were of the opinion that the second wave was caused by the association and dissociation of ion pairs while Ibl was of the opinion that the second wave was caused by the convection currents set up in the cell.

The first set of experiments carried out to determine the cause of the second wave involved the use of zinc perchlorate as the electrolyte between the zinc electrodes. It was thought, at the time, that few ion pairs would exist in this solution and the second wave should, therefore, not occur. The type of fringe patterns obtained are shown in Fig. XII; photographs (g) and (h). The pH of the 0.10 M $Zn(ClO_4)_2$ solution was found to be 2.5. It was later found that ion pairs do exist in $Zn(ClO_4)_2$ solutions so these experiments could not be considered conclusive.

TABLE X - CONCENTRATION CHANGE EXPRESSED BY FIRST WAVE

ELECTRODES No. 3, AREA = 0.4897 cm^2, T - 25.0°C

CURRENT DENSITY ma/cm^2	CONC. ANODE gm/1.	CONC. CATHODE gm/1	DIST. OF FIRST WAVE FROM ANODE mm.	DIST. OF FIRST WAVE FROM CATHODE mm.
A - 0.001 M $ZnSO_4$				
0.076	0.11	0.11	0.346	0.392
0.118	0.15	0.15	0.331	0.362
0.226	0.19	—	0.338	—
0.343	0.29	—	0.331	—
B - 0.010 M $ZnSO_4$				
0.111	0.13	0.13	0.213	0.221
0.112	0.10	0.13	0.353	0.382
0.237	0.21	0.23	0.213	0.221
0.795	0.45	0.50	0.221	0.221
1.10	0.58	0.63	0.235	0.221
1.39	0.68	0.73	0.198	0.191
1.64	0.77	0.84	0.206	0.221
1.91	0.81	0.77	0.191	0.191
2.13	0.89	0.86	0.235	0.221
2.12	0.94	0.89	0.235	0.250
C - 0.10 M $ZnSO_4$				
0.010	0	0		
0.036	0.10	0.10	0.236	0.236
0.046	0.10	0.10	0.206	0.206
0.077	0.18	0.18	0.221	0.221
0.148	0.233	0.23	0.236	0.236
0.269	0.27	0.37	0.221	0.236
0.545	0.45	0.55	0.250	0.265
0.710	0.55	0.55	0.236	0.236

TABLE X - Cont.

CURRENT DENSITY ma/cm^2	CONC. ANODE gm/l	CONC. CATHODE gm/l	DIST. OF FIRST WAVE FROM ANODE mm.	DIST. OF FIRST WAVE FROM CATHODE mm.
C - 0.10 M $ZnZO_4$				
0.724	0.53	0.63	0.236	0.250
1.064	0.81	0.93	0.236	0.265
1.958	1.11	1.16	0.221	0.191
D - 0.25 M $ZnSO_4$				
0.051	0.06	0.06	0.165	0.165
0.086	0.11	0.16	0.230	0.230
0.210	0.36	0.36	0.221	0.221
0.283	0.24	0.31	0.247	0.238
0.389	0.36	0.42	0.247	0.238
0.506	0.57	0.65	0.206	0.221
0.625	0.37	0.37	0.247	0.247
1.069	0.69	0.69	0.230	0.238
1.645	0.86	0.94	0.230	0.230
1.744	0.77	0.92	0.205	0.235

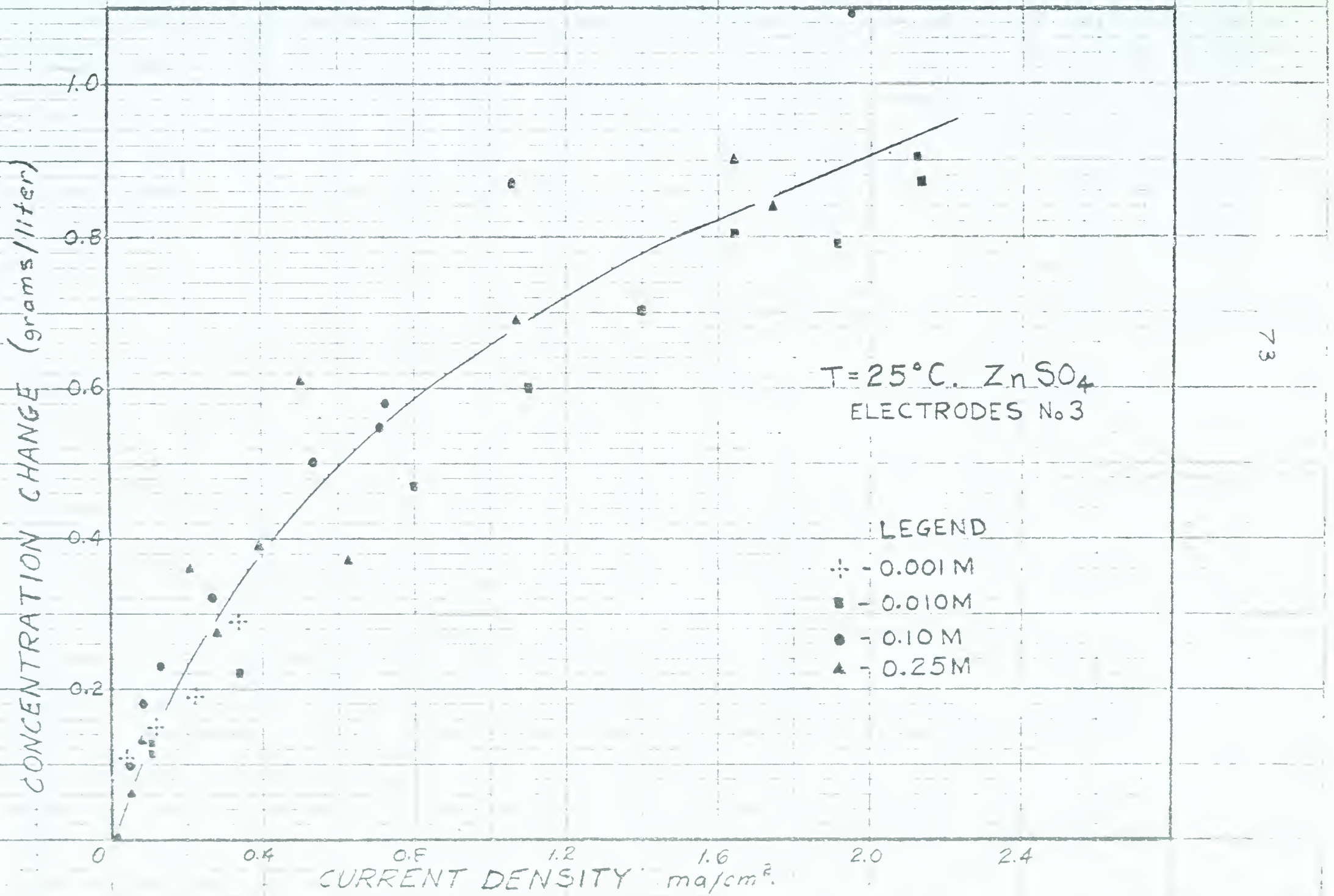

FIG. 29 - CONCENTRATION CHANGE AT ELECTRODES - FIRST WAVE.

ELECTRODES IN VARIOUS POSITION

To confirm that convection currents play a major role in the formation of the second wave it was decided to carry out experiments with the cell in various positions. Up to this point all the experiments were carried out in what we shall now call the normal position. Fig. 30 shows, diagramatically, the location of the electrodes in each of the positions used.

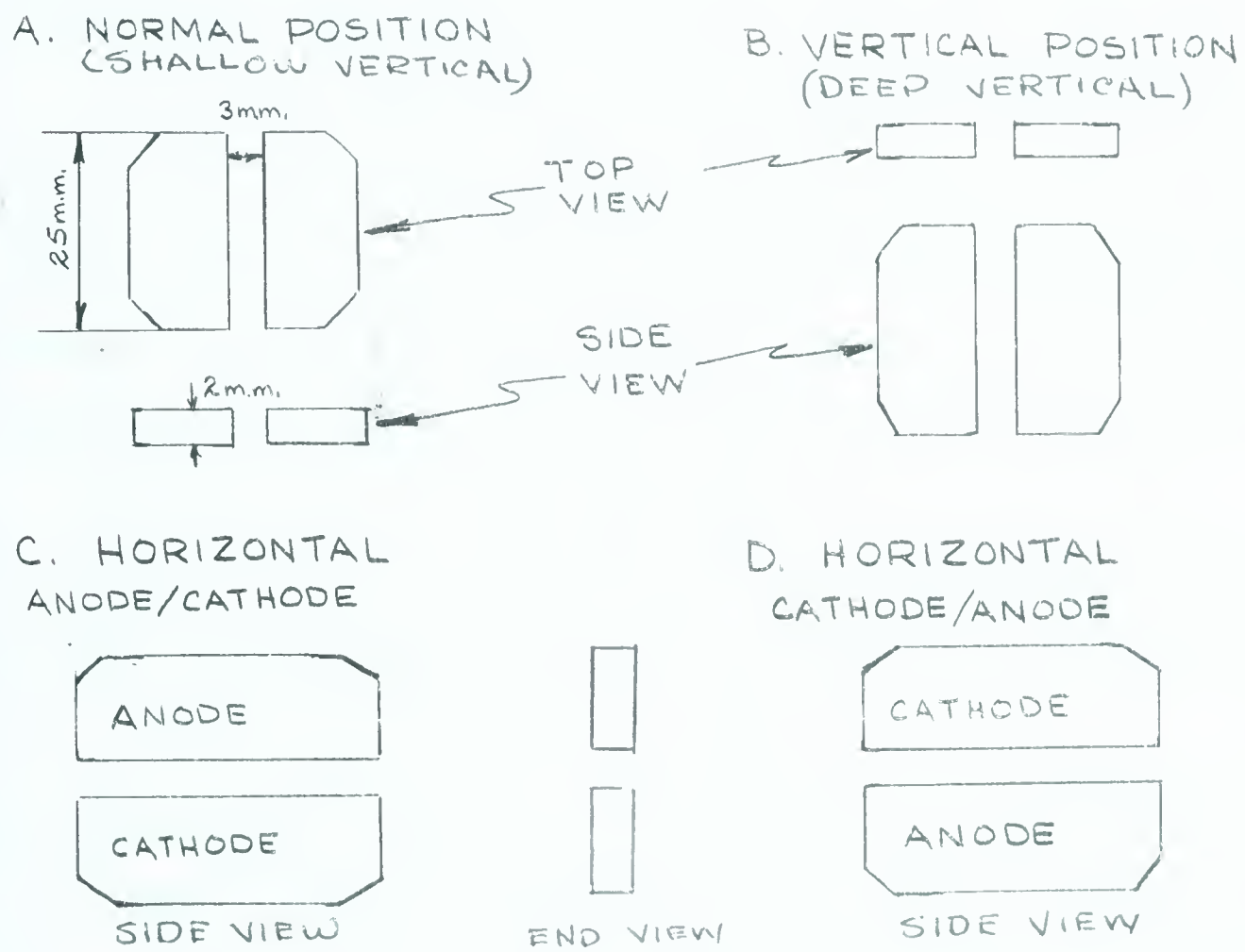

FIG. 30 Location of Electrodes in the Various Positions

Since it was necessary to tilt the cell apparatus on its side to obtain all the positions except the normal position and since no provision

was made in the original design of the apparatus to prevent spillage of the electrolyte through the top of the cell it was necessary to seal the top of the cell with molten paraffin before each run. Table XI and Fig. 31 show the results that were obtained from voltage-current density readings obtained in the four positions for 0.10M $ZnSO_4$ at 25.0°C. Table XII and Fig. 32 show the results obtained for the concentration changes at the anode and cathode expressed by the first wave. Only one run was made in each position.

The type of fringe patterns obtained in the four positions are shown in Fig. III to Fig. XI inclusive. Build up and decay of the patterns at a given current density as well as the patterns at various current densities are shown. Although the photographs are self-explanatory the following points should be noted:

Normal Position - Fig. III and IV

1. Second wave is evident at a current density of about 2.5 ma/cm^2.
2. The concentration of the bulk of the electrolyte increases from cathode to anode.
3. Less than 120 seconds is required for the fringe pattern to stabilize at 16.39 ma/cm^2.
4. Approximately 15 seconds is required for the second wave to disappear and about 40 seconds for the first wave during decay.

Vertical Position - Fig. V, VI and VII

(Top of photograph is towards top of cell)

1. The second wave starts to form at a current density of about 3 ma/cm^2.

2. The formation of the second wave at a current density of 16 ma/cm^2 appears to be different in Fig. V than in Fig. VI and VII. This difference is produced by changing the direction of the wedge angle. Although the mechanism of formation is different the end fringe pattern is the same.
3. The second wave is formed first at the top of the cell. The formation gradually progresses down the cell, taking about four minutes to reach the center of the cell where these photographs were taken at a current density of 16.75 ma/cm^2. More time is required at smaller current densities.
4. The second wave is much greater in the vertical position than in the normal position.
5. About 60 seconds is required for the second wave to disappear during decay.
6. There is very little if any concentration gradient in the bulk of the electrolyte.

Horizontal (Anode/Cathode) - Fig. VIII and IX

1. The second wave forms as is indicated by the photograph for 3.876 ma/cm^2. The fringe patterns are continually changing position due to movement of parcels of electrolyte down from the anode and up from the cathode.
2. The first wave is very small.
3. The parcels of moving electrolyte are formed even at very low current densities, but only in isolated spots. At high current densities the fringe distortion occurs in the manner illustrated in the build up sequence at 15 seconds in Fig. IX.

Horizontal (Cathode/Anode) - Fig. X and XI

1. The first wave is very large.
2. The second wave is not formed.
3. Build up of a needle-like deposit on the cathode occurs very rapidly as is illustrated in Fig. XI.
4. The decay is very slow, taking more than 12 minutes at a current density of 16.81 ma/cm^2.

Fig. 33 shows the time required for the fringe distortion at the anode to start falling and that at the cathode to start rising. It was noticed that, while in most cases the distortion at the anode and cathode started at the same time, there were cases when there was a definite lag (up to 3 seconds) between these occurences. In some cases the formation left the cathode first and in others it left the anode first.

A run was also carried out with the electrodes in the anode over cathode position but located such that the electrode faces made an angle of 10° with the horizontal. This yielded the same type of fringe pattern except that the parcels of electrolyte which rose vertically intersected the fringes which were perpendicular to the electrode faces.

It was also noted that, if the fringe pattern was developed in the vertical position and the cell quickly rotated to the anode/cathode position after the current was turned off, the fringe pattern decayed very rapidly with the formation of falling and rising parcels of electrolyte.

Calculations carried out by Rosenfield indicated that convection currents should not be set up in the size of cell used in her work. Since the cell used in this work was the same size as that used by Rosenfield it was decided to carry out a few runs using much thinner electrodes. The fringe patterns obtained are shown in Fig. XII. The second wave is not formed in the normal or vertical position. However, rising and falling parcels of electrolyte are evident in the anode/cathode position. Photograph (f) shows the needle-like deposit growing out from the cathode.

ALTERNATING CURRENT FRINGE PATTERNS

Experiments were also carried out using alternating current. A variac was placed in series with the cell and the output of an 8.5 volt transformer. A 110 volt, 60 cycle source was used. The voltage drop across the cell and a known resistance in the circuit were measured with a voltohmyst. The voltage-current density curves for the three positions are shown in Fig. 34 and the fringe patterns obtained are shown in Fig. II. Some movement of parcels of electrolyte was noticed in the one electrode above the other position. It should be noted that at low voltages the fringe displacement at the electrodes is not consistent while at high voltages there is a definite difference between the concentration at the electrode faces and that in the bulk; the concentration at the electrode faces being greater.

DETERMINATION OF pH CHANGE

An attempt to determine whether a pH change of the $ZnSO_4$ electrolyte did occur at the electrode faces while current was being passed was also made. A universal indicator was added to the 0.10M $ZnSO_4$ electrolyte

and white light was passed through the cell. A color change in the indicator due to a pH change could not be observed in any of the four positions even at 1.5 volts across the cell.

TABLE XI - VOLTAGE-CURRENT DENSITY RESULTS FOR ALL POSITIONS

ELECTRODES No. 1, 0.10 M $ZnSO_4$, T - 25.0°C AREA = 0.4894 cm^2

VOLTAGE ACROSS CELL VOLTS	CURRENT DENSITY ma/cm^2	DIST. BET. ELECTRODES cm	EQUIVALENT CONDUCTIVITY
A - Normal Position			
0.033	0.368	0.323	18.1
0.056	0.700	"	20.4
0.084	1.340	"	25.8
0.115	1.989	"	28.0
0.179	3.900	"	35.2
0.296	7.419	"	40.3
0.435	11.72	"	43.5
0.577	16.91	"	47.2
B - Vertical Position			
0.037	0.368	0.323	16.3
0.053	0.721	"	22.1
0.078	1.505	"	31.1
0.118	1.836	"	25.3
0.140	3.900	"	45.1
0.255	7.457	"	47.2
0.290	7.435	"	41.3
0.311	11.66	"	45.9
0.533	16.75	"	50.8

TABLE XI - cont.

VOLTAGE ACROSS CELL VOLTS	CURRENT DENSITY ma/cm^2	DIST. BET. ELECTRODES cm	EQUIVALENT CONDUCTIVITY
C - Horizontal Anode Above Cathode			
0.043	0.368	0.323	13.7
0.078	0.826	"	17.2
0.084	1.340	"	25.8
0.115	1.503	"	21.0
0.209	3.876	"	30.0
0.284	7.443	"	42.4
0.416	11.71	"	45.5
0.566	16.91	"	48.6
D - Horizontal Cathode Over Anode			
0.043	0.368	0.323	13.8
0.054	0.831	"	20.8
0.091	1.505	"	26.8
0.128	1.989	"	25.3
0.167	3.902	"	37.9
0.282	7.443	"	42.8
0.408	11.63	"	46.3
0.574	16.81	"	47.2

TABLE XII - CONCENTRATION CHANGE EXPRESSED BY FIRST WAVE IN VARIOUS POSITIONS.

ELECTRODES No. 1, 0.10 M $ZnSO_4$, T = 25.0°C, Area = 0.4894 cm^2

CURRENT DENSITY ma/cm^2	CONC. CHANGE AT ANODE gm/l	CONC. CHANGE AT CATHODE gm/l	DIST. TO FIRST WAVE AT ANODE mm.	DIST. TO FIRST WAVE AT CATHODE mm.
A - Normal Position				
0.358	0.28	0.43	0.311	0.311
1.213	0.82	0.87	0.233	0.233
2.413	1.36	1.41	0.210	0.202
4.609	1.86	2.16	0.202	0.171
B - Vertical Position				
0.368	0.60	0.67	0.476	0.507
0.721	1.10	1.17	0.472	0.503
1.505	2.08	2.23	0.457	0.457
1.836	2.54	2.54	0.414	0.479
3.900	3.14	4.24	0.395	0.473
C - Horizontal - Anode over Cathode				
0.368	0.28	0.51	0.222	0.348
0.826	0.53	1.00	0.206	0.379
1.340	0.52	1.14	0.222	0.363
1.503	0.52	0.23	0.191	0.319
3.876	0.78		0.192	0.222

TABLE XII - cont.

CURRENT DENSITY ma/cm^2	CONC. CHANGE AT ANODE gm/l	CONC. CHANGE AT CATHODE gm/l	DIST. TO FIRST WAVE AT ANODE mm.	DIST. TO FIRST WAVE AT CATHODE mm.
D - Horizontal - Cathode over Anode				
0.358	0.82	0.82	0.793	0.793
0.831	1.99	1.95	0.785	0.785
1.505	4.00	3.88	0.988	0.956
1.989	4.95	4.88	1.025	1.057
3.902	—	—	1.142	1.110

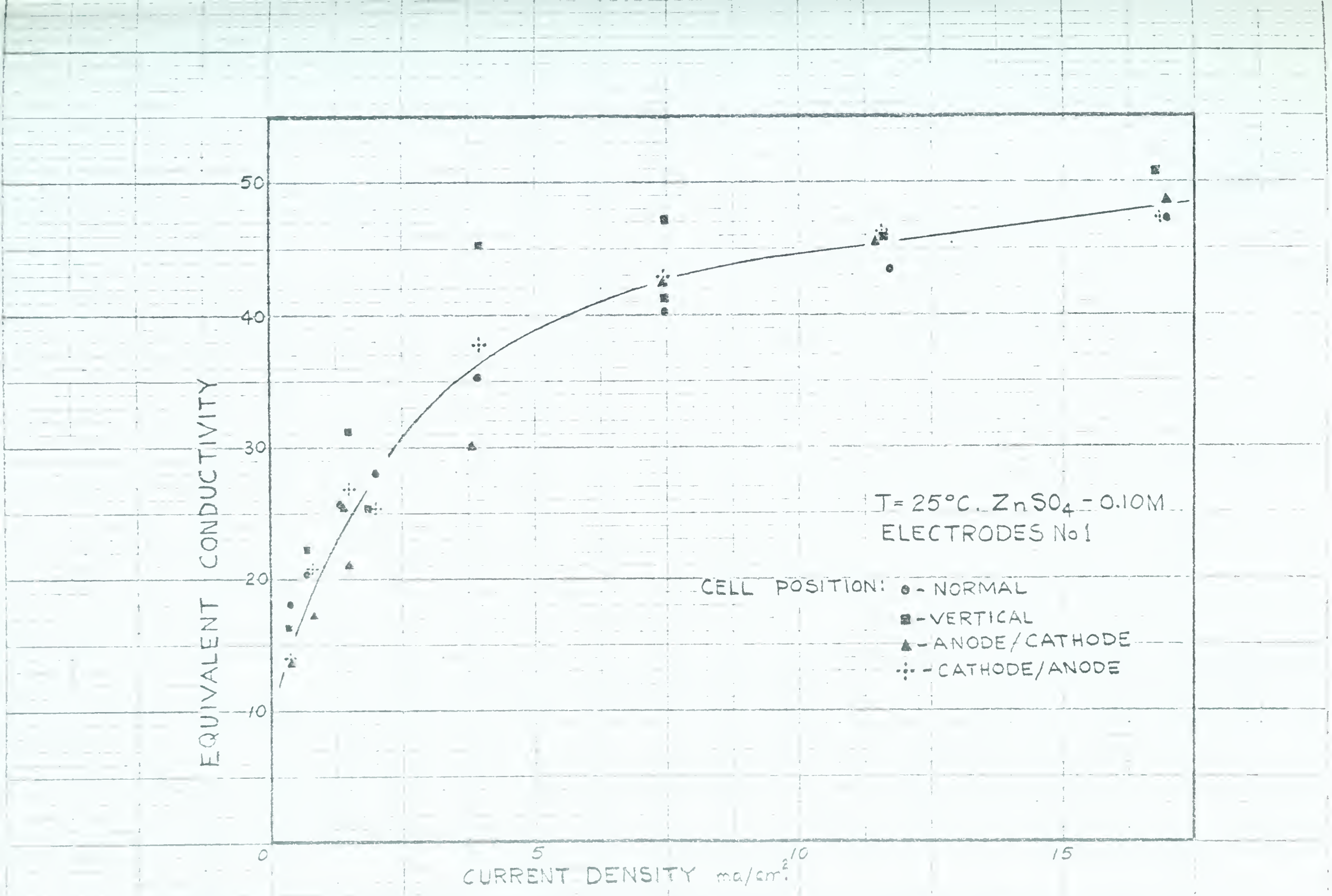

FIG. 31 - CONDUCTANCE - WITH ELECTRODES IN VARIOUS POSITIONS.

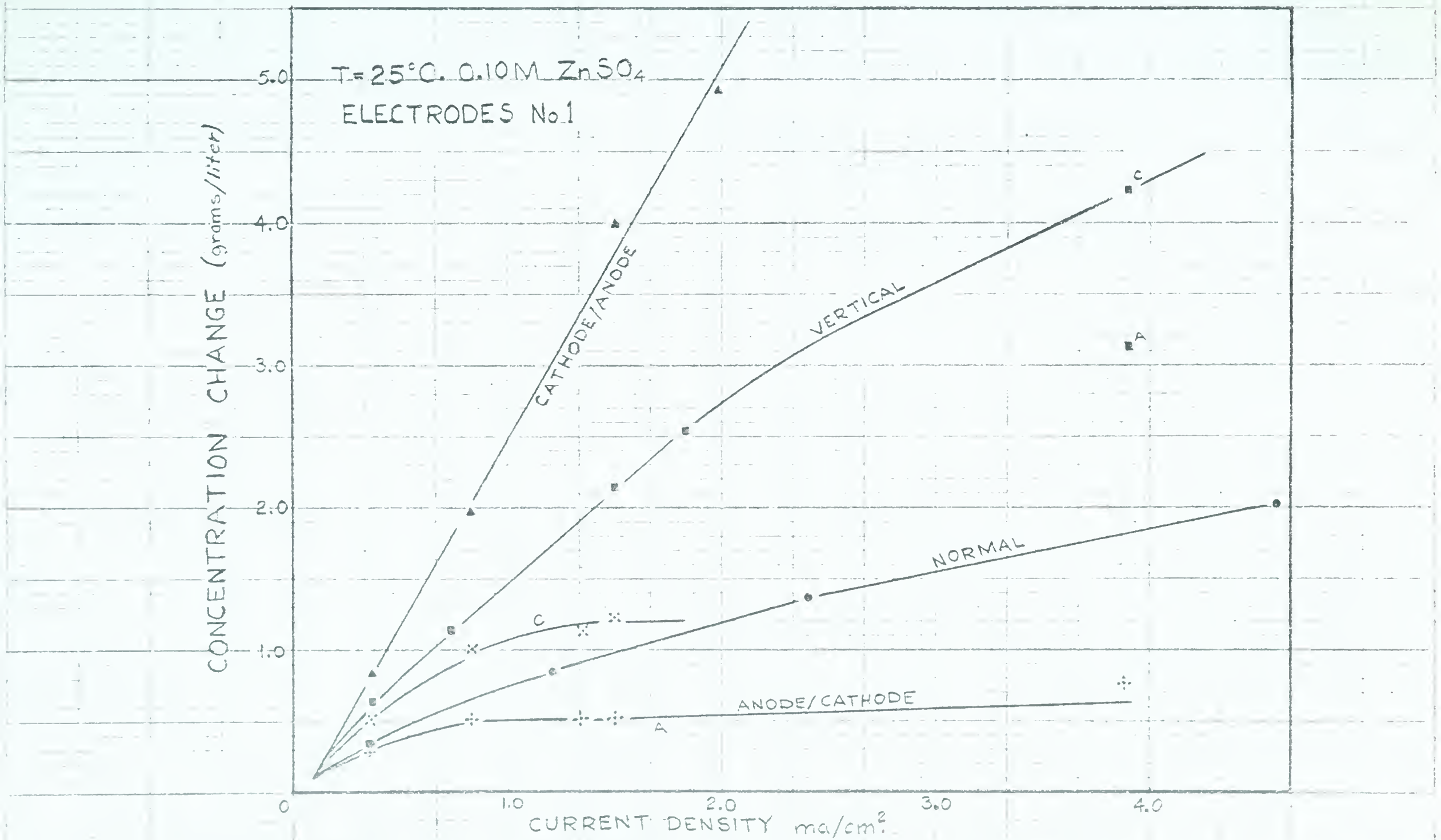

FIG. 32 - CONCENTRATION CHANGE - FIRST WAVE - VARIOUS POSITIONS.

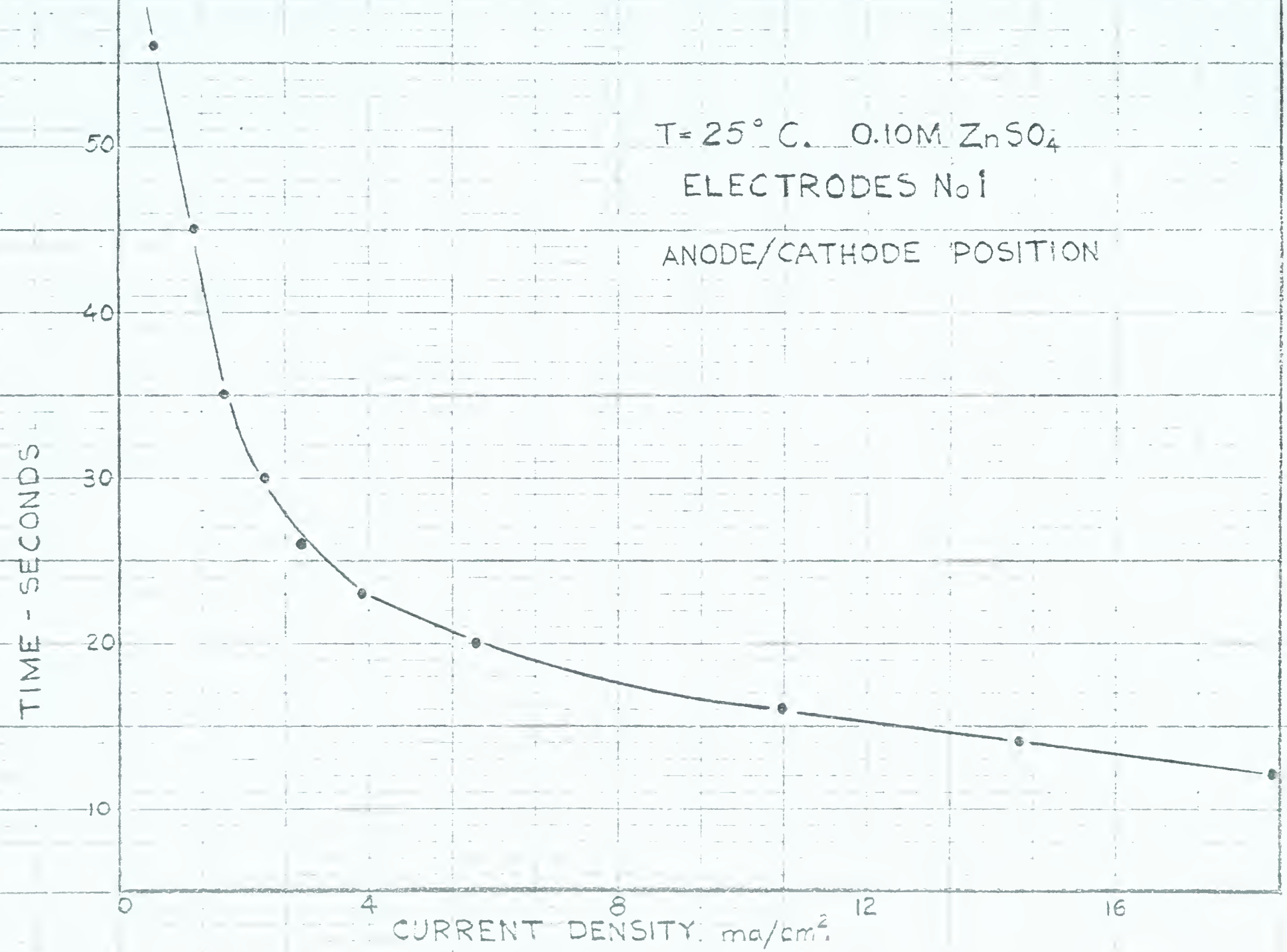

FIG. 33 - TIME REQUIRED FOR FRINGE DISTORTION TO START.

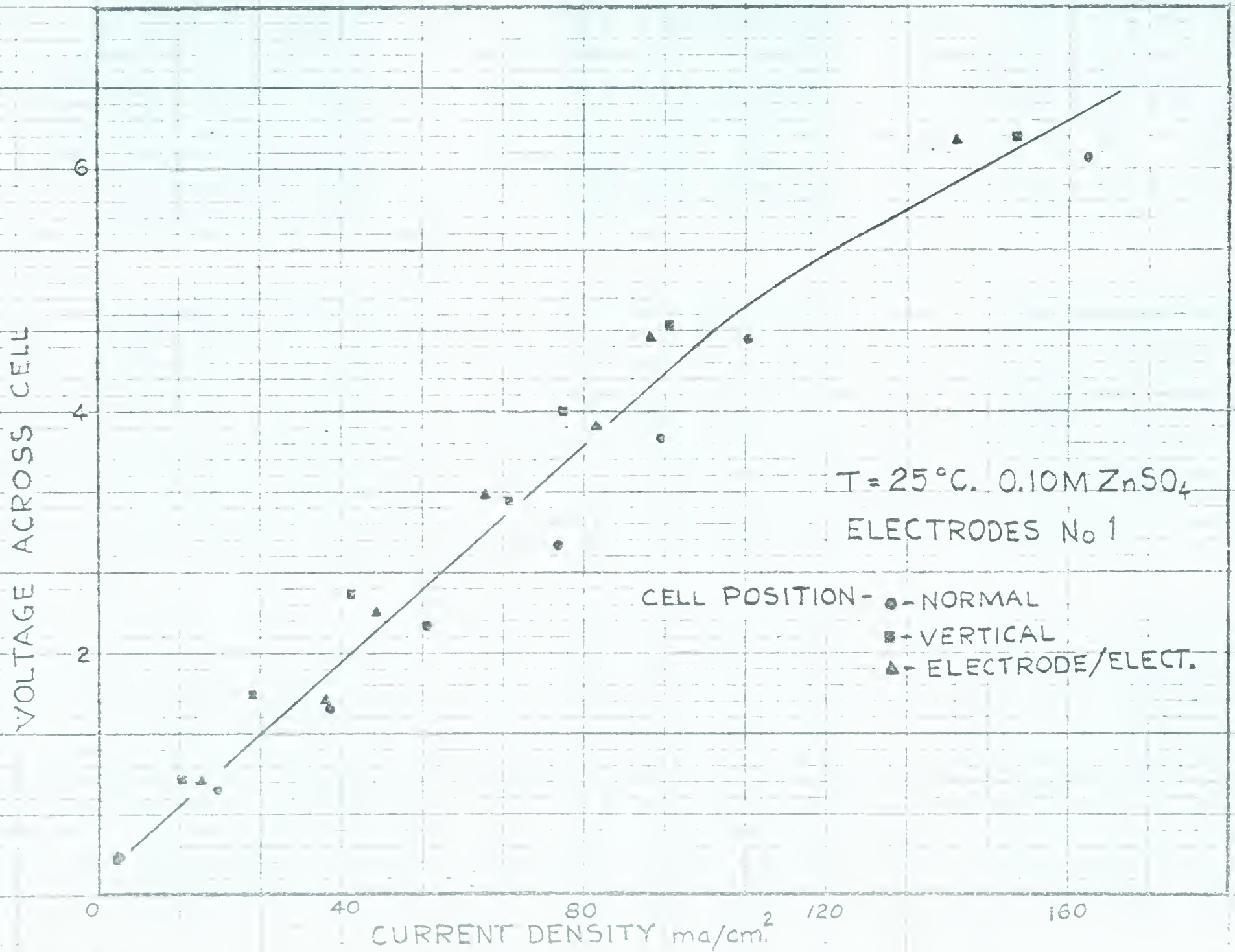

FIG. 37- ALTERNATING CURRENT CURVES - VARIOUS POSITIONS.

NORMAL POSITION

0.31 VOLTS | 2.24 VOLTS | 6.10 VOLTS

VERTICAL POSITION

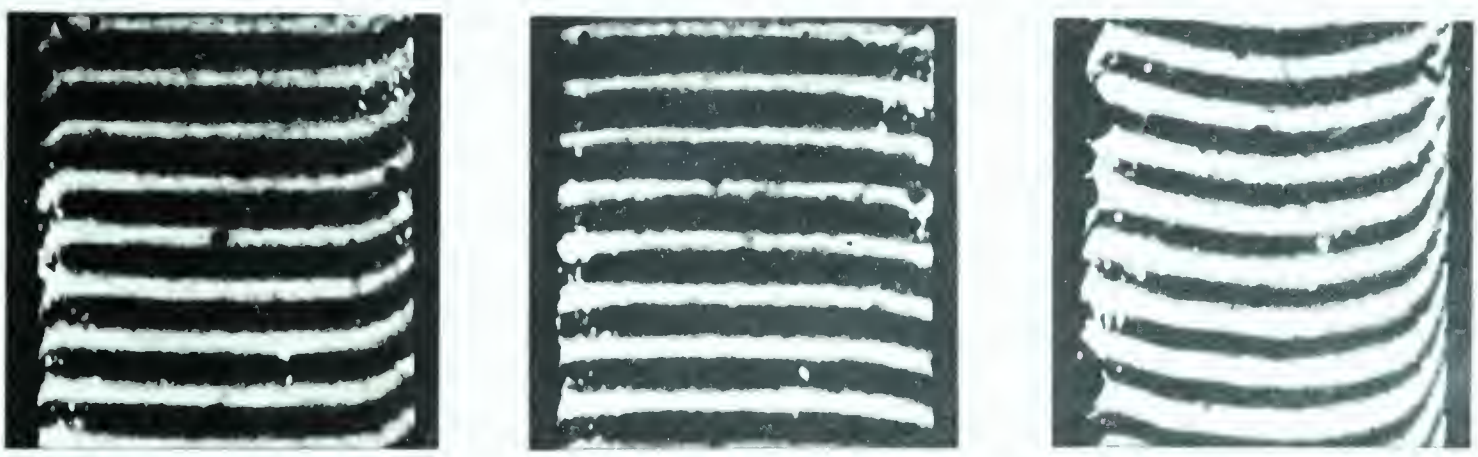

0.28 VOLTS | 2.51 VOLTS | 6.27 VOLTS

ONE ELECTRODE ABOVE THE OTHER

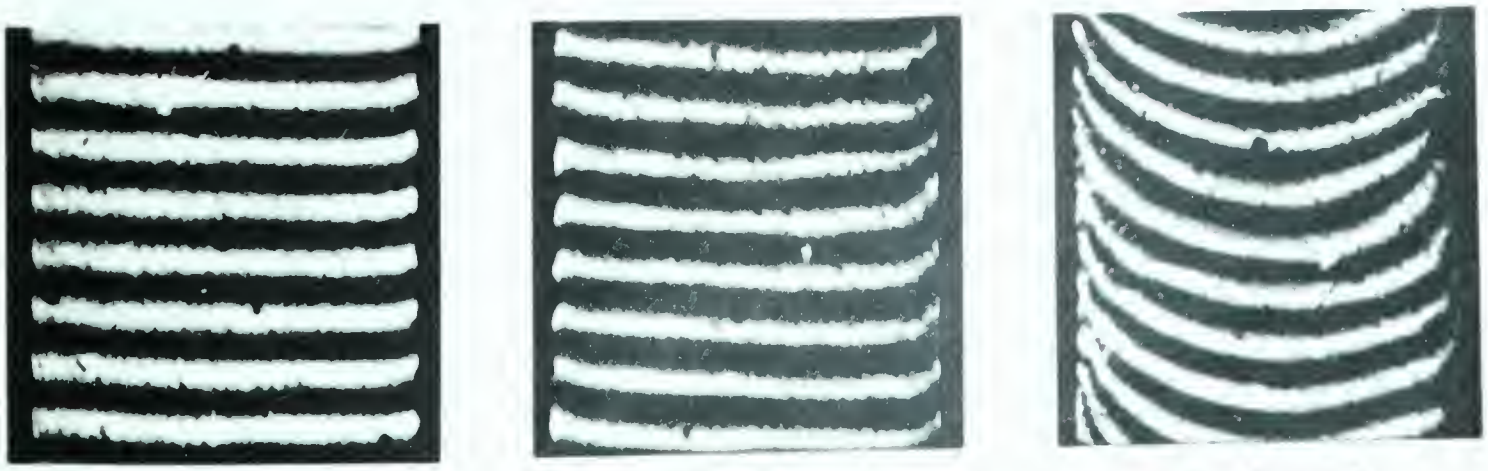

0.30 VOLTS | 2.33 VOLTS | 6.25 VOLTS

Fig. 11 FRINGE PATTERNS PRODUCED BY ALTERNATING CURRENTS.- 25.0°C. 0.01 $ZnSO_4$. 3 MIN. AFTER CURRENT TURNED ON.

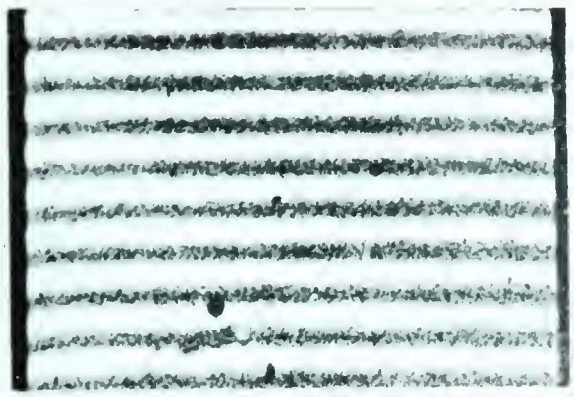

NO CURRENT

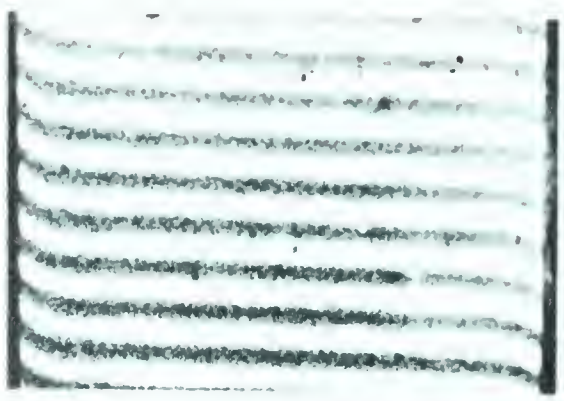

0·357 ma/cm² 0·035V

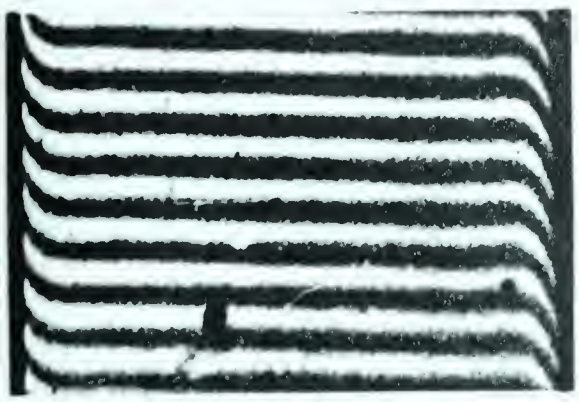

1·21 ma/cm² 0·074V

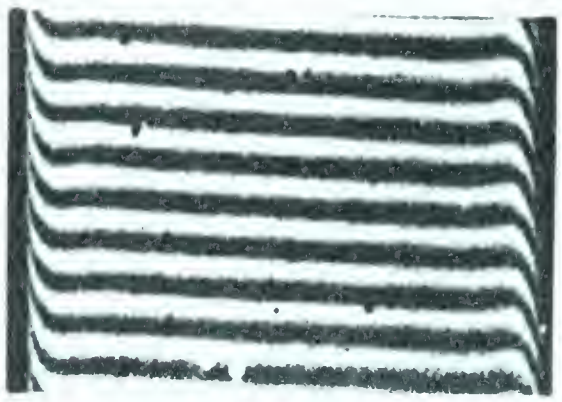

2·41 ma/cm² 0·112V

4·61 ma/cm² 0·178V

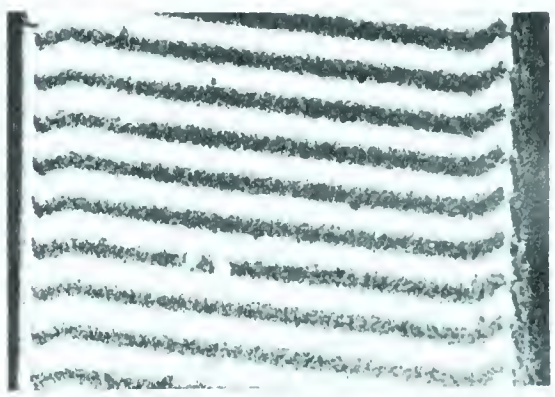

9·79 ma/cm² 0·355V

anode cathode

16·38 ma/cm² 0·562V

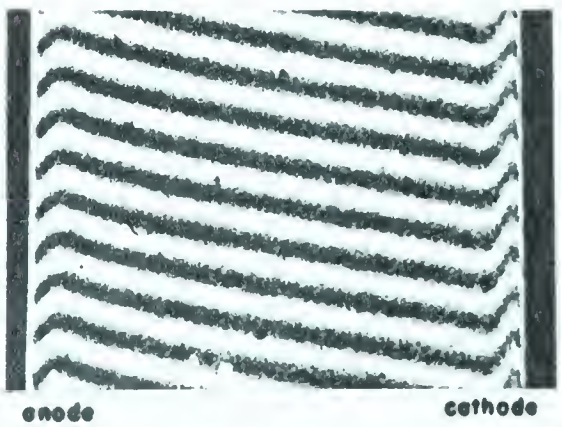

anode cathode

22·58 ma/cm² 0·8[illegible]V

Fig III FRINGES AT VARIOUS CURRENT DENSITIES – 3 min after current turned on

25°C, 0·10M $ZnSO_4$

NORMAL POSITION

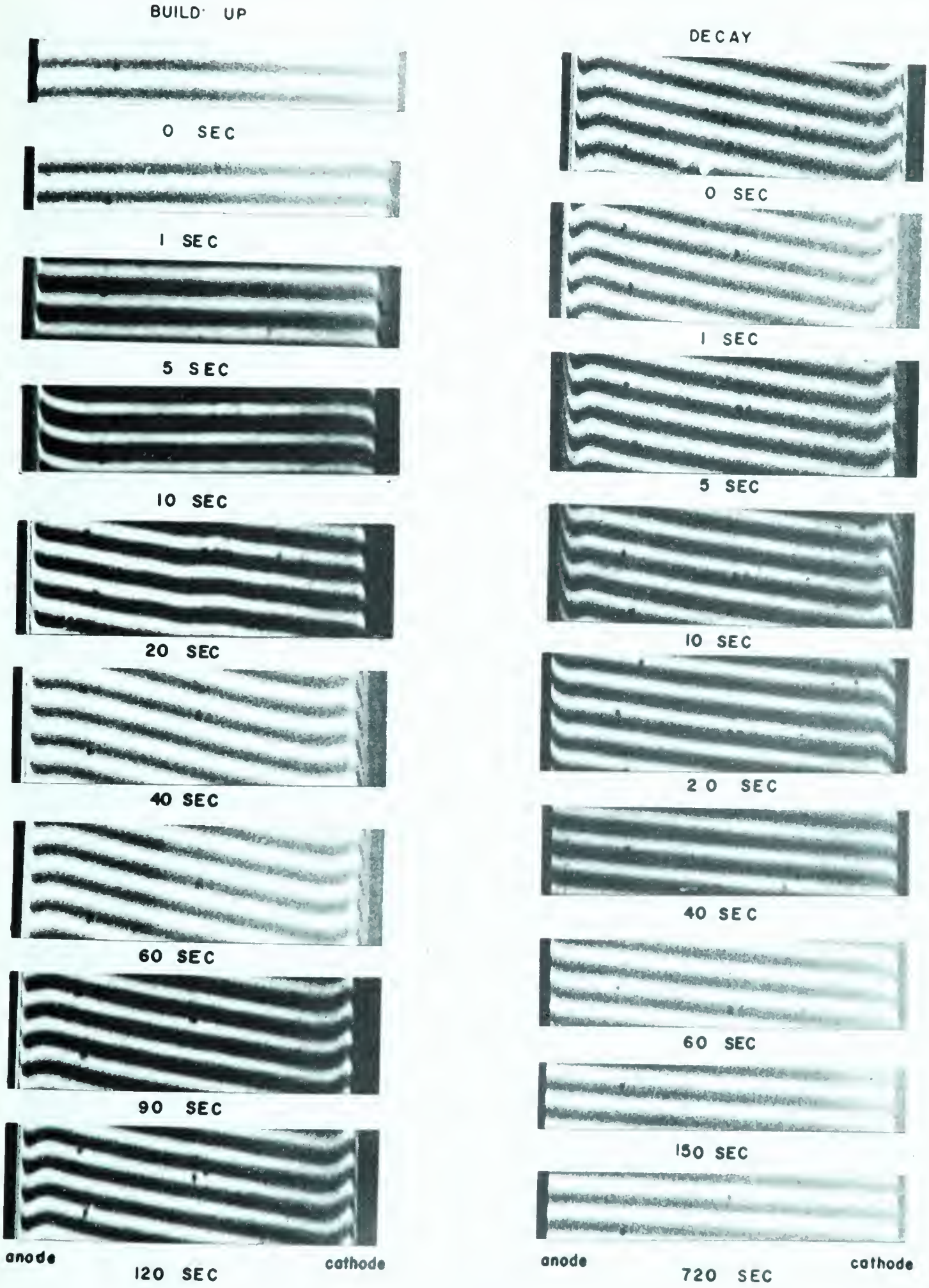

Fig IV BUILD UP AND DECAY OF FRINGE PATTERN AT 16·39 ma / cm²

NORMAL POSITION

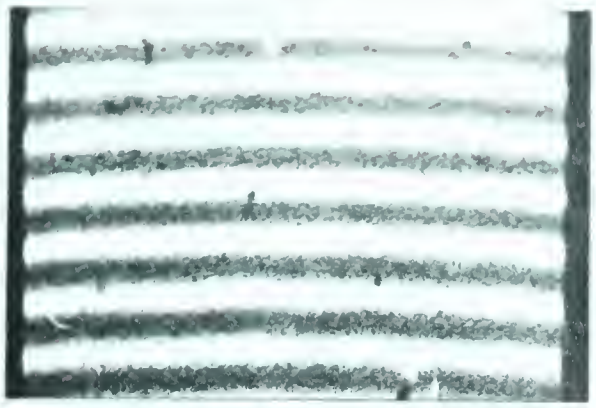

No Current

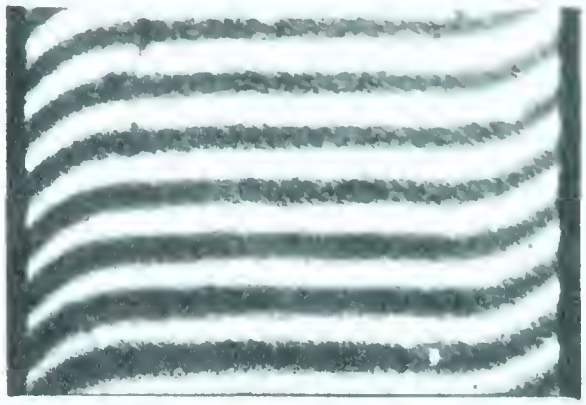

0·368 ma/cm²

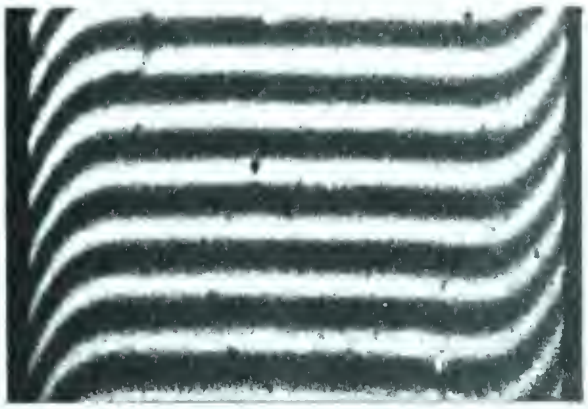

0·721 ma/cm²

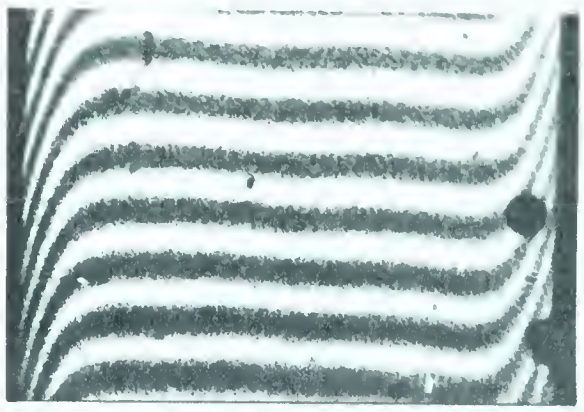

1·505 ma/cm²

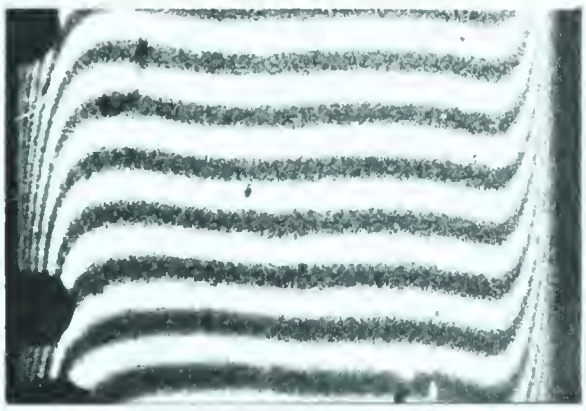

3·900 ma/cm²

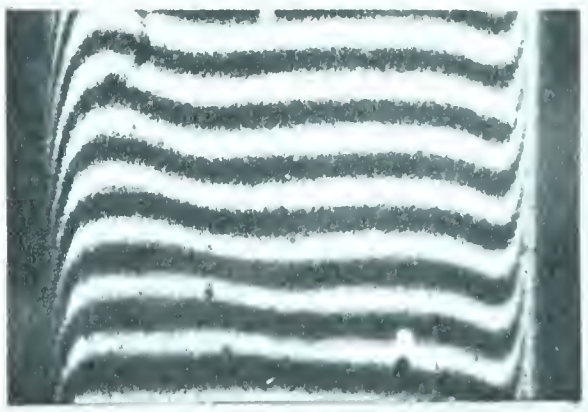

7·435 ma/cm²

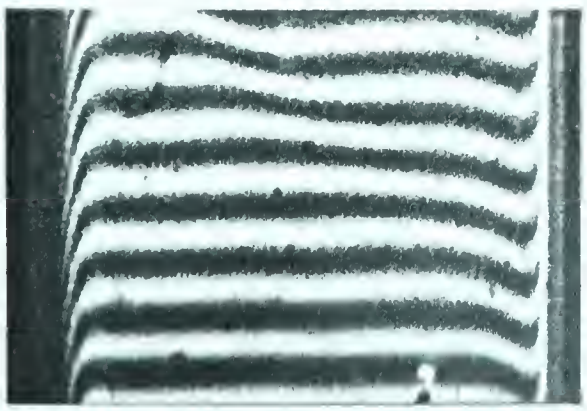

cathode anode

11·66 ma/cm²

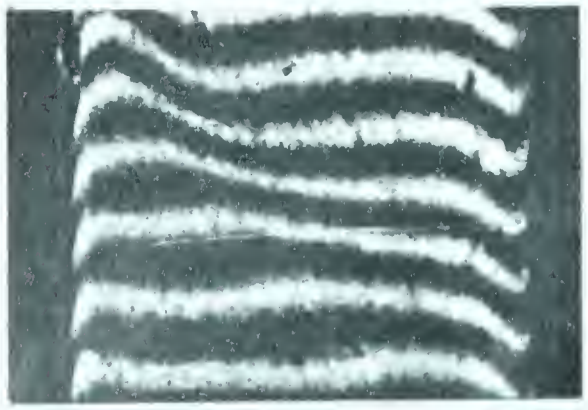

cathode anode

16·84 ma/cm²

FIG V FRINGE PATTERNS AT VARIOUS CURRENT DENSITIES – 5 min. after current turned on. 0·10M $ZnSO_4$, 25·0° C.
VERTICAL POSITION

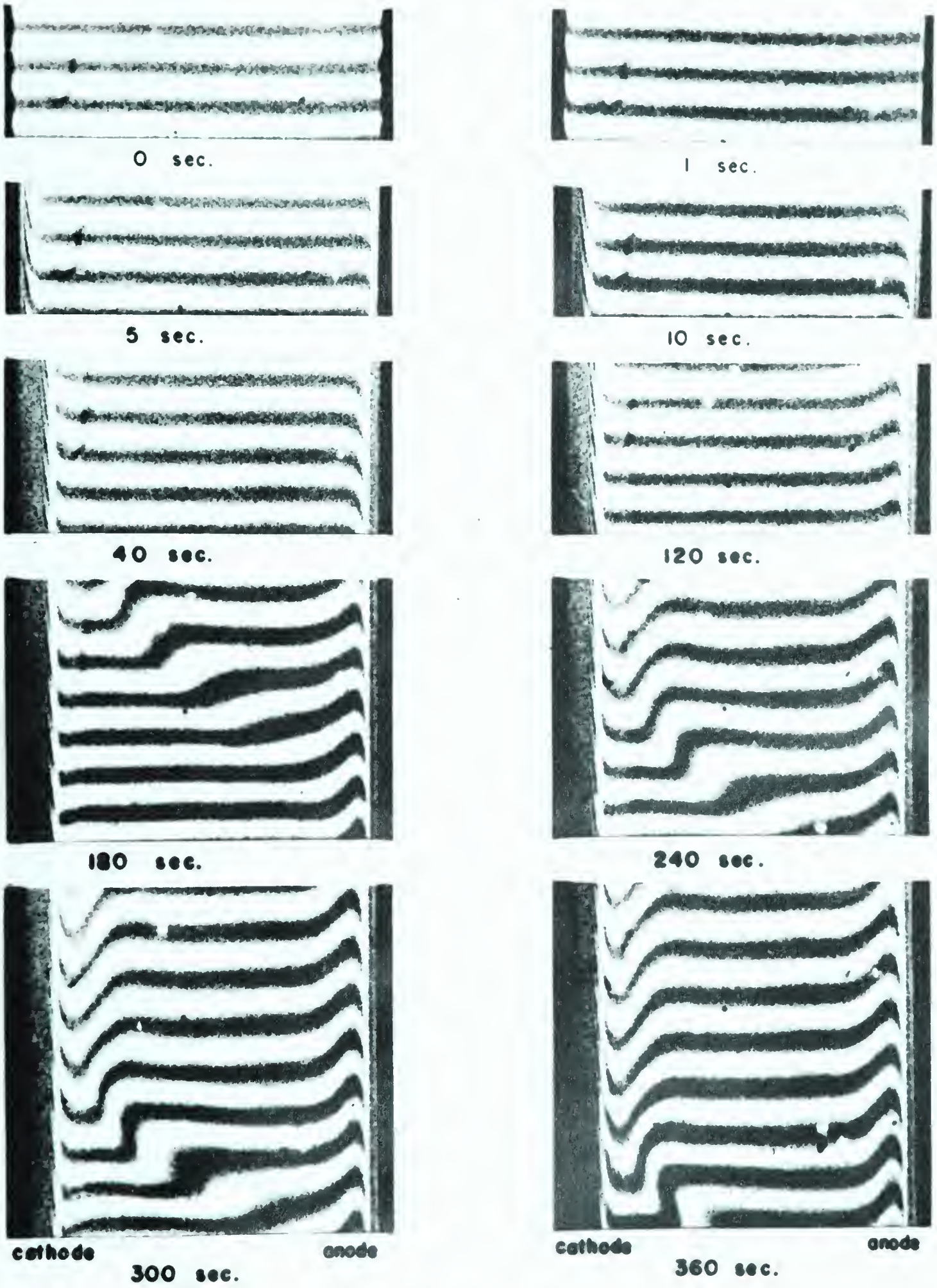

FIG. VI BUILD UP OF FRINGE PATTERN AT 16·75 ma/cm^2. 0·10 M $ZnSO_4$. 25·0° C. VERTICAL POSITION

0 SEC.

80 SEC.

1 SEC.

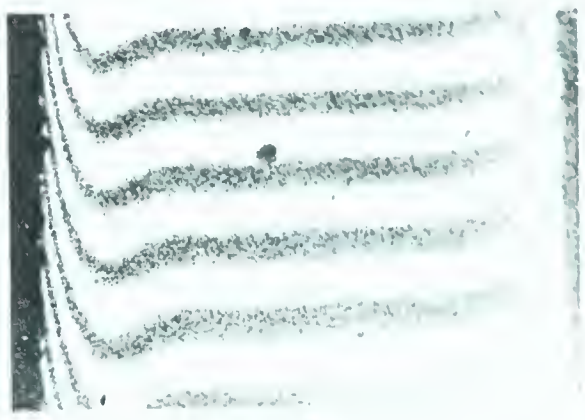

40 SEC.

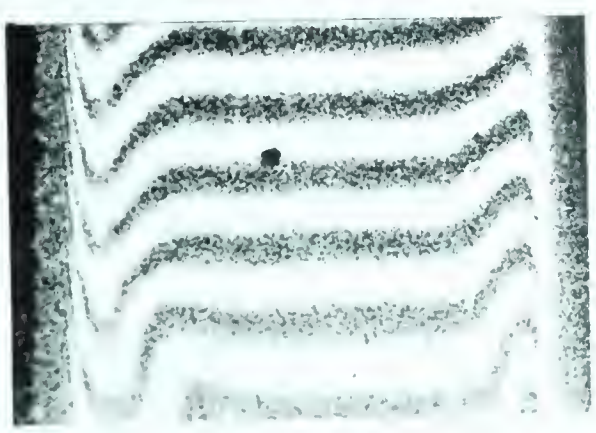

5 SEC.

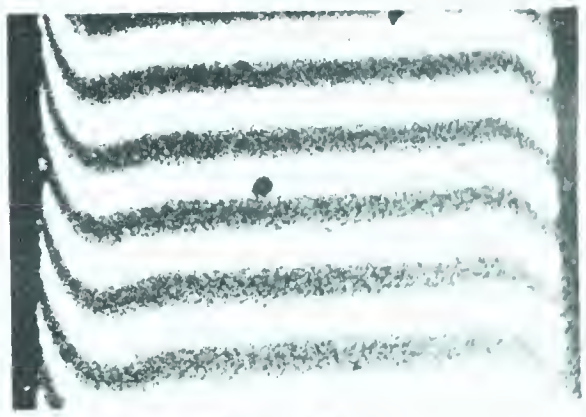

60 SEC.

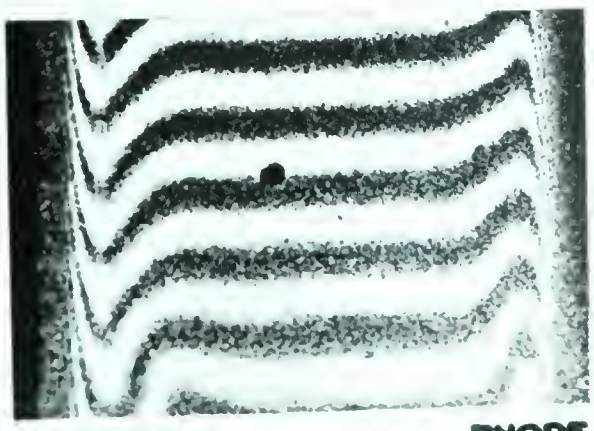

CATHODE RHODE

10 SEC.

CATHODE RHODE

180 SEC.

Fig VII DECAY OF FRINGE PATTERN AT 16.75 ma/cm^2
0.10 M $ZnSO_4$. 25.0°C VERTICAL POSITION

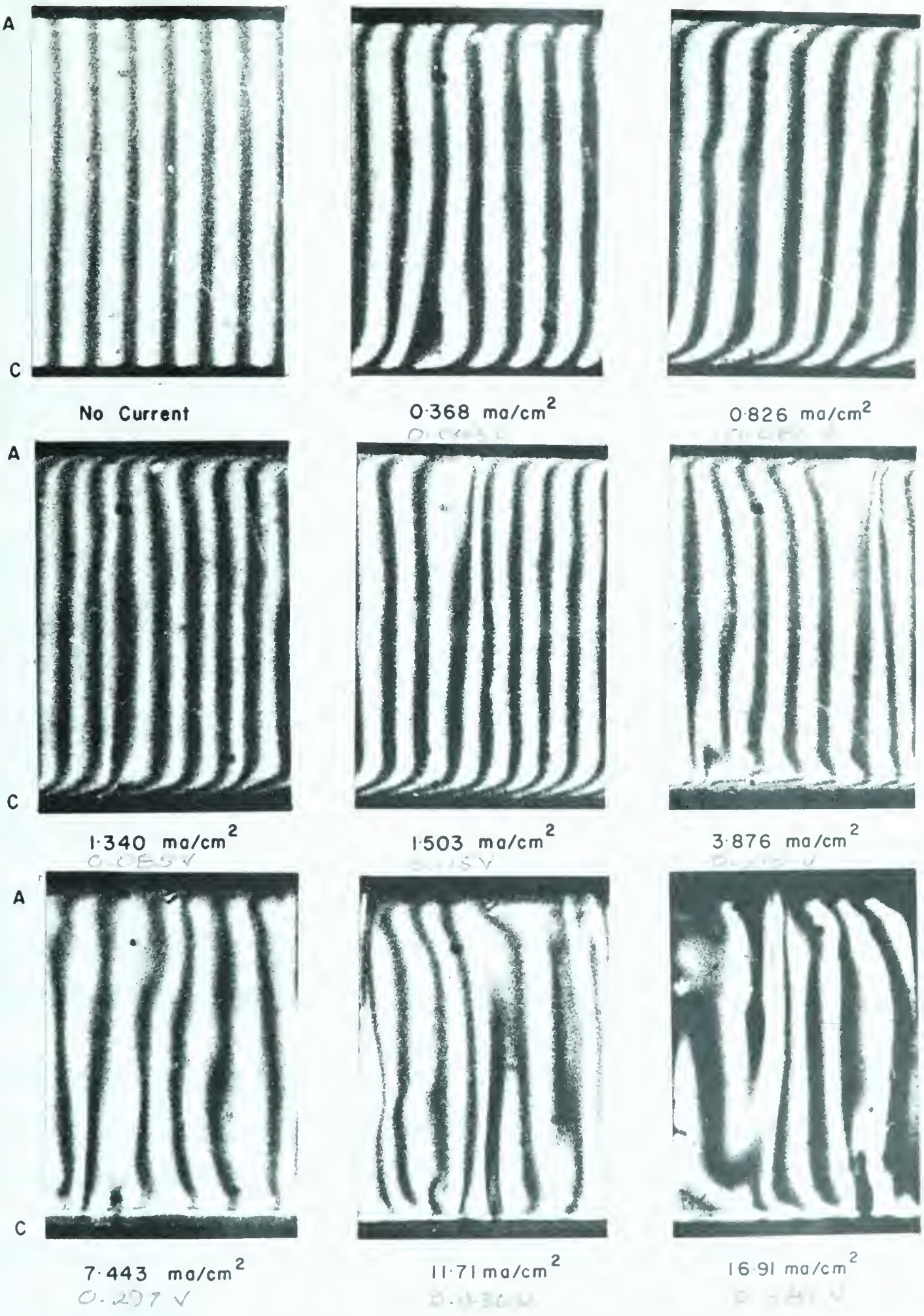

FIG VIII FRINGE PATTERN AT VARIOUS CURRENT DENSITIES

3 min. after current turned on. 0·10 M $ZnSO_4$, 25·0° C

HORIZONTAL (anode/cathode) POSITION

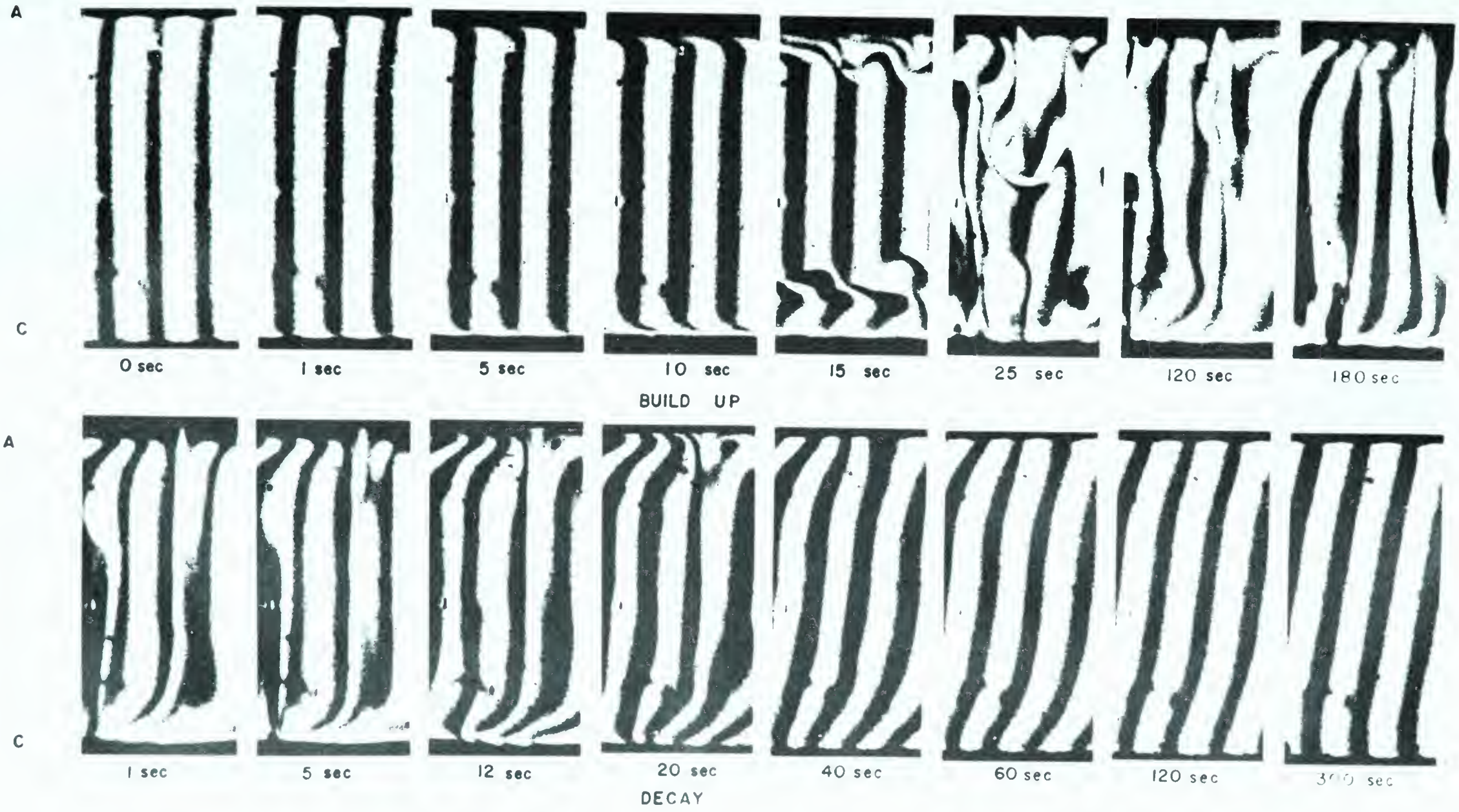

FIG IX . BUILD UP AND DECAY OF FRINGE PATTERN AT 16·91 ma / cm^2 , 25·0 °C , 0·10 M $ZnSO_4$

HORIZONTAL (anode / cathode) POSITION

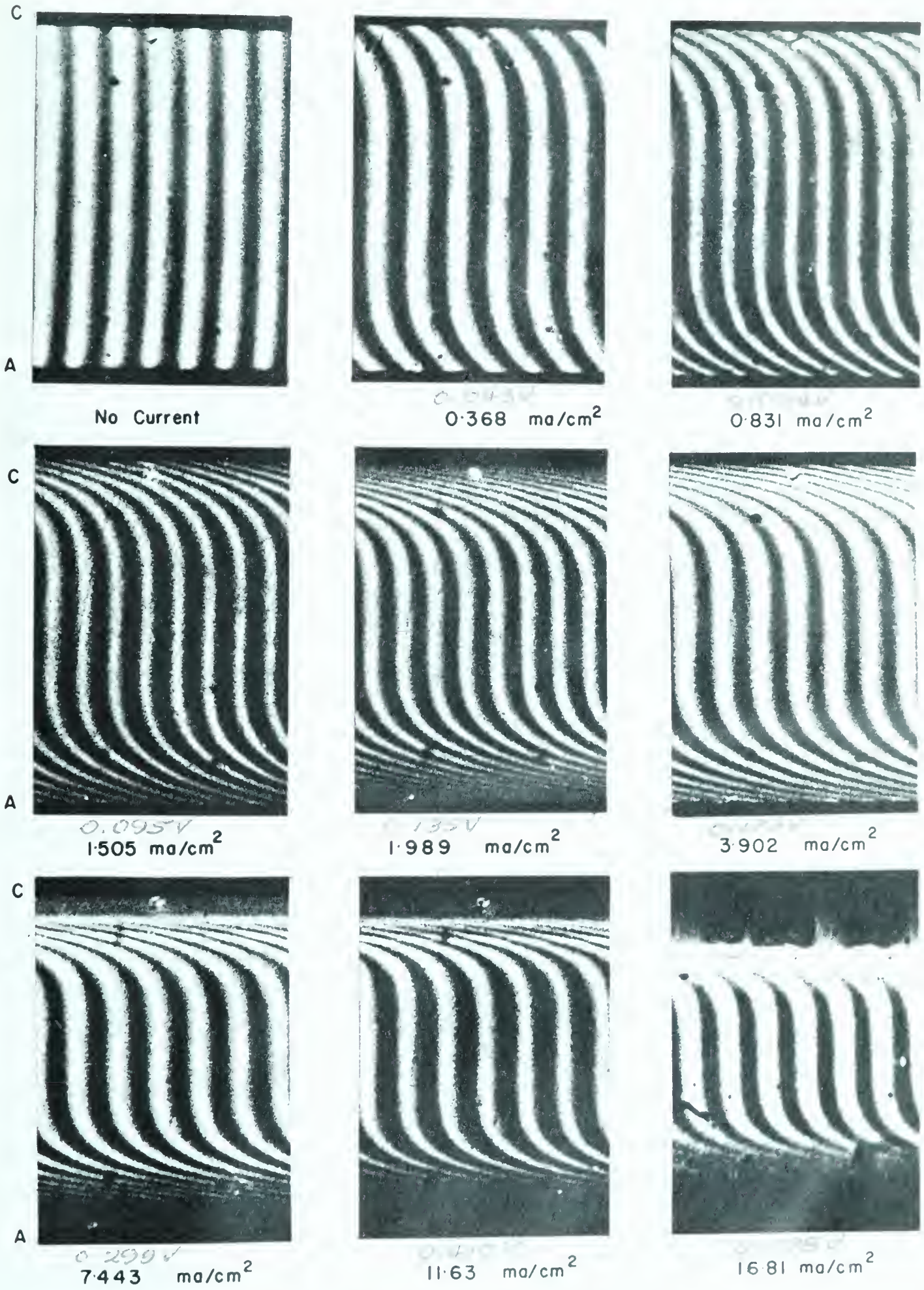

FIG X FRINGE PATTERNS AT VARIOUS CURRENT DENSITIES

3 min. after current turned on. 0 1 M $ZnSO_4$, 25 0°C

HORIZONTAL (cathode/anode) POSITION

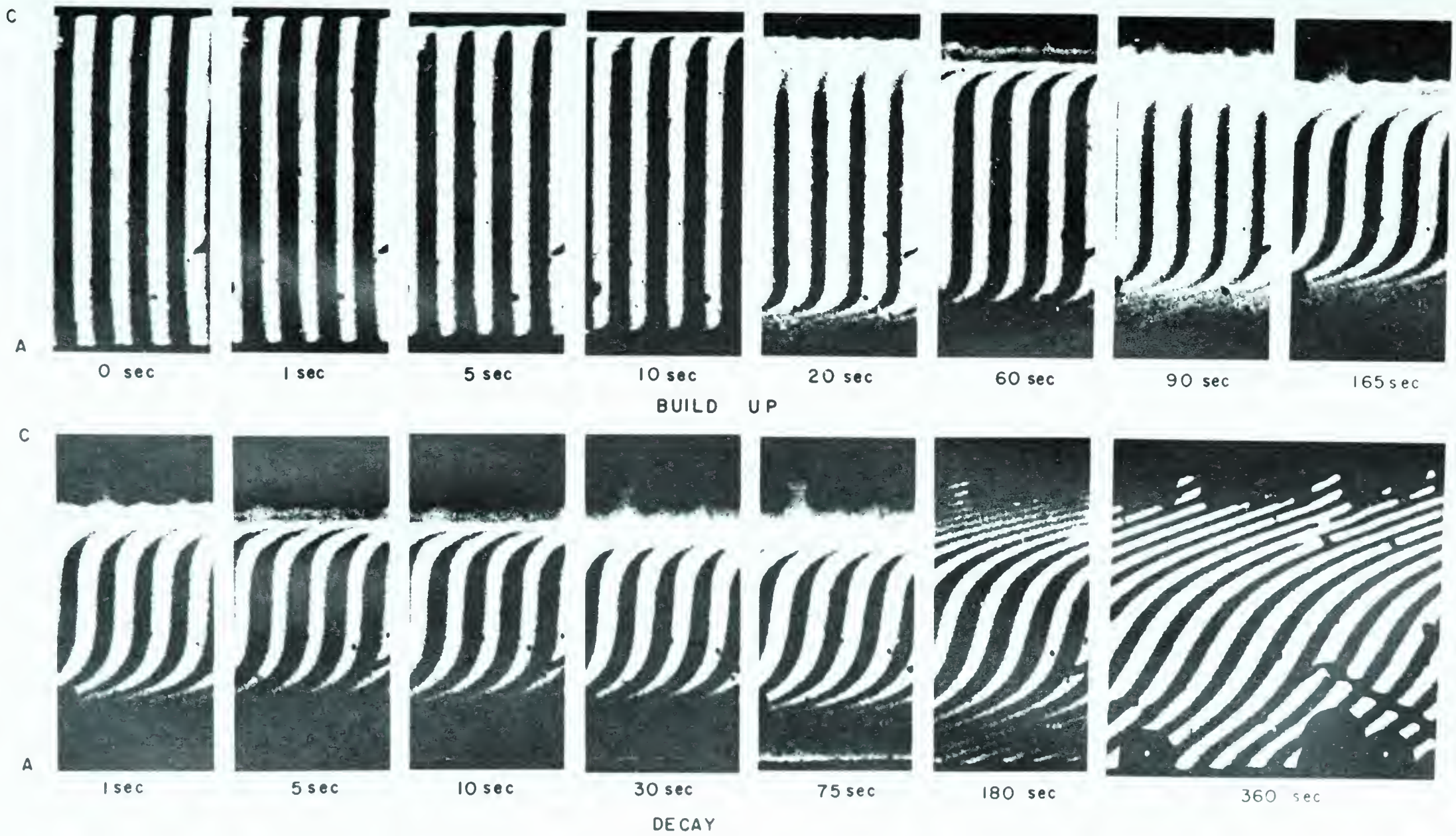

FIG XI BUILD UP AND DECAY OF FRINGE PATTERN AT 16·81 ma/cm², 25·0°C, 0·10M $ZnSO_4$

HORIZONTAL (cathode/anode) POSITION

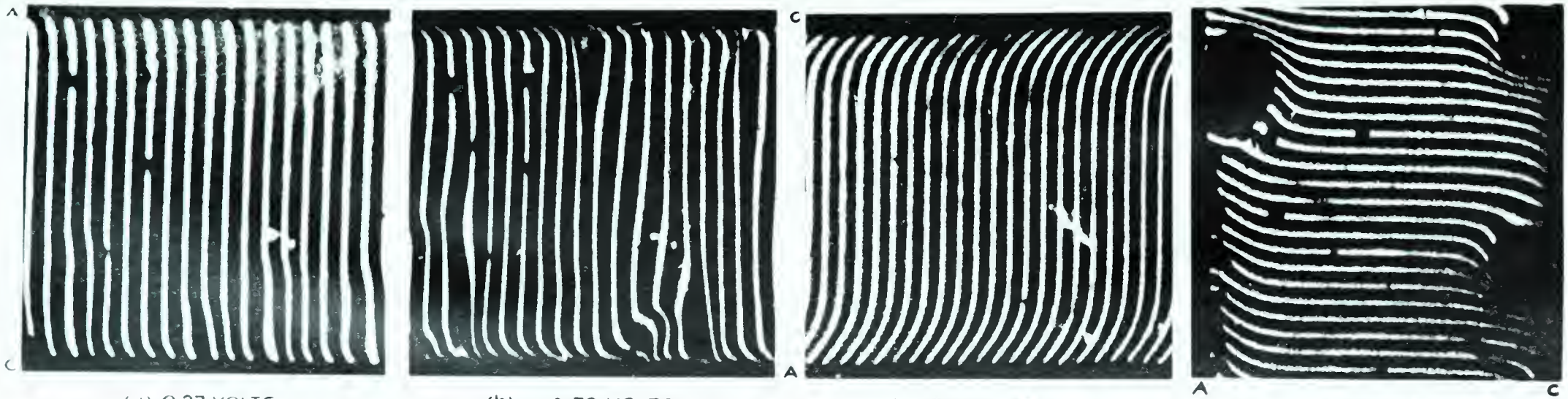

(a) 0.27 VOLTS (b) 0.59 VOLTS (C) 0.52 VOLTS (d) 0.60 VOLTS

ANODE OVER CATHODE CATHODE OVER ANODE VERTICAL

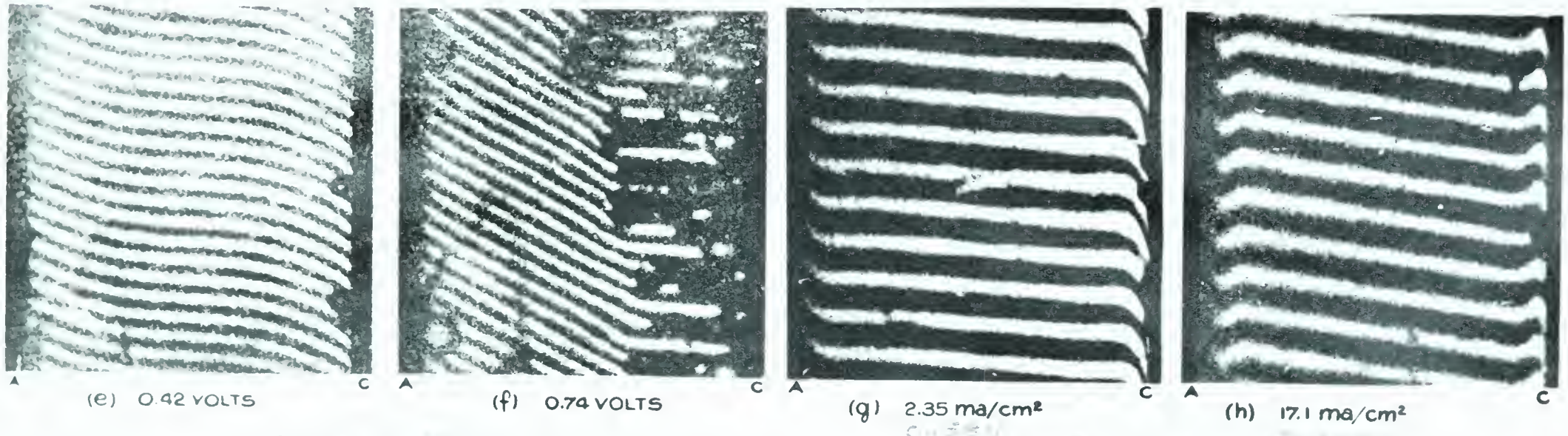

(e) 0.42 VOLTS (f) 0.74 VOLTS (g) 2.35 ma/cm² (h) 17.1 ma/cm²

NORMAL POSITION NORMAL POSITION USING $Zn(ClO_4)_2$

Fig. XII FRINGE PATTERNS PRODUCED USING THIN ELECTRODES AND $Zn(ClO_4)_2$ 25.0°C. 3 MIN. AFTER CURRENT TURNED ON.

MOVEMENT OF PARTICLES IN THE ELECTROLYTE

During some of the runs tiny particles of lint or dust were observed moving around in the electrolyte while current was being passed. Experiments were therefore carried out to determine the route of these particles in the various electrode positions. Fig. 35 shows the type of routes obtained. It was found that the direction of a particle was reversed by reversing the direction of the current. It was also noticed that there was a movement of particles at current densities below that required for the formation of the second wave.

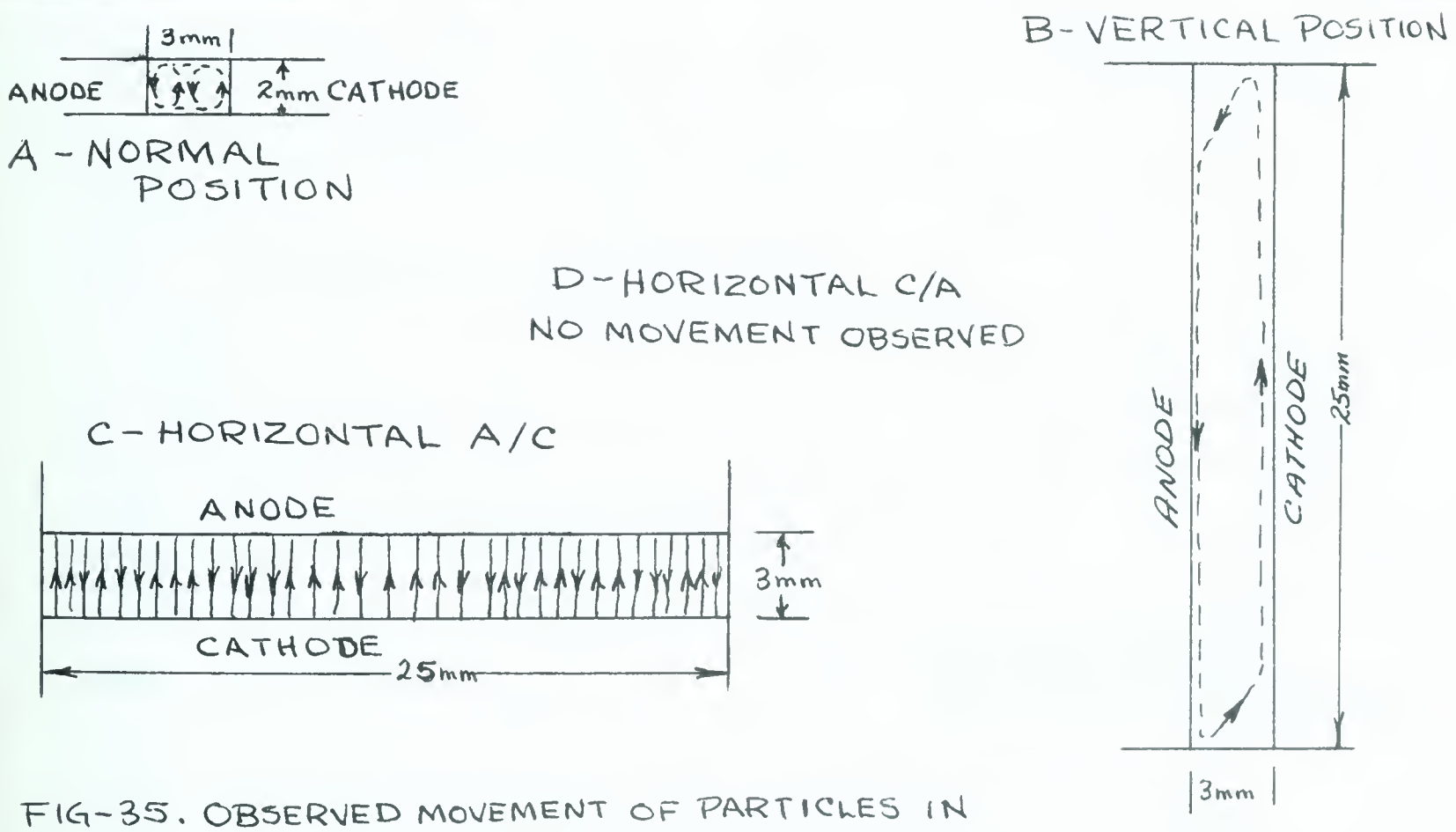

FIG-35. OBSERVED MOVEMENT OF PARTICLES IN VARIOUS POSITIONS.

RESULTS USING $Cu-CuSO_4$ SYSTEM

The system of $CuSO_4$ electrolyte between copper electrodes was used to determine whether the same type of fringe patterns would be obtained

in the four positions as those obtained with the Zn - $ZnSO_4$ system and to determine whether some of the problems encountered in the Zn - $ZnSO_4$ system were due to the system intself or due to the apparatus used. Experiments showed that the highest voltage across the cell at no impressed current was only 0.5 m.v. and that the voltage across the cell at a given current density was much more constant with time than for the Zn - $ZnSO_4$ system. Fig. 36 illustrates some of the voltage time curves obtained for the Cu - $CuSO_4$ in the normal position.

All the experiments on the Cu - $CuSO_4$ system were carried out using 0.10 M $CuSO_4$ as the electrolyte and at a temperature of 25.0°C.

Difficulty was encountered in trying to obtain voltage-current density readings in the cathode/anode position. The voltage across the cell remained resonably constant with time up to a current density of about 3 ma/cm^2; at higher current density values the voltage increased with time to values greater than 1 volt. An inspection of the electrodes after the voltage had been allowed to increase in this manner showed that the cathode was coated with a reddish-brown film. A similar deposit was also noticed in the other positions, but to a much lesser extent, after high current densities.were passed. It is believed that this is an oxide film formed by the presence of the cuprous ion.

Table XIII gives the results obtained for the Cu - $CuSO_4$ system at varying electrode separations. These data are plotted in Fig. 37 to 43. Fig. 37 is a plot of the equivalent conductivity against the current density for electrode separations of 0.325 c.m. and 0.052 c.m. for the

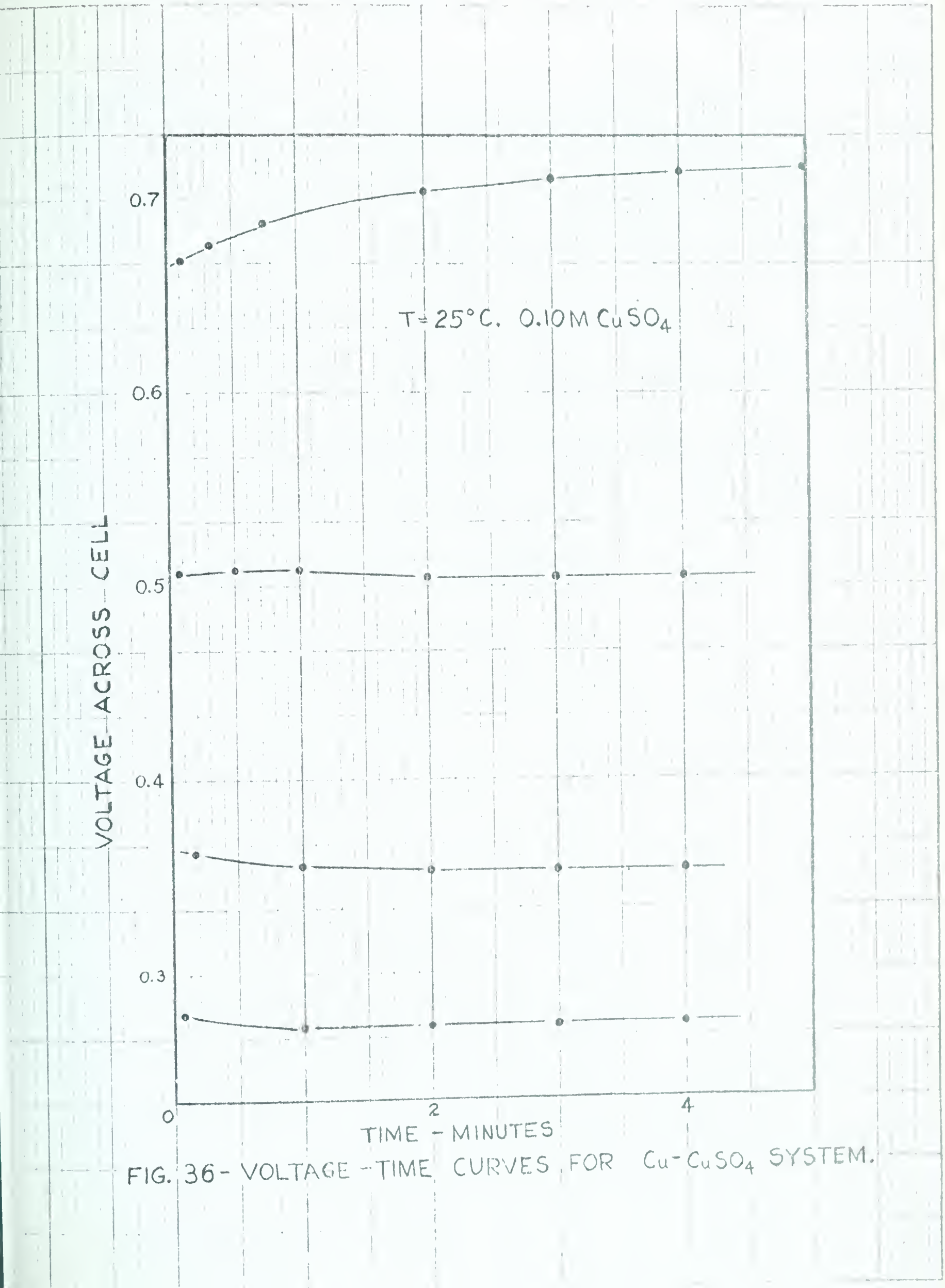

FIG. 36 - VOLTAGE - TIME CURVES FOR Cu - $CuSO_4$ SYSTEM.

four electrode positions. Fig. 38 gives the variation of equivalent conductivity with electrode separation for the four positions. Equivalent conductivity values were taken at current density values of about 6 ma/cm^2. Fig. 39 is a plot of the voltage required to produce a current density of 6 ma/cm^2. Fig. 40 to 43 are voltage-current density plots for the various positions at varying electrode separations.

All voltage and current density data obtained for the Cu - $CuSO_4$ system were taken at 3 minutes after the current was turned on.

Fig. XIII to XVI indicate the type of fringe patterns obtained at varying electrode separations in the four positions. It was found that it was very difficult to obtain photographs of the fringe patterns at electrode separations of less than 0.76 mm.

TABLE XIII - VOLTAGE-CURRENT DENSITY DATA FOR VARIOUS POSITIONS AND ELECTRODE SEPARATIONS

0.10 $CuSO_4$, 25.0°C Cu ELECTRODES, AREA = APPROX 0.50 cm^2

VOLTAGE ACROSS CELL VOLTS	CURRENT DENSITY ma/cm^2	DIST. BET. ELECTRODES cm	EQUIVALENT CONDUCTIVITY
A - Normal Position			
0.026	0.347	0.325	21.9
0.058	1.187	"	33.6
0.097	2.305	"	38.6
0.170	4.498	"	43.0
0.263	7.213	"	44.5
0.372	10.35	"	45.3
0.019	0.352	0.263	24.1
0.045	1.213	"	35.4
0.078	2.363	"	40.1
0.141	4.615	"	42.9
0.222	7.420	"	44.0
0.320	10.67	"	43.9
0.020	0.359	0.185	16.7
0.039	1.224	"	29.4
0.062	2.373	"	35.2
0.109	4.609	"	39.3
0.168	7.356	"	40.4
0.237	10.68	"	41.7

TABLE XIII - Cont.

VOLTAGE ACROSS CELL VOLTS	CURRENT DENSITY ma/cm^2	DIST. BET. ELECTRODES cm	EQUIVALENT CONDUCTIVITY
0.016	0.364	0.117	13.2
0.029	1.245	"	25.4
0.044	2.436	"	32.0
0.076	4.734	"	36.6
0.116	7.616	"	38.5
0.171	10.95	"	37.6
0.017	0.374	0.095	10.8
0.028	1.285	"	22.0
0.042	2.505	"	28.4
0.070	4.896	"	33.2
0.110	7.874	"	34.0
0.155	11.34	"	34.8
0.017	0.370	0.076	8.5
0.027	1.264	"	17.9
0.040	2.462	"	23.6
0.065	4.816	"	28.1
0.103	7.746	"	28.7
0.147	11.16	"	28.9

TABLE XIII - cont.

VOLTAGE ACROSS CELL VOLTS	CURRENT DENSITY ma/cm^2	DIST. BET. ELECTRODES cm	EQUIVALENT CONDUCTIVITY
0.016	0.388	0.070	8.6
0.025	1.324	"	18.2
0.037	2.582	"	24.5
0.061	5.050	"	29.1
0.095	8.135	"	29.9
0.155	11.69	"	26.5
0.015	0.386	0.062	8.1
0.024	1.316	"	17.1
0.035	2.568	"	23.0
0.057	5.023	"	27.6
0.089	8.091	"	28.1
0.144	11.63	"	25.1
0.013	0.382	0.052	7.6
0.022	1.305	"	15.5
0.032	2.544	"	21.0
0.051	4.977	"	25.3
0.079	8.025	"	26.5
0.137	11.53	"	21.8

TABLE XIII - Cont.

VOLTAGE ACROSS CELL VOLTS	CURRENT DENSITY ma/cm^2	DIST. BET. ELECTRODES cm	EQUIVALENT CONDUCTIVITY
B - Vertical Position			
0.023	0.347	0.325	24.4
0.055	1.187	"	35.3
0.095	2.307	"	39.6
0.170	4.494	"	43.1
0.262	7.212	"	44.7
0.368	10.36	"	45.7
0.025	0.354	0.263	18.9
0.052	1.213	"	30.4
0.087	2.359	"	35.8
0.154	4.605	"	39.2
0.241	7.359	"	40.4
0.350	10.62	"	39.9
0.028	0.357	0.185	12.0
0.047	1.226	"	24.2
0.072	2.381	"	30.6
0.124	4.638	"	34.7
0.192	7.420	"	35.8
0.304	10.56	"	32.2

TABLE XIII - Cont.

VOLTAGE ACROSS CELL VOLTS	CURRENT DENSITY ma/cm^2	DIST. BET. ELECTRODES cm.	EQUIVALENT CONDUCTIVITY
0.027	0.364	0.117	7.9
0.039	1.247	"	18.5
0.058	2.423	"	24.6
0.094	4.726	"	29.4
0.148	7.576	"	30.0
0.292	10.72	"	21.5
0.018	0.368	0.076	7.9
0.031	1.264	"	15.5
0.048	2.455	"	19.6
0.080	4.801	"	22.9
0.129	7.717	"	22.7
0.291	10.88	"	14.2
0 016	0.383	0.062	7.3
0.027	1.316	"	15.4
0.039	2.565	"	20.4
0.066	5.014	"	23.4
0.125	8.040	"	20.0
0.301	11.29	"	11.6

TABLE XIII - Cont.

VOLTAGE ACROSS CELL VOLTS	CURRENT DENSITY ma/cm^2	DIST. BET. ELECTRODES cm	EQUIVALENT CONDUCTIVITY
0.015	0.382	0.052	6.7
0.025	1.305	"	13.7
0.036	2.544	"	18.4
0.062	4.968	"	21.0
0.110	7.982	"	18.8
0.270	11.27	"	10.9
C - Horizontal - Anode/Cathode			
0.025	0.347	0.325	22.9
0.054	1.187	"	35.6
0.081	1.971	"	39.7
0.167	4.500	"	43.7
0.262	7.221	"	44.8
0.372	10.36	"	45.3
0.022	0.354	0.263	20.8
0.047	1.213	"	33.7
0.080	2.363	"	39.1
0.142	4.611	"	42.6
0.222	7.409	"	43.9
0.316	10.67	"	44.4

TABLE XIII - Cont.

VOLTAGE ACROSS CELL VOLTS	CURRENT DENSITY ma/cm^2	DIST. BET. ELECTRODES cm	EQUIVALENT CONDUCTIVITY
0.023	0.357	0.185	14.6
0.041	1.226	"	27.5
0.065	2.384	"	34.2
0.110	4.650	"	39.2
0.167	7.454	"	41.4
0.232	10.70	"	42.6
0.022	0.362	0.117	9.9
0.035	1.245	"	20.8
0.052	2.419	"	27.5
0.083	4.730	"	33.5
0.126	7.608	"	35.4
0.173	10.95	"	37.0
0.020	0.368	0.076	7.1
0.033	1.261	"	14.7
0.047	2.460	"	19.7
0.072	4.807	"	25.3
0.103	7.748	"	28.6
0.141	11.17	"	30.2

TABLE XIII - Cont.

VOLTAGE ACROSS CELL VOLTS	CURRENT DENSITY ma/cm^2	DIST. BET. ELECTRODES cm	EQUIVALENT CONDUCTIVITY
0.017	0.388	0.070	7.9
0.028	1.324	"	16.6
0.041	2.582	"	27.3
0.065	5.050	"	27.3
0.097	8.135	"	29.4
0.142	11.71	"	28.9
0.016	0.383	0.062	7.7
0.025	1.316	"	16.3
0.035	2.568	"	23.1
0.055	5.023	"	28.4
0.079	8.104	"	31.7
0.116	11.70	"	31.3
0.016	0.382	0.052	6.0
0.027	1.305	"	12.8
0.037	2.544	"	17.7
0.058	4.973	"	22.3
0.086	8.017	"	24.3
0.124	11.56	"	24.2

TABLE XIII - Cont.

VOLTAGE ACROSS CELL VOLTS	CURRENT DENSITY ma/cm^2	DIST. BET. ELECTR. DES cm.	EQUIVALENT CONDUCTIVITY
D - Horizontal - Cathode/Anode			
0.022	0.347	0.325	25.8
0.055	1.189	"	35.4
0.101	2.307	"	37.2
0.75	4.47	"	9.7
0.021	0.354	0.263	22.7
0.049	1.213	"	32.5
0.089	2.358	"	34.8
0.065	4.58	"	9.3
0.0 9	0.359	0.185	17.4
0.041	1.226	"	28.0
0.071	2.381	"	30.9
0.28	4.62	"	15.3
0.017	0.362	0.117	12.3
0.033	0.245	"	22.1
0.056	2.419	"	25.3
0.146	4.71	"	18.9

TABLE XIII - Cont.

VOLTAGE ACROSS CELL VOLTS	CURRENT DENSITY ma/cm^2	DIST. BET. ELECTR. CM	EQUIVALENT CONDUCTIVITY
0.014	0.370	0.076	13.2
0.030	1.264	"	16.0
0.046	2.460	"	21.4
0.079	4.801	"	23.1
0.015	0.383	0.062	8.2
0.026	1.316	"	15.7
0.043	2.561	"	18.3
0.077	5.005	"	20.1
0.014	0.382	0.052	6.9
0.025	1,303	"	13.6
0.037	2.542	"	17.7
0.070	4.962	"	18.5

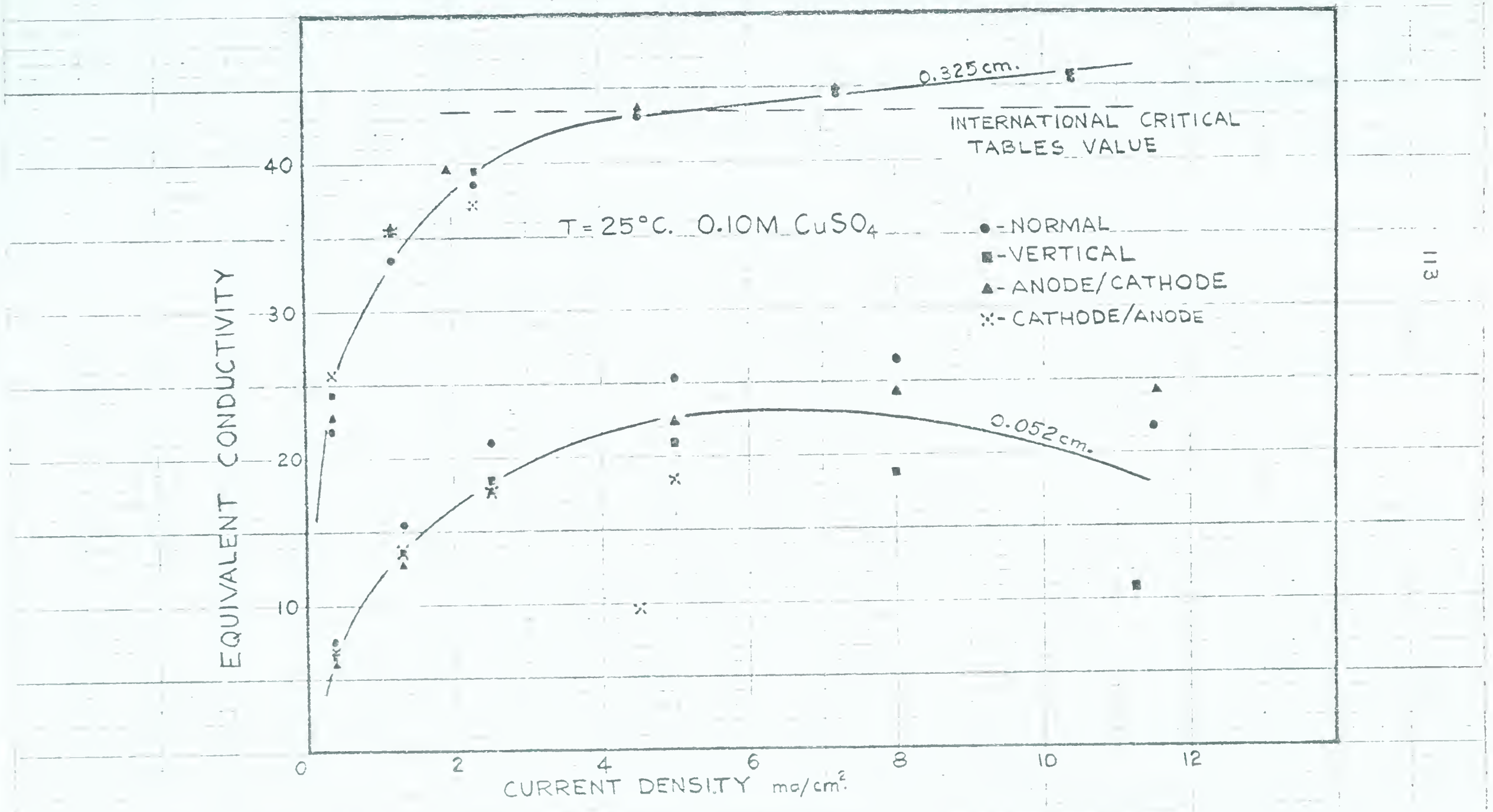

FIG. 37 - CONDUCTANCE - VARIOUS POSITIONS AND SEPARATIONS.

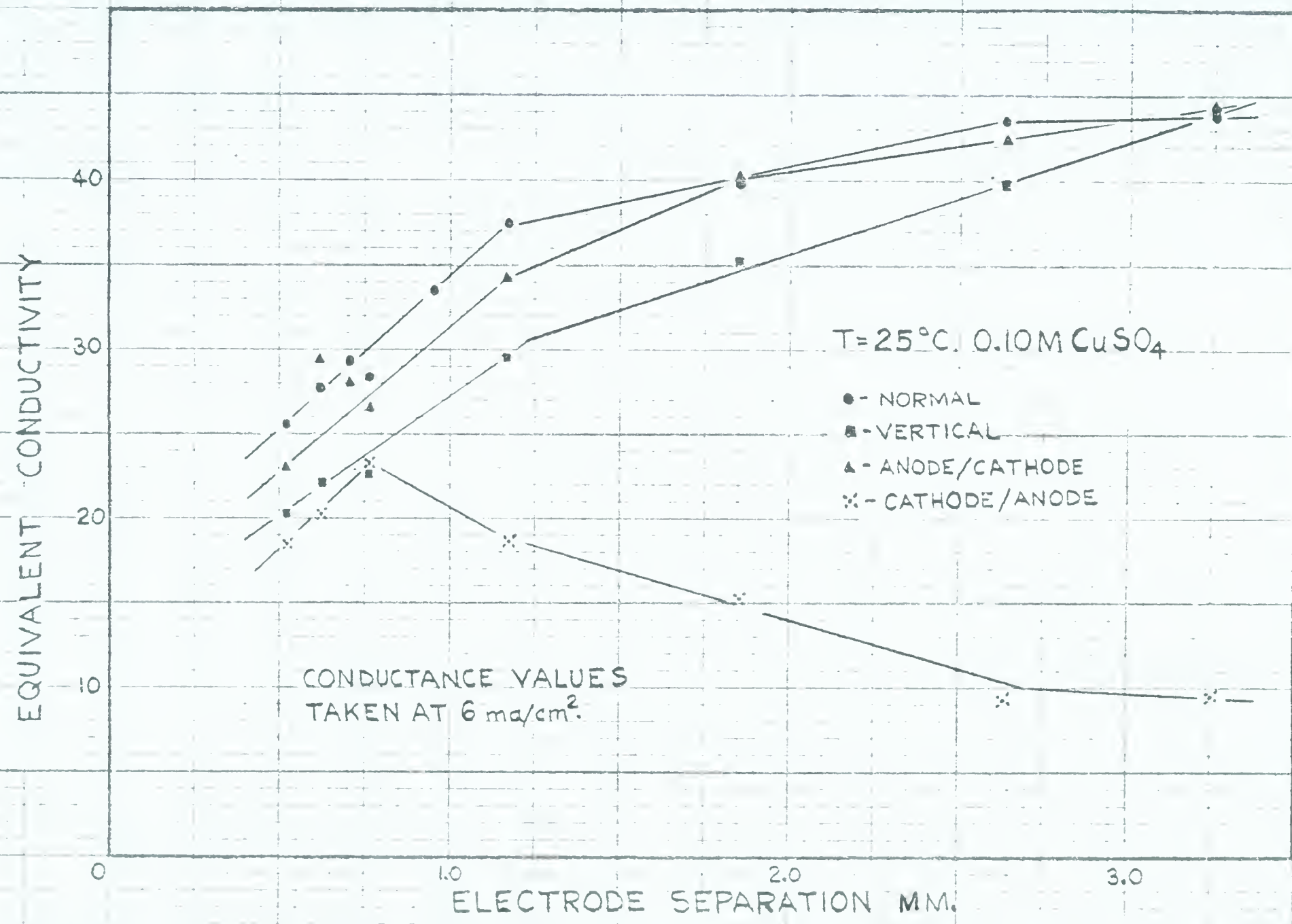

FIG. 38 - CONDUCTANCE VERSUS ELECTRODE SEPARATION - VARIOUS POSITIONS.

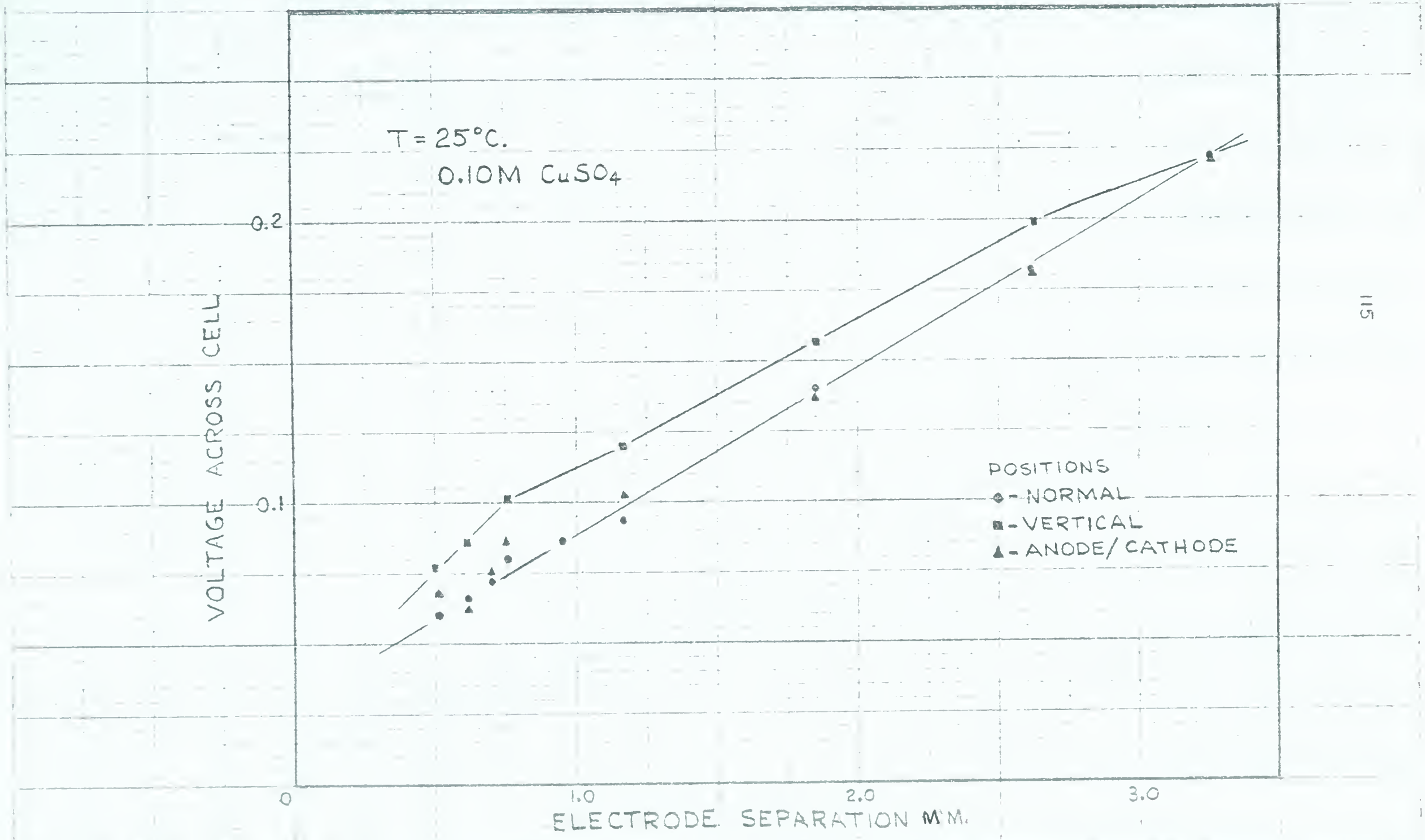

FIG. 39 - VOLTAGE TO PRODUCE C.D. OF 6.0 ma/cm².

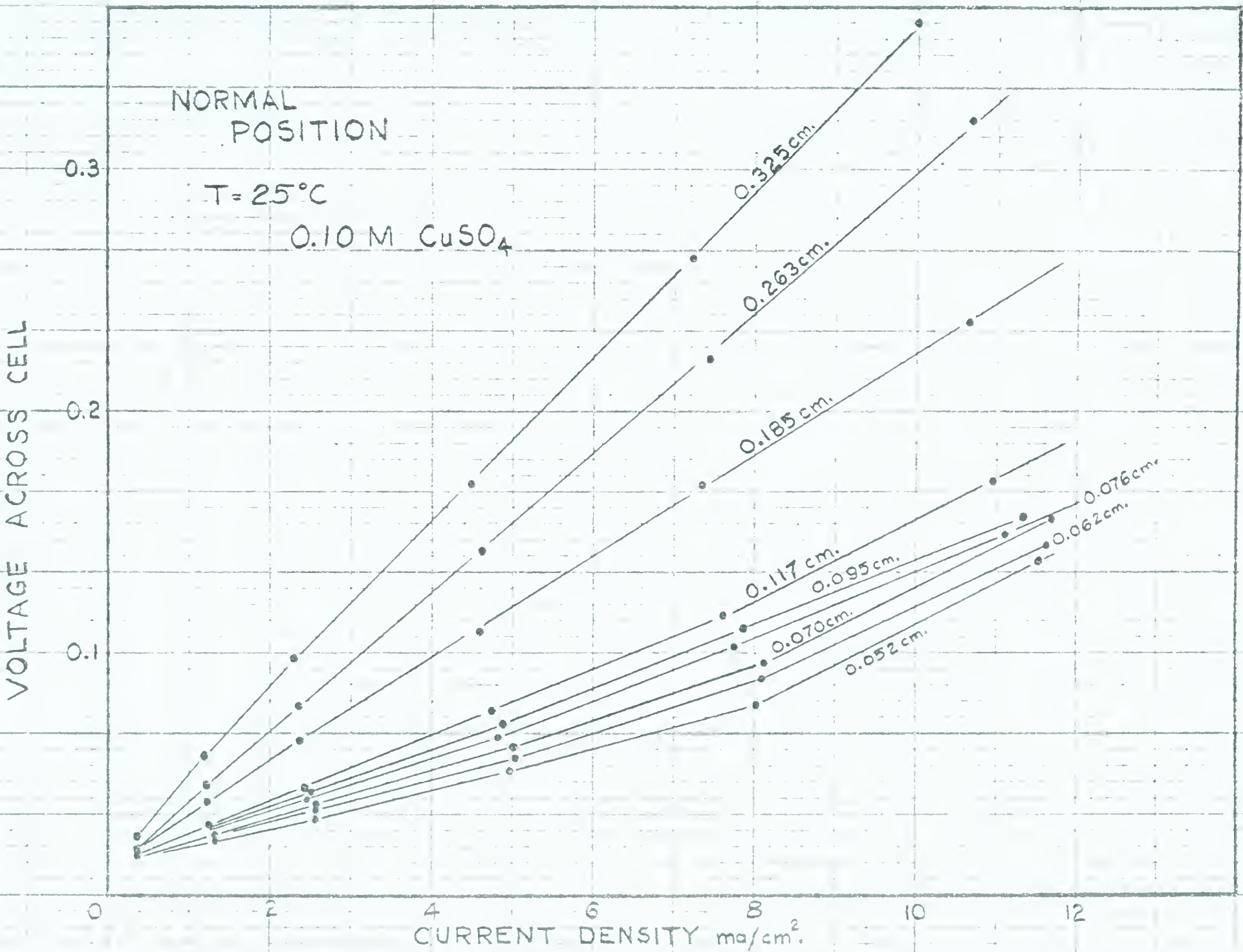

FIG. 40 - VOLTAGE - C.D. CURVES FOR VARIOUS ELECTRODE SEPARATIONS.

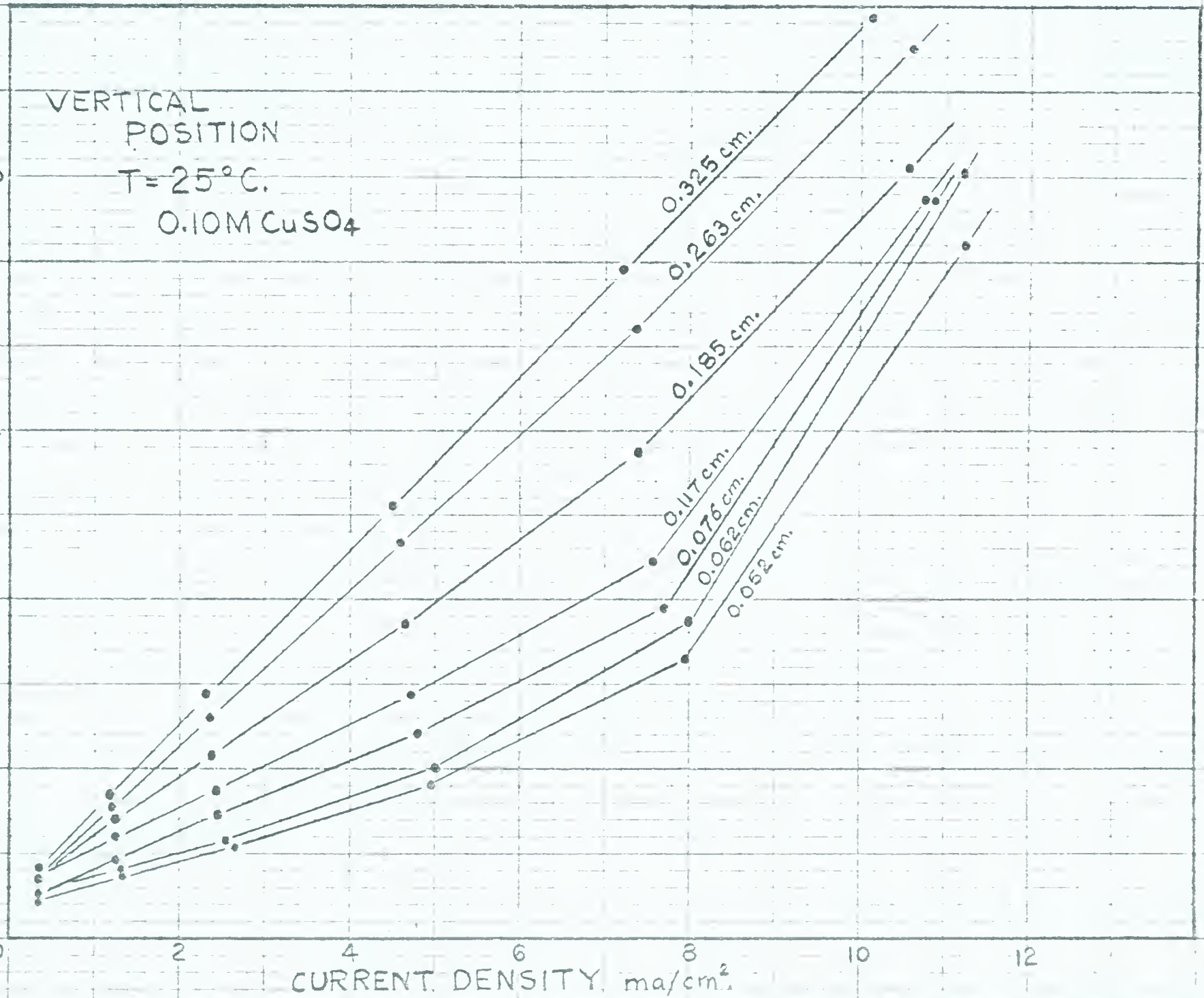

FIG. 41 - VOLTAGE - C.D. CURVES FOR VARIOUS ELECTRODE SEPARATIONS.

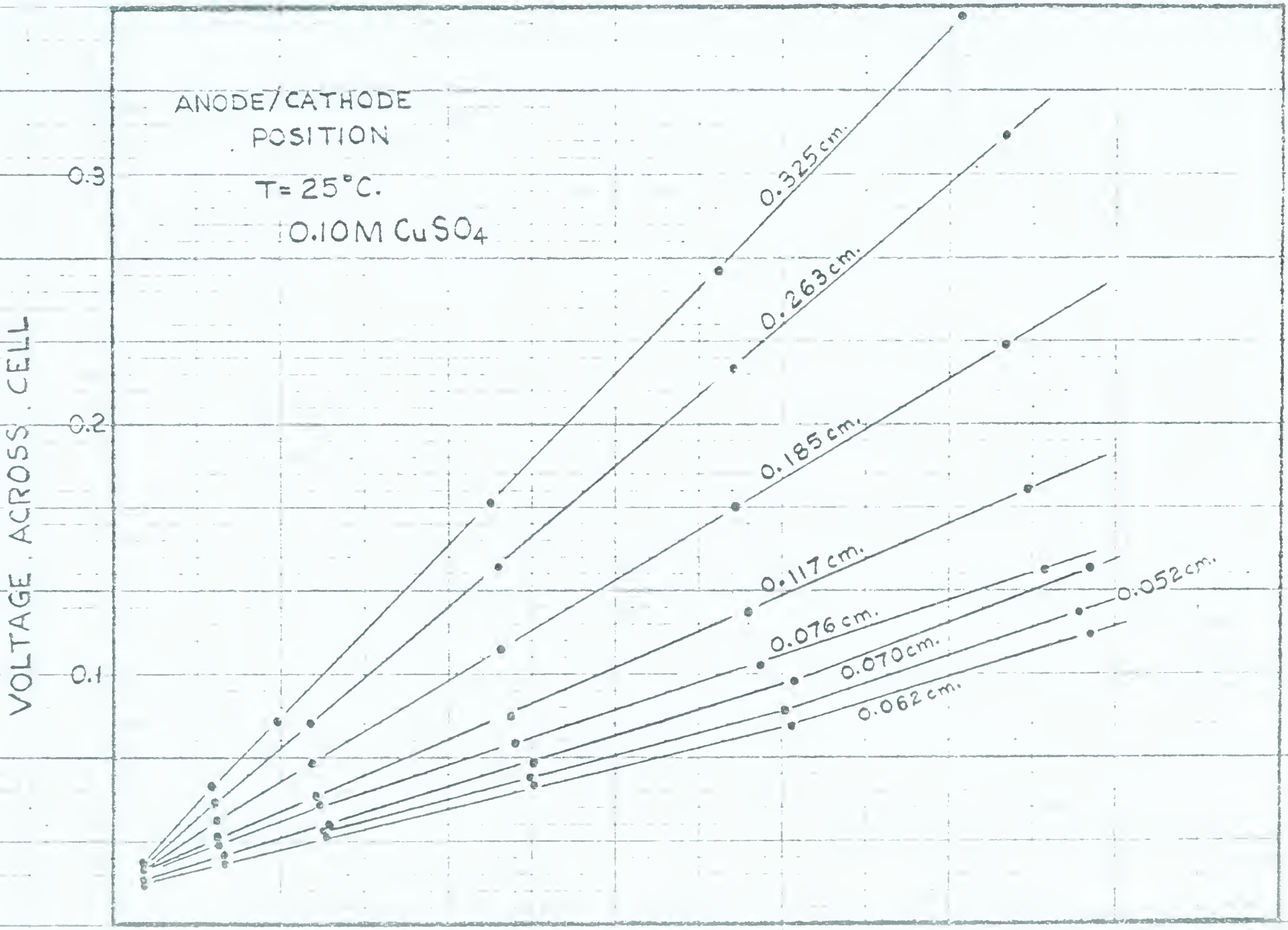

FIG. 42 - VOLTAGE - C.D. CURVES FOR VARIOUS ELECTRODE SEPARATIONS

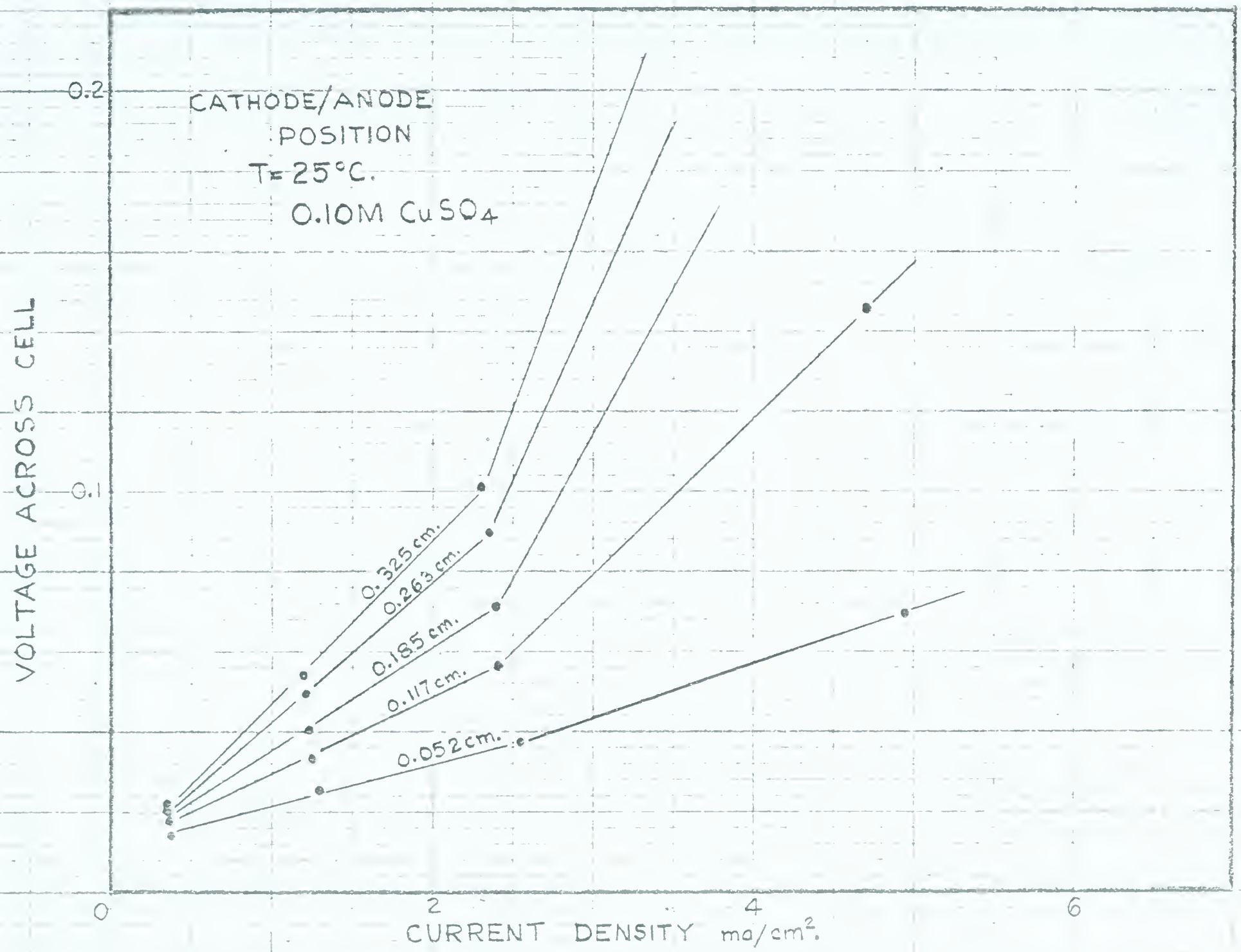

FIG. 43 - VOLTAGE - C.D. CURVES FOR VARIOUS ELECTRODE SEPARATIONS.

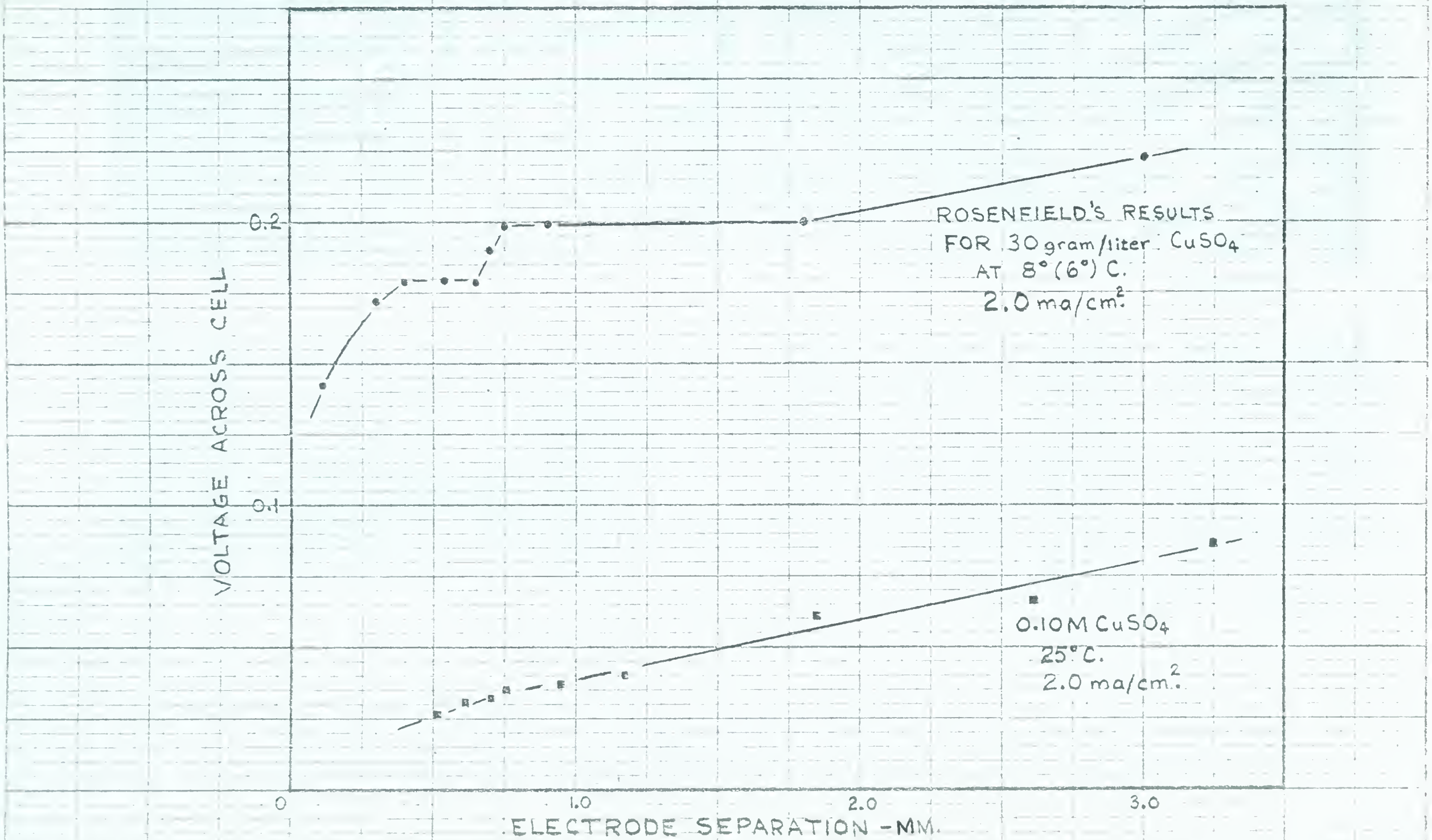

FIG. 44 - COMPARISON OF RESULTS WITH ROSENFIELD'S.

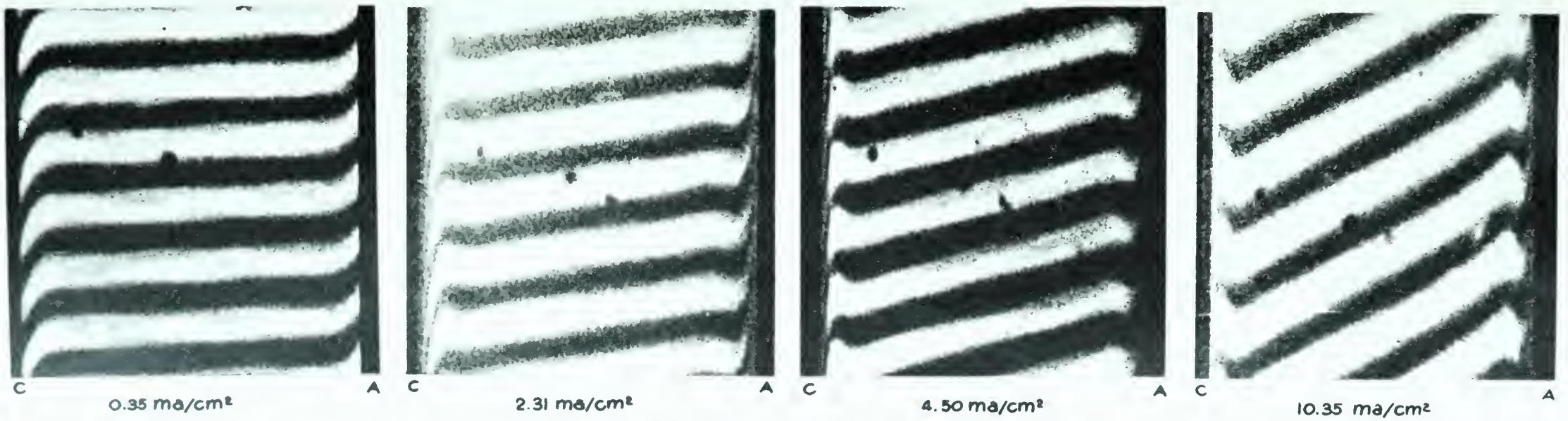

Fig. XIII FRINGE PATTERNS PRODUCED AT VARIOUS CURRENT DENSITIES AND ELECTRODE SEPARATIONS.

0.10M $CuSO_4$, 25.0°C. 3 MIN. AFTER CURRENT TURNED ON. NORMAL POSITION.

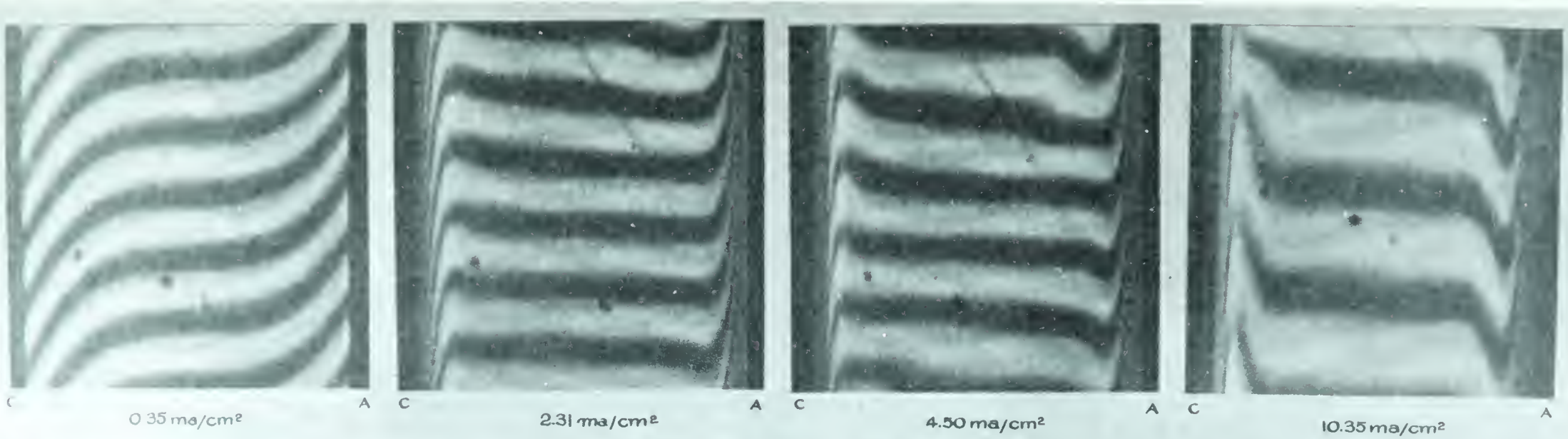

Fig XIV FRINGE PATTERNS PRODUCED AT VARIOUS CURRENT DENSITIES AND ELECTRODE SEPARATIONS.

0.10 M $CuSO_4$, 25.0°C. 3 MIN. AFTER CURRENT TURNED ON. VERTICAL POSITION.

Fig. XV - FRINGE PATTERNS PRODUCED AT VARIOUS CURRENT DENSITIES AND ELECTRODE SEPARATIONS. 0.10 M $CuSO_4$, 25.0°C. 3 MIN. AFTER CURRENT TURNED ON. ANODE OVER CATHODE POSITION.

0.35 ma/cm²

1.19 ma/cm²

2.31 ma/cm²

3.25 mm BETWEEN ELECTRODES

0.38 ma/cm²

4.61 ma/cm²

2.63 mm BETWEEN ELECTRODES

0.36 ma/cm²

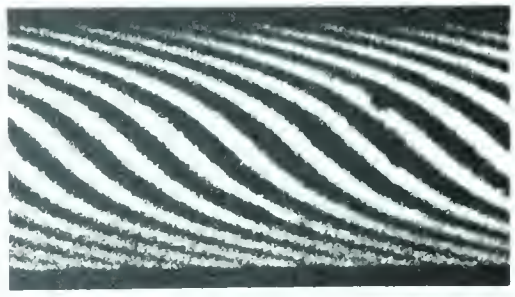

1.23 ma/cm²

1.85 mm BETWEEN ELECTRODES

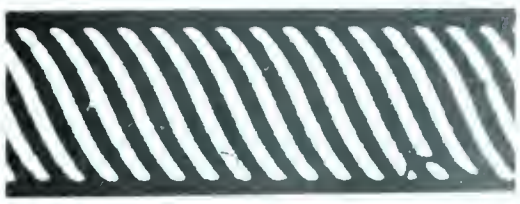

0.36 ma/cm²

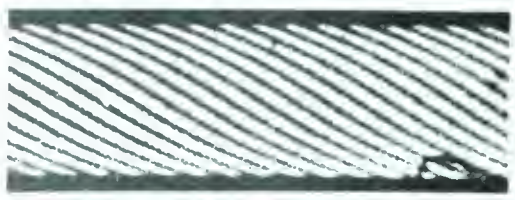

1.25 ma/cm²

1.17 mm BETWEEN ELECTRODES

0.37 ma/cm²

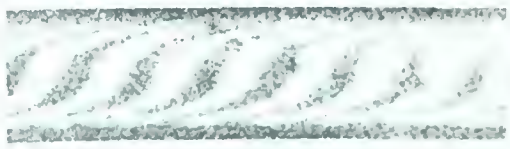

1.26 ma/cm²

0.76 mm BETWEEN ELECTRODES

Fig. 16 XVI - FRINGE PATTERNS PRODUCED AT VARIOUS CURRENT DENSITIES AND ELECTRODE SEPARATIONS. 0.10 M $CuSO_4$, 25.0°C. 3 MIN. AFTER CURRENT TURNED ON. CATHODE OVER ANODE POSITION.

DISCUSSION

The experiments carried out during this work do not give any indication that ion-pairs play a part in the formation of the second wave. The results obtained, however, do indicate that the formation of the second wave is a phenomenon closely associated with the type of convection currents that are formed in the cell. These statements are borne out by the results obtained in the cathode over anode position and while using very thin electrodes.

A second wave is not developed in the cathode over anode position. There is no reason why, if ion-pairs are localized in a specific region to cause the formation of the second wave in the normal position, they should not also be localized in the same region in the cathode over anode position. On the other hand, since mass movement of the electrolyte was not observed in the Cathode over Anode position, a second wave would not be expected to exist if its formation was due to convection.

By extrapolating the variables (height of cell, width, etc.) in Ibl's equation for the rate of convection, Greenfield determined that convection currents should not be found to exist in the size of cell that she used. This extrapolation has been proven erroneous as mass movement of the electrolyte was found to exist in the cell (which was of the same dimensions as Greenfield's) used in this work. Experiments carried out using very thin electrodes (0.19 mm. thick) show that the second wave is not formed even at 0.42 volts (40 ma/cm^2.)

across the cell, in either the normal or vertical position. At electrode thicknesses of only 0.19 mm. convection should not exist or should be small as was found in the anode over cathode position.

The fact that particles in the electrolyte moved in different paths in each position and that different fringe patterns were formed in each position strengthens the supposition that convection currents play the major role in the formation of the fringe patterns (excluding the first wave) in an electrolyte between two electrodes.

It is evident from the fringe patterns formed at low current densities (below that required for the formation of the second wave) that some movement of the electrolyte at the electrode faces must be occurring. This is shown by the fact that the concentration change at the electrodes, expressed by the shift in the first wave, is not the same in the four positions (Fig. 32). Although there is relatively no concentration gradient in the bulk of the solution at these low current densities, the overall concentration difference between the anode and cathode is different for each position. For the same cell and at identical current densities the overall concentration change should be the same in all the positions unless a faster mode of transfer of the cation, than that produced by diffusion alone, is obtained. Mass transfer by convection is such a mode. This indicates that very small concentration changes are sufficient to cause movement of the electrolyte. Some movement of particles in the electrolyte was observed at current densities of 2 ma/cm^2.

Fig. 32 shows that the greatest concentration change at an electrode face for a given current density is obtained for the Cathode over Anode Position. The Vertical Position exhibits the next greatest concentration change, then the Normal Position and lastly the Anode over Cathode position Since convection currents are not set up in the Cathode over Anode Position it is expected that this position should exhibit the greatest concentration change. Also the Anode over Cathode position should have the least concentration change. (This was not found to be so at the cathode at very small current densities.) There are two reasons why the concentration change at the electrodes should be greater in the vertical position than in the normal position. Essentially the same types of convection currents are set up in these two positions. The only difference in the cell between the two positions is the height of the cell in the vertical direction. Therefore, the time during which the electrolyte flows parallel to the electrode face is much longer in the vertical position. The flow in the normal position is mainly towards or away from the electrodes and thus a more efficient stirring of the electrolyte is obtained in this position.

Secondly, there is a difference in the direction of the light producing the fringes with respect to the direction of convection flow in the two positions. In the vertical position the direction of the light is perpendicular while in the normal position, the light is parallel, to the direction of the flow at the electrode face. It can be expected that the concentration of the electrolyte at the top of the

cell will be less than that at the bottom of the cell. This has been shown to be so in the vertical position. (However in order to measure these concentration differences motion pictures would have to be taken of the fringe formation across the whole height of the cell. The photographs shown in this thesis were taken in the center of the cell and do not illustrate this difference.) In the normal position any difference in the concentration between the top and bottom of the cell will not be shown, but rather an average value of the concentration will be obtained.

This averaging effect will be quite small at low current densities, however, it is felt that this effect may partially account for the formation of a smaller second wave in the normal position, than in the vertical position. The amount of averaging that is obtained could be determined by building a cell with the dimensions 3 mm. x 3 mm. x 3 mm. and observing the patterns formed in the normal and vertical positions.

It is very difficult to describe the method of formation of the fringe pattern in the vertical position. In order to really see what is happening photographs should be taken of the whole length of the cell with a motion picture camera. All photographs shown in this thesis were taken at the center of the cell, and therefore, the fringe distortion at the very top and bottom on the cell is not shown. The formation of the second wave starts at the top of the cell, appearing first at the anode, and then progresses slowly downwards.

It was noticed that, in the vertical position, the method of formation was determined by the direction of the wedge angle. This difference is illustrated by photographs numbered 16.84 ma/cm^2 in Fig. V and 300 sec. in Fig. VI. These photographs were taken under the same conditions except that the wedge angle formed by the glass flats is such that the distance between the glass flats is smaller at the top of the cell in Fig. V and greater at the top in Fig. VI (top of photographs is towards top of cell in both cases.) Since there is no apparent difference in the fringe patterns once they are formed, it is felt that this difference in fringe pattern formation is a positional effect only.

It is difficult to compare the voltage-current density data obtained in the four positions since effects were produced in the cathode over anode position that were not produced in the other positions. In the $Zn\text{-}ZnSO_4$ system a needle-like deposit grew out from the cathode at the higher current densities producing a smaller separation between the electrodes while in the $Cu\text{-}CuSO_4$ system a reddish-brown film was formed on the cathode causing the voltage to rise quickly with time.

It is interesting to note that when the data in Fig. 33 was plotted on semi-log paper two approximately straight lines were obtained with the change in slope occurring at 3 ma/cm^2. Also when equivalent conductivity is plotted against current density as in Fig. 27 and 31 for $ZnSO_4$ and Fig. 37 for $CuSO_4$ a similar change in slope was obtained at about 4 ma/cm^2. It would be convenient to be able to relate these occurrences to the appearance of the second wave which starts to form in

normal and vertical positions at about 2.5 to 3.5 ma/cm^2. A form of the second wave is also present in the anode over cathode position at 3 ma/cm^2. However, it is felt that results should be obtained in the four positions in a system in which interfering effects are not produced in the Cathode over Anode Position before this correlation can be made. The Ag-$AgNO_3$ system may be suitable for this purpose.

Much speculating can be done concerning the cause of the variation of the voltage with time in all positions in the Zn-$ZnSO_4$ system. Since this same variation was not observed in the Cu-$CuSO_4$, it is felt that this effect is produced by the formation of Zinc complex ions in the electrolyte. An attempt to measure pH changes in the solution was made, however, it is felt that the method employed (Universal Indicator) may not be sufficiently sensitive. A method similar to the pin hole method of Read and Graham, whereby solution at the electrode interface is withdrawn, could be used to give an indication of pH changes. Another method would be to use microelectrode probes.

Experiments on the Cu-$CuSO_4$ system were carried out for two reasons: (1) to compare the results obtained with the results for $ZnSO_4$ and (2) to determine whether the same results would be obtained as those shown by Rosenfield when the electrode separation is gradually decreased Voltage-current density results were obtained in the four positions for each electrode separation. The electrodes were polished and etched at the start of the run for each given electrode separation, whereas all the values presented by Rosenfield were obtained during a single run.

comparison of the results obtained, at 25.0°C. and at a concentration of 0.10 M, to those obtained by Rosenfield, at 8.0°C. and at a concentration of 30 grams/liter is shown in Fig. 44.

Photographs of the type of fringe patterns obtained in the various positions using alternating current are shown in Fig. II. At low voltages (below 2.5 volts) there is no apparent consistency in the direction of the fringe shift at the electrodes in the three positions. The fringe shift may be up in one location and down in another on the same electrode. It is believed that this is due to the difference in potentials existing between different grains. The grains in the zinc electrodes were relatively large. No alternating current results were taken using copper electrodes which had relatively small grains.

At high voltages the fringe patterns take on a definite shape; the concentration of the bulk of the electrolyte is less than that of the electrode faces. Therefore, the electrolyte at the electrode faces has been enriched or the electrolyte in the bulk has been depleted. Although there is no evidence for support, other than the formation of bubbles, it is felt that zinc may be dissolving when the current is in one direction and hydrogen ions plating out (due to higher mobility) when the current is reversed.

BIBLIOGRAPHY

1 Ibl, N., International Committee of Electrochemical Thermodynamics and Kinetics, Seventh Edition Pages 112-133, (1955)

2 Kurtz, L U. and Samartsev, A.G J. of Physical Chemistry, 5, 1424-28, (1934).

3 Berg, W.F., Discussions of the Faraday Society, Vol 1, Pages 44-45, (1947)

4. Proc. Roy Soc. A. (1938), 164, 79.

5. Ibl, N and Muller, R., Z. Elektrochem., 59, 671-6, (1955)

6. Ibl, N. and Muller, R., J. Electrochem. Soc., 105, 346-53 (1958)

7. O'Brien, R.N., Thesis, "An Optical Study of Electrodeposition", University of Manchester, (1955).

8 Rosenfield, Christine Ann Culp, Thesis, "An Interferometric Study of Concentration Polarization at Low Current Densities", University of Alberta, (1960)

9 Tolansky, S., "Multiple Beam Interferometry", Oxford University Press, (1948).

10 Handbook of Chemistry and Physics, Chemical Rubber Publishing Co., Cleveland, Ohio, 37th Edition (1955-56).

11 Baxter, G.P., Burgess, L.L. and Daudt, H.W. J. of the American Chemical Society, Vol. 33, 893-901 (1911)